# Characterization of a small molecule inhibitor of small G proteins regulating AT1R trafficking and signaling

Jenna Giubilaro

Department of Pharmacology & Therapeutics
Faculty of Medicine
McGill University
Montreal, Quebec, Canada
April 2020

A thesis submitted to McGill University in partial fulfillment of the requirements of the degree of Doctor of Philosophy.

**ABSTRACT**

G protein–coupled receptors (GPCRs) are important therapeutic targets that activate various downstream signaling events, like mitogen-activated protein kinases (MAPK, for instance ERK1/2), via both G proteins and β-arrestins. GPCR-mediated ERK1/2 signaling occurs both at the plasma membrane and in endosomes from receptor/β-arrestin complexes. However, deciphering where ERK1/2 signals occur in cells, as well as the role(s) of β-arrestin in such spatiotemporal signaling remains a challenge due to the dearth of tools. Here, using BRET-based sensors in a high-throughput screen for angiotensin II type 1 receptor (AT1R) trafficking, a small molecule, named Rasarfin, was identified that selectively inhibits small GTPases Ras and Arf6 but not heterotrimeric or other small G proteins. Rasarfin blocks agonist-promoted endocytosis of the AT1, Bradykinin B2 (B2R) and β2-adrenergic (β2AR) receptors and inhibits the activation of ERK1/2 by these receptors, including EGFR, as well as the activation of Akt. Molecular dynamics (MD) simulations reveal that Rasarfin binds Ras at the interface between Ras and its guanine nucleotide exchange factor (GEF) SOS1 domain. Structure-activity relationship studies on Rasarfin identify functionally selective analogs that inhibit AT1R endocytosis and/or MAPK activation. This project has also allowed for the development of novel biosensors that measure receptor-mediated signaling events in live cells. This study is the first to report a small molecule inhibitor of both Ras and Arf6 that can be further optimized for the functional characterization of Ras-mediated MAPK signaling versus Arf6-mediated receptor internalization in normal and cancer cells.

**RÉSUMÉ**

Les récepteurs couplés aux protéines-G, ou RCPG, sont des cibles thérapeutiques importantes qui activent les protéines-G et les β-arrestines pour induire l'activation de voies de signalisation, telles que les protéines kinases activées par des signaux mitogéniques (MAPK, par exemple ERK1/2). La séquestration des complexes arrestine/récepteurs à l'intérieur des endosomes conduit à l'activation de ERK1/2 et est distincte de celle opérant au niveau de la membrane plasmique. Actuellement, il y a un manque d'outils pharmacologiques pour déchiffrer l'endroit d'où proviennent ces signaux ERK1/2, ainsi que déterminer la contribution des arrestines dans cette régulation spatio-temporelle. Ici, en utilisant des biosenseurs BRET dans un crible à haut rendement pour l'étude du trafic du récepteur de l'angiotensine II de type 1 (AT1R), une petite molécule, appelée Rasarfin, a été identifiée. Elle inhibe sélectivement Ras et Arf6, mais pas les autres protéines-G monomériques ou hétérotrimériques. La Rasarfin bloque l'endocytose des récepteurs AT1, B2 de la bradykinine (B2R) et beta 2-adrénergique (β2AR) et inhibe l'activation de ERK1/2 par ces RCPG, ainsi que par l'EGFR, ainsi que l'activation de Akt. Des simulations de dynamique moléculaire démontrent que la Rasarfin se lie à Ras autour de la surface de contact entre Ras et son facteur d'échange de nucléotides guanyliques (GEF) SOS1. À la lumière des relations quantitatives structure-activité, des analogues de Rasarfin ont été identifiés qui inhibent l'endocytose de l'AT1R et/ou l'activation des MAP kinases. Ce projet a également permis le développement de nouveaux biosenseurs BRET capables de mesurer la signalisation de protéines médiée par des récepteurs dans des cellules vivantes. On rapporte le premier inhibiteur de Ras et Arf6 qui peut être optimisé pour l'étude de la signalisation de MAPK médiée pas Ras par rapport à l'internalisation du récepteur médiée par Arf6 dans des cellules normales et malignes.

**TABLE OF CONTENTS**

**ACKNOWLEDGEMENTS**

First of all, I wish to express my deepest gratitude to my supervisor and mentor, Dr. Stéphane A. Laporte, who took me on as an unexperienced undergraduate student in 2014 and gave me the opportunity to explore graduate student life. This pleasant experience gave me the courage to continue and start my graduate studies in his lab. Here, I had the chance to participate in several interesting research projects and attend various conferences. I feel very grateful to have learnt from the best in the field. His support, encouragement and fruitful discussions were crucial in training me how to become the researcher I am today. I also appreciate all his help, guidance, advice, criticism and insight throughout my Ph.D. studies, as well as providing me with an excellent environment to complete my work for the past 6 years.

I am deeply indebted to my advisor, Dr. Terry Hébert, for all his advice, guidance and constant support since my undergraduate studies. I would like to thank the members of my thesis committee, namely Dr. Simon Rousseau, Dr. Christian Rocheleau and Dr. Louise Larose for all their helpful discussions, suggestions, comments and support during my Ph.D. studies.

I would also like to extend my most sincere thanks to the past and present members of the Laporte lab (known as “Laporte Crew”) starting with research associate Dr. Yoon Namkung for her great discussions and unconditional support. I thank postdoctoral fellow Dr. Lama Yamani, graduate students Ljiljana Nikolajev, Sahil Kumar, Dana Sedki, Frank Cao, Aaron Cho and Laurence Gagnon for providing a fun working environment every day. I cherish the great friendships we have formed.

I would also like to thank all the members of the polypeptide lab for being the best group of students, technicians, research assistants, research associates and principal investigators I had

the pleasure to work with. Special thanks to Mary Lapenna for taking such great care of the whole group.

I am also thankful for the opportunity to carry out my work at the state-of-the-art facility of the Research Institute of the McGill University Health Centre (RI-MUHC) and the CIHR for their financial support.

Finally, I would like to express my deepest gratitude for the constant support, understanding and love that I received from my family throughout my graduate studies. More specifically, I dedicate this thesis to my parents whose unconditional support have played a major role in helping me proudly achieve this thesis.

## AUTHOR CONTRIBUTIONS

This thesis is assembled in accordance with the regulations of the Faculty of Graduate Studies of McGill University. It is written in traditional format with unpublished data from an original submitted manuscript entitled "Discovery of a dual Ras and ARF6 inhibitor from a GPCR endocytosis screen." Dr. Stéphane A. Laporte provided global supervision of the research work, contributed to the interpretation of data and helped with the critical reading and editing of the thesis.

Chapter 2:

The high-throughput screening was performed by Dr. Jean Duchaine at the Institute for Research in Immunology and Cancer (IRIC) and hits were validated by Drs. Sylvain Armando, Olivier Radresa and Yoon Namkung prior to me taking over the project. I analyzed the spreadsheet data. Dr. Etienne Khoury designed and performed the microscopy experiments in Figure 2.1C.

Chapter 4:

Dr. Yoon Namkung designed and generated the four BRET sensors constructs.
I contributed to the characterization of these sensors by performing and analyzing all experiments.

Chapter 5:

Dr. Etienne Khoury designed and performed the microscopy experiments in Figure 5.1D and E. Dr. Doris A. Schuetz designed, performed and analyzed all of the computational data, as well as produced Figure 5.10. I designed, performed and analyzed all other experiments.

Chapter 6:

I designed, performed and analyzed all experiments.

I am also co-author of the following publications for which my contributions are explained below:

**Beautrait A*, Paradis JS*, Zimmerman B*, Giubilaro J, Nikolajev L, Armando S, Kobayashi H, Yamani L, Namkung Y, Heydenreich FM, Khoury E, Audet M, Roux PP, Veprintsev DB, Laporte SA, Bouvier M.** A new inhibitor of the β-arrestin/AP2 endocytic complex reveals interplay between GPCR internalization and signalling. *Nat Commun* **8,** 2017 (15054). *These authors contributed equally to this work.

My contribution to this project was in response to reviewers' comments. I provided helpful discussion for complementary experiments, where I performed BRET and MAPK assays, analyzed data, and proofread the final manuscript.

**Namkung Y*, LeGouill C*, Kumar S, Cao Y, Teixeira LB, Lukasheva V, Giubilaro J, Simões SC, Longpré JM, Devost D, Hébert TE, Piñeyro G, Leduc R, Costa-Neto CM, Bouvier M, Laporte SA.** Functional selectivity profiling of the angiotensin II type 1 receptor using pathway-wide BRET signaling sensors. *Sci Signal*. 2018, 11(559). *These authors contributed equally to this work.

My contribution to this project was in the characterization of the Rho and p63 BRET sensors and editing of the manuscript.

**ABBREVIATIONS**

| | |
|---|---|
| $\beta_2$AR | $\beta_2$-adrenergic receptor |
| AngII | Angiotensin II |
| AP-2 | Clathrin adaptor protein 2 |
| ARF6 | ADP-ribosylation factor 6 |
| ARNO | Arf nucleotide binding site opener |
| AT1R | Angiotensin II type 1 receptor |
| B2R | Bradykinin type 2 receptor |
| BK | Bradykinin |
| BRAG | Brefeldin-resistant Arf GEF |
| BRET | Bioluminescence resonance energy transfer |
| CCP | Clathrin-coated pit |
| CCV | Clathrin-coated vesicle |
| CRISPR/Cas9 | Clustered regularly interspaced short palindromic repeats/CRISPR-associated protein 9 |
| EDTA | Ethylenediaminetetraacetic acid |
| EFA6 | Exchange factor for Arf6 |
| EGF | Epidermal growth factor |
| EGFR | Epidermal growth factor receptor |
| ERK1/2 | Extracellular-signal regulated kinase |
| FRET | Fluorescence resonance energy transfer |
| G protein | Guanine nucleotide-binding protein |
| GAP | GTPase activating protein |
| GDP | Guanosine diphosphate |
| GEF | Guanine nucleotide exchange factor |
| GFP | Green fluorescent protein |
| GGA3 | Golgi-localized, gamma adaptin ear-containing, ARF-binding protein 3 |
| GPCR | G protein-coupled receptor |
| GRK | G protein-coupled receptor kinase |

| | |
|---|---|
| GST | Glutathione S-transferase |
| GTP | Guanosine-5’-triphosphate |
| HEK293 | Human embryonic kidney cells |
| HTS | High-throughput screen |
| ISO | Isoproterenol |
| MANT | N-Methylanthraniloyl |
| MAPK | Mitogen-activated protein kinase |
| MD | Molecular dynamics simulation |
| PAK | p21-activating kinase |
| PBD | Protein-binding domain |
| PI3K | Phosphoinositide 3-kinase |
| PKA | Protein kinase A |
| PKC | Protein kinase C |
| RBD | Ras-binding domain |
| rGFP | *Renilla reniformis* green fluorescent protein |
| RlucII | *Renilla reniformis* luciferase |
| RTK | Receptor tyrosine kinase |
| SAR | Structure activity relationship |
| WT | Wild type |
| YFP | Yellow fluorescent protein |

**LIST OF FIGURES**

**Chapter 1**



**Chapter 2**



**Chapter 4**

**Chapter 5**



**Chapter 6**



**Chapter 7**

# CHAPTER 1. INTRODUCTION AND LITERATURE REVIEW

## 1.1. G protein-coupled receptors

Historically, the evolutionary survival of organisms has relied heavily on the ability of cells to communicate with each other, to sense and adapt to their environment. As such, the cellular membrane provides a barrier between the internal and external milieu and houses many integral proteins for adhesion, ion conductivity, and transducing cellular signals for second messenger production, gene transcription and translation. Among these proteins, the plasma-membrane-bound receptors provide the capacity for cells to respond to external stimuli. Among these cell-membrane receptors are the family of G protein-coupled receptors (GPCRs), which form the largest superfamily of over 1000 genes encoding seven-transmembrane receptors (Larhammar, Blomqvist, & Wahlestedt, 1993). They are referred to as GPCRs based on the notion that most of them interact with one or more G proteins (continued in Chapter 1.3). The diverse functional coupling of the GPCRs to G proteins and sequence homology contribute to their GRAFS classification into the following five families: Glutamate (clan C), Rhodopsin (clan A), Adhesion, Frizzled/taste2, Secretin (clan B) (Foord et al., 2005; Fredriksson, Lagerstrom, Lundin, & Schioth, 2003; Latek, Modzelewska, Trzaskowski, Palczewski, & Filipek, 2012). It has been estimated that more than half of all modern drugs are targeted at these receptors (Flower, 1999) or their downstream effectors, making them a focus of many drug discovery and research programs (Lagerstrom & Schioth, 2008; Marinissen & Gutkind, 2001; Overington, Al-Lazikani, & Hopkins, 2006). In fact, several ligands for GPCRs are found among the worldwide top-100-selling pharmaceutical products. The variety of ligands (ions, organic odorants, amines, peptides, proteins, lipids, nucleotides, and photons) allows for GPCR regulation of numerous biological processes ranging from neurotransmission and hormonal control of virtually all physiological responses, to

perception of taste, vision, smell, light and pain. The highly selective detection of chemical signals results in the transduction of the signal from these ligand–receptor interactions into specific intracellular responses. Upon stimulation, heptahelical receptors undergo conformational changes that allow binding of heterotrimeric G proteins, leading to the activation of different effectors and signaling pathways. These effectors generate second messengers, which in turn regulate a wide variety of cellular processes including gene transcription, protein synthesis, cell growth and differentiation (Figure 1.1) (S. J. Hill, 2006; Marinissen & Gutkind, 2001).

For example, the peptide hormone angiotensin II (AngII) regulates numerous physiological responses through its central actions in the brain, where it functions as a neurotransmitter to influence cardiovascular function, fluid and electrolyte homeostasis, pituitary hormone secretion and several neuroendocrine processes. AngII acts primarily at the angiotensin II type 1 receptor (AT1R) in a variety of tissues including vascular smooth muscle, kidney and adrenal gland to influence vasoconstriction, vasopressin release and sodium reabsorption (de Gasparo, Catt, Inagami, Wright, & Unger, 2000). Furthermore, AngII acts within cardiac tissues to regulate blood homeostasis through the renin-angiotensin-aldosterone system (RAAS) to directly stimulate heart rate, cardiac contractility and growth by binding to AT1R located on the plasma membrane (PM). As such, AT1R also mediates the direct actions of AngII in the development of cardiac hypertrophy and heart failure (Matsubara et al., 1994; Peach, 1977).

## 1.2. GPCR activation

The GPCR possesses seven α-helical hydrophobic transmembrane domains (TM1-TM7), which are oriented perpendicularly to the plasma membrane and are connected by three

extracellular loops (ECL1-ECL3) and three intracellular loops (ICL1-ICL3) (Kobilka, 2007). These transmembrane domains form the orthosteric ligand binding site for many classes of GPCRs, which is the binding site for the endogenous ligand of the receptor. GPCRs are synthesized in the endoplasmic reticulum and are then transported to the cell surface, fully matured and accessible for ligand activation. The receptor's amino N-terminus, which is found in the extracellular milieu, and residues of the extracellular loops undergo post-translational modifications, such as glycosylation, which are vital for maturation, receptor expression at the plasma membrane, and the binding of some endogenous ligands to the receptor. Indeed, agonist-activated GPCRs undergo conformational changes within their seven-transmembrane-spanning domain, rearranging the connected cytoplasmic loops and receptor C-tail thus providing an intracellular surface for productive G protein coupling. The receptor's carboxy C-terminus, which is found exclusively in the cytosol, and intracellular loops provide sites for palmitoylation and phosphorylation, which are important for G protein and effector coupling (Figure 1.1) (Bannert et al., 2001; Khoury, Clement, & Laporte, 2014; Maurice et al., 2011).

Agonists of low efficacy activate only the most efficiently coupled G protein. Whereas, agonists of high efficacy can induce several conformational changes of one particular GPCR, allowing them to activate various G proteins. This is known as receptor promiscuity and leads to the activation of different effectors and signaling pathways, even when the expression level of receptor and the strength of stimulus-response coupling are the same (Kenakin, 1995; Zheng, Loh, & Law, 2010).

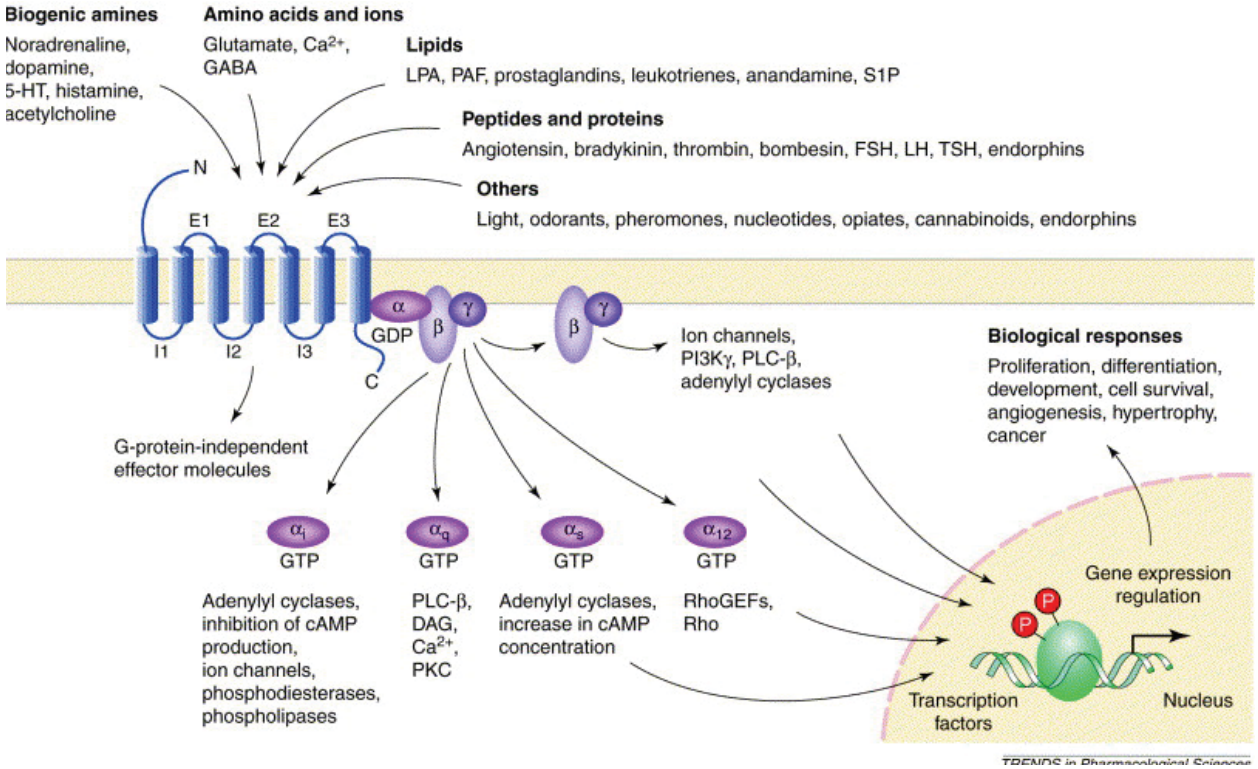


**Figure. 1.1. The activation of GPCRs and their effectors.** A wide variety of GPCR ligands and stimuli include biogenic amines, amino acids, ions, light, lipids, peptides and proteins. These agonists stimulate cytoplasmic and nuclear targets through heterotrimeric G protein-dependent and -independent effectors. GPCRs are known to couple to $G\alpha_i$, $G\alpha_{q/11}$, $G\alpha_{s/olf}$, $G\alpha_{12/13}$ and $G\beta\gamma$ to activate second messengers and propagate signaling pathways that regulate key biological responses such as cell proliferation, cell survival and differentiation. Abbreviations: E1-E3: extracellular loops; I1-I3: intracellular loops; N: amino terminus; C: carboxy terminus. Figure used and text adapted with permission from Elsevier (Marinissen & Gutkind, 2001).

Some ligands and stimuli can bind a receptor at an allosteric site, a topographically distinct site from the orthosteric site in the receptor. The intrinsic activities of GPCR ligands to initiate downstream signaling events can vary. Depending on the efficacies, receptor ligands can be classified into four main categories: full agonists, partial agonists, neutral antagonists and inverse agonists (Rosenbaum, Rasmussen, & Kobilka, 2009). A ligand is classified into each category according to its ability to stabilize the "on" state of the receptor: full agonists are defined as ligands that fully activate the receptor; partial agonists induce submaximal activation of the G protein even at saturating concentrations; neutral antagonists can bind to the receptor and cause no discernible effect or change in conformation; and inverse agonists inhibit basal activity (Kenakin, 2003; Kobilka, 2007). Antagonists have no effect on basal activity, but competitively block access of the ligand, whereas the inverse agonist can bind to basally active receptors and induce a conformational change that will lead to their activation and promote a converse activation.

Although receptors are activated by different ligands, some receptors share a common mechanism of activation as they retain the ability to couple to the same G protein. When comparing sequences, GPCRs undergo similar structural changes in the cytoplasmic regions of TM2 and TM3 where the receptor interacts with G proteins (Kobilka, 2007). In addition, biased ligands can also induce structural changes and control the efficiency of G protein coupling and GPCR signalling. Specifically, agonists acting on pleiotropically coupled receptors have the potential to cause bias towards some signalling pathways and not others. In general, biased agonists may have beneficial therapeutic profiles in many disease areas, including the treatment of pain, heart failure, osteoporosis and metabolic diseases. However, in some of these indications, biased signalling may also be associated with undesirable side effects and even contribute to disease. These beneficial

and undesirable side effects usually depend on the ligand's bias towards favoring G protein signaling over β-arrestin signaling or vice-versa (Kenakin, 2019).

Activation of GPCRs also triggers receptor endocytosis (continued in Chapter 1.5) with different functional outcomes, depending on the further fate of the receptor. The receptor can be directed toward late endosomes and then be degraded in the lysosomal compartment, thus desensitizing the functional response (continued in Chapter 1.4) or the receptor can be sorted toward recycling endosomes and redirected back to the plasma membrane, thus resensitizing the functional response (continued in Chapter 1.6) (Delom & Fessart, 2011).

Receptor activation is typically turned-off by G protein-coupled receptor kinases (GRKs) that either directly compete for G protein binding to GPCRs or modify the receptor by phosphorylating serine and threonine residues within its C-tail (continued in Chapter 1.4). GPCR phosphorylation increases the affinity for β-arrestins, which upon recruitment to the receptor impairs G protein coupling (continued in Chapter 1.5). Binding of G proteins, GRKs, and β-arrestins to the receptor occurs through multiple contact points located in intracellular loops and the C-tail of the receptor (Maurice et al., 2011).

## 1.3. Heterotrimeric G protein signaling

The heterotrimeric guanine nucleotide-binding proteins are present in all eukaryotic cells, assisting in the control of metabolic, humoral, neural, and developmental functions. The ternary complex is formed by one alpha (α) subunit, one beta (β) subunit, and one gamma (γ) subunit. These G proteins interact with cell surface receptors undergoing ligand-mediated conformational changes, and this binding event is transduced into an intracellular signal (Gilman, 1987). They act

as switches that can exist in either of two states depending on bound nucleotide: GDP- or GTP-bound states. Upon receptor activation, the GDP-bound G protein interacts with the intracellular face and C-terminus of the receptor, promoting the exchange of GDP to GTP within the α subunit and subsequent dissociation of the Gα and Gβγ subunits, hence the receptor acts as a guanine nucleotide exchange factor (GEF). The now active Gα and Gβγ subunits then bind to their respective downstream effectors, including kinases, phosphatases, small guanosine triphosphatases (GTPases), integral membrane proteins, enzymes, and transcription factors and a multitude of additional targets and signaling cascades (Figure 1.1). Termination of the signal occurs when the GTP is hydrolyzed to GDP by a GTPase activating protein (GAP), thereby re-associating the α subunit and the βγ heterodimer back to its basal state (Bridges & Lindsley, 2008; Marinissen & Gutkind, 2001; Simon, Strathmann, & Gautam, 1991). To date, twenty-eight α subunit subtypes, six β subunit subtypes, and twelve γ subunit subtypes have been described. Each G protein is able to activate and/or couple to a multitude of effectors, depending on the subtype. These G protein subtypes are extremely conserved in evolution and can recruit a protein to the plasma membrane, activate multiple effectors directly or indirectly, or activate one protein while inactivating another (Gonzalez-Maeso & Meana, 2006). The following sections will describe these subunits, their subtypes and their effectors in more detail.

### 1.3.1. Gα subunits and their downstream effectors

The G protein α-subunit can be divided into four groups: $G\alpha_s$, $G\alpha_{i/o}$, $G\alpha_{q/11}$ and $G\alpha_{12/13}$, and some of these also have different isotypes. There is approximately 20% homology between

the amino acids sequenced from these subunits. The N-terminal region of the Gα subunit interacts with the βγ subunits for heterotrimer formation; Gα proteins $G\alpha_o$, $G\alpha_{i1}$, $G\alpha_{i2}$, $G\alpha_{i3}$ have a post-translational myristoylation modification at the N-terminal region that increases the affinity of the α subunit for the βγ subunit (Simon et al., 1991). The C-terminal region is involved in interactions with the receptor. Antibodies and peptides designed to recognize the Gα C-terminus have shown to block the receptor/Gα protein interaction (Hamm, Deretic, Hofmann, Schleicher, & Kohl, 1987; Simon et al., 1991). The $G\alpha_s$ proteins are coupled to the stimulation of adenylyl cyclase (AC); $G\alpha_i$ proteins are coupled to the inhibition of AC as well as to the activation of G protein-coupled inwardly rectifying potassium (GIRK) channels; $G\alpha_{q/11}$ proteins are coupled to the activation of phospholipase Cβ; and $G\alpha_{12/13}$ proteins are coupled to the activation of Rho GEFs (Pierce, Premont, & Lefkowitz, 2002). These four Gα subunits are described individually in more detail below.

#### 1.3.1.1. $G\alpha_{s/olf}$ signaling

$G\alpha_s$ shows 88% amino acid sequence identity with $G\alpha_{olf}$. Both proteins are able to activate adenylyl cyclase (AC) to increase intracellular cAMP levels. $G\alpha_s$ is named the stimulatory regulator of AC, a plasma membrane-bound enzyme that catalyzes the conversion of adenosine triphosphate (ATP) to cyclic adenosine monophosphate (cAMP) (Rodbell, Birnbaumer, Pohl, & Krans, 1971; Simon et al., 1991). When $G\alpha_s$ or $G\alpha_{olf}$ are bound to GTP, they will activate AC to enhance the synthesis of the second messenger cAMP, which will activate protein kinase A (PKA). PKA is a serine/threonine kinase that phosphorylates many substrates, including GPCRs, other

downstream kinases like mitogen-activated protein kinase (MAPK), transcription factors and phosphatases for cell proliferation and differentiation (Pierce et al., 2002). The $G\alpha_s$ subunit is also capable of regulating sodium, chloride, and L-type calcium channels (Bridges & Lindsley, 2008; Simon et al., 1991). Examples of GPCRs that couple to $G\alpha_s$ include the $\beta_2$-adrenergic receptor, dopamine receptor $D_1$, and 5-$HT_{4,6\text{ and }7}$ serotonin receptors. $G\alpha_{olf}$-activated adenylyl cyclase increases intracellular cAMP levels, which open cyclic-nucleotide-gated ions channels and cause the depolarization of sensory neurons and subsequent transduction of action potentials to the brain (Ebrahimi & Chess, 1998). $G\alpha_{olf}$ is only expressed in neural tissues and neurons in the olfactory epithelium; therefore, it is solely activated by olfactory GPCRs in response to odorant molecules.

1.3.1.2. $G\alpha_{i/o}$ signaling

The family of $G\alpha_{i/o}$ proteins include the subtypes $G\alpha_{i1}$, $G\alpha_{i2}$, $G\alpha_{i3}$, $G\alpha_{o1}$ and $G\alpha_{o2}$. They inhibit AC to lower intracellular cAMP levels (Simon et al., 1991). As such, $G\alpha_i$ is named the inhibitory regulator of AC. Activated $G\alpha_{i/o}$ binds the catalytic region of AC to prevent ATP catalysis to cAMP, thus blocking the activation of PKA or its downstream effectors. However, $G\alpha_{i/o}$ has the potential to activate c-Src tyrosine kinases, including the extracellular regulated kinase (ERK)/MAPK and phosphatidylinositol-3-kinase (PI3K)/Akt cascades. $G\alpha_{i1}$ and $G\alpha_{i3}$ couple to GIRK channels, whereas $G\alpha_o$ increases phosphoinositide release, regulates neuronal and atrial potassium channels, as well as calcium channels in the dorsal root ganglia (Birnbaumer et al., 1989; Hescheler, Rosenthal, Trautwein, & Schultz, 1987). Examples of GPCRs that couple to $G\alpha_{i/o}$ include the AT1R, γ-aminobutyric acid receptor ($GABA_BR$), dopamine receptor $D_2$ and both subtypes of cannabinoid receptors ($CB_1$ and $CB_2$).

1.3.1.3. $G\alpha_{q/11}$ signaling

The amino acid sequences of the $G\alpha_q$ and $G\alpha_{11}$ isotypes differ from each other by less than 12% and almost all of these changes are found in the N-terminal region of the molecule, which determines the specificity of interaction with the Gβγ subunit. Therefore, they could interact with different subsets of receptors and effectors (Simon et al., 1991). $G\alpha_{q/11}$ proteins couple to phospholipase C-β (PLCβ), a plasma membrane-bound enzyme which hydrolyzes the lipid phosphatidylinositol-4,5-biphosphate ($PIP_2$) to generate two second messengers: diacylglycerol (DAG) and inositol-1,4,5-triphosphate ($IP_3$) (Gutkind, 2000; Rhee & Bae, 1997). Cytosolic $IP_3$ binds and activates the $IP_3$ receptor ($IP_3R$) on the endoplasmic reticulum or sarcoplasmic reticulum surface, resulting in the release of calcium ($Ca^{2+}$) from internal stores into the cytosol. Thus, $IP_3$ controls various $Ca^{2+}$-dependent cellular functions, including but not limited to cell proliferation, differentiation, muscular contraction, immune responses, brain functions, and light transduction (Berridge, 1993; Berridge & Irvine, 1984). Whereas, DAG is a physiological activator of protein kinase C (PKC), a serine/threonine kinase that phosphorylates many substrates, including GPCRs. The production of DAG in the membrane facilitates the translocation of PKC from the cytosol to the plasma membrane, thereby activating it and its downstream effectors, such as the Ras/Raf/MEK/ERK cascade (continued in Chapter 1.7.1) (Nishizuka, 1984, 1988). Examples of GPCRs that couple to $G\alpha_{q/11}$ include the B2 Bradykinin receptor (B2R), oxytocin receptor and AT1R.

#### 1.3.1.4. $G\alpha_{12/13}$ signaling

The $G\alpha_{12}$ and $G\alpha_{13}$ subunits are ubiquitously expressed and primarily linked to the activation of four small GTP-binding protein members of the Rho family, through Rho guanine nucleotide exchange factors (RhoGEFs): p115-RhoGEF, PSD-95/Disc-large/ZO-1 homology (PDZ)-RhoGEF, leukemia-associated RhoGEF (LARG), and lymphoid blast crisis (Lbc)-RhoGEF (Dutt, Nguyen, & Toksoz, 2004; Fukuhara, Murga, Zohar, Igishi, & Gutkind, 1999; Kozasa et al., 1998). Rho GEFs contain a common Dbl oncogene homology (DH) domain which confers GEF activity, followed by an adjacent pleckstrin homology (PH) domain, which together (the DH-PH module) promote nucleotide exchange. RhoGEFs also contain unique N- or C-terminal regions which represent regulatory regions. GTPases, such as Rho, bind guanine nucleotides and their activation state is determined by whether they bind GDP in the inactive state, or GTP in the active state. Activated GTP-bound $G\alpha_{12/13}$ proteins mediate the translocation of RhoGEFs from the cytosol to the plasma membrane. Rho GEFs are key Rho regulators since they transduce extracellular signals to Rho and directly activate Rho GTPase by inducing rapid GDP/GTP exchange, resulting in GTP-bound Rho (Schmidt & Hall, 2002). The downstream Rho-dependent pathways will then affect cytoskeletal structure, nuclear gene expression, cellular growth, contraction, and migration (continued in Chapter 1.7.2). Examples of GPCRs that couple to $G\alpha_{12/13}$ include M1 and M3 muscarinic acetylcholine receptors, AT1R and B2R.

### 1.3.2. Gβγ subunits and their downstream effectors

The Gβγ heterodimer is a single entity tightly bound through non-covalent hydrophobic interactions. Several of its functions include stabilizing the Gα subunit at the N-terminus in a conformation that allows it to interact with the receptor at the Gα subunit's C-terminus, modulating downstream effects of the activated Gα subunit, and indirectly regulating ion channel and phospholipase activity at the plasma membrane (Simon et al., 1991). There are six distinct Gβ subunits and thirteen Gγ subunits, sharing between 79 and 90%, and 26 and 76% amino acid sequence identity, respectively. Originally, the Gβγ dimer was viewed as a negative regulator of Gα signaling, inactivating Gα subunits and allowing them to reassociate with the receptor for subsequent rounds of signaling and preventing spontaneous Gα activation in the absence of receptor stimulation. It is now understood that the Gβγ subunit can itself modulate many other effectors that are also regulated by Gα subunits, including twelve AC isoforms, PLCβ, GIRKs, voltage-gated $Ca^{2+}$ channels, PI3K, and MAPKs, among others (Khan et al., 2013). The variety of responses the Gβγ subunit mediates is due to their ability to crosstalk with different Gα subunits, specifically since Gβγ can activate Gα subunits and vice versa (Rondard et al., 2001). For example, the Gβγ-activated inwardly rectifying potassium channel is activated by $G\alpha_i$ and $G\alpha_o$-coupled receptors (Q. Zhang, Dickson, & Doupnik, 2004). All receptors signal through Gβγ.

## 1.4. GPCR desensitization

In the presence of continued stimulus, GPCRs have their own internal mechanism to dampen the physiological response. Following receptor activation by an agonist, the receptor

undergoes the process of desensitization, defined as the "off-switch" of all receptor signaling functions. This process is fairly rapid (seconds to minutes) and involves the functional "uncoupling" of G proteins from the receptors (Hausdorff, Caron, & Lefkowitz, 1990). Desensitization is mediated by the phosphorylation of serine and threonine residues within the third intracellular loop (ICL3) or C-terminal tail of the receptor by PKA, PKC and/or G protein-coupled receptor kinases (GRKs) (Freedman et al., 1995; Hausdorff, Lohse, et al., 1990; Premont, Inglese, & Lefkowitz, 1995).

### 1.4.1. Heterologous desensitization

PKA and PKC are phosphotransferases that catalyze the transfer of the $\gamma$-phosphate group of ATP to serine and threonine residues contained within specific amino acid consensus sequences of proteins. They can phosphorylate a receptor even in the absence of its agonist, resulting in "heterologous" desensitization (Pierce et al., 2002). These kinases are activated in response to GPCRs-stimulated increases in intracellular second messengers, such as cAMP, $Ca^{2+}$ and diacylglycerol (DAG), and participate in GPCRs signaling by mediating the phosphorylation of the receptor itself or other downstream target proteins. These second messenger kinase pathways can provide classical feedback regulatory loops or cross-talk between different second messenger systems (Hausdorff, Caron, et al., 1990).

### 1.4.2. Homologous desensitization

Homologous desensitization requires high agonist occupancy of the receptor and involves the recruitment of G protein-coupled receptor kinases (GRKs) to the receptor (Benovic, Strasser,

Caron, & Lefkowitz, 1986; Hausdorff, Lohse, et al., 1990). Seven mammalian GRK genes have been identified, GRK1-GRK7, which are most closely related to PKC and PKA families. They have three distinct domains that contribute to their specificity for receptors. Furthermore, the activity of the kinases toward the receptor is enhanced in the presence of activated conformations of the receptors (Pitcher, Freedman, & Lefkowitz, 1998). The GRK phosphorylation of the receptor leads to the binding of β-arrestins and subsequent uncoupling of the receptor from heterotrimeric G proteins, preventing further signalling from the receptor via the G protein (Attramadal et al., 1992; Lohse, Benovic, Codina, Caron, & Lefkowitz, 1990). Here, the binding of β-arrestins then targets GPCRs for internalization in clathrin-coated vesicles (Ferguson, 2001). For most receptors, the phosphorylation status of the activated GPCR and the GRK-mediated phosphorylation clusters regulate the stability of receptor/arrestin complexes and interaction (Krupnick & Benovic, 1998; Oakley, Laporte, Holt, Barak, & Caron, 1999).

### 1.5. Clathrin-dependent GPCR endocytosis

Over the years much research has shown there are biological GPCR responses that are not mediated by heterotrimeric G proteins but by canonical β-arrestin signalling, following receptor desensitization and involves clathrin-dependent endocytosis (Daaka et al., 1998; Khoury, Clement, et al., 2014; Marinissen & Gutkind, 2001).

Clathrin is a triskelion protein that forms a lattice of pentagons and hexagons that wraps around to enclose an invagination of the lipid bilayer. Clathrin-coated vesicles (CCVs) are ubiquitously found in all nucleated cells. They remove proteins and lipids from the plasma membrane and transport them into internal compartments (endosomes). They also export proteins

and lipids from the *trans*-Golgi network to endosomes. The cycle of CCV formation begins with the nucleation or initiation of a pit, followed by the propagation of the clathrin lattice, invagination of the bilayer and cargo recruitment (Kirchhausen, 2000).

Clathrin-mediated endocytosis is the well-described mechanism for entry of molecules into cells. GRK phosphorylation of receptor promotes the recruitment of the cytoplasmic accessory proteins β-arrestin (step 1, Figure 1.2). β-arrestins act as scaffold intermediates by binding components of the clathrin-coated-pit machinery and sequestering receptors in clathrin-coated pits (CCPs) (steps 2 and 3, Figure 1.2). The GTPase activity of dynamin pinches off clathrin-coated vesicles from the plasma membrane to invaginate formed pits and release them into the cytosol as a free CCV (steps 3 and 4, Figure 1.2). All the vesicle components must now be disassembled so that the CCV can fuse with an early endosome (step 5, Figure 1.2), which sorts proteins into different compartments. The early endosome determines the fate of receptors, directing them to recycling endosomes and back to the cell surface (step 6, Figure 1.2), or directing them to late endosomes or lysosomes for degradation (step 7, Figure 1.2) (Delom & Fessart, 2011).

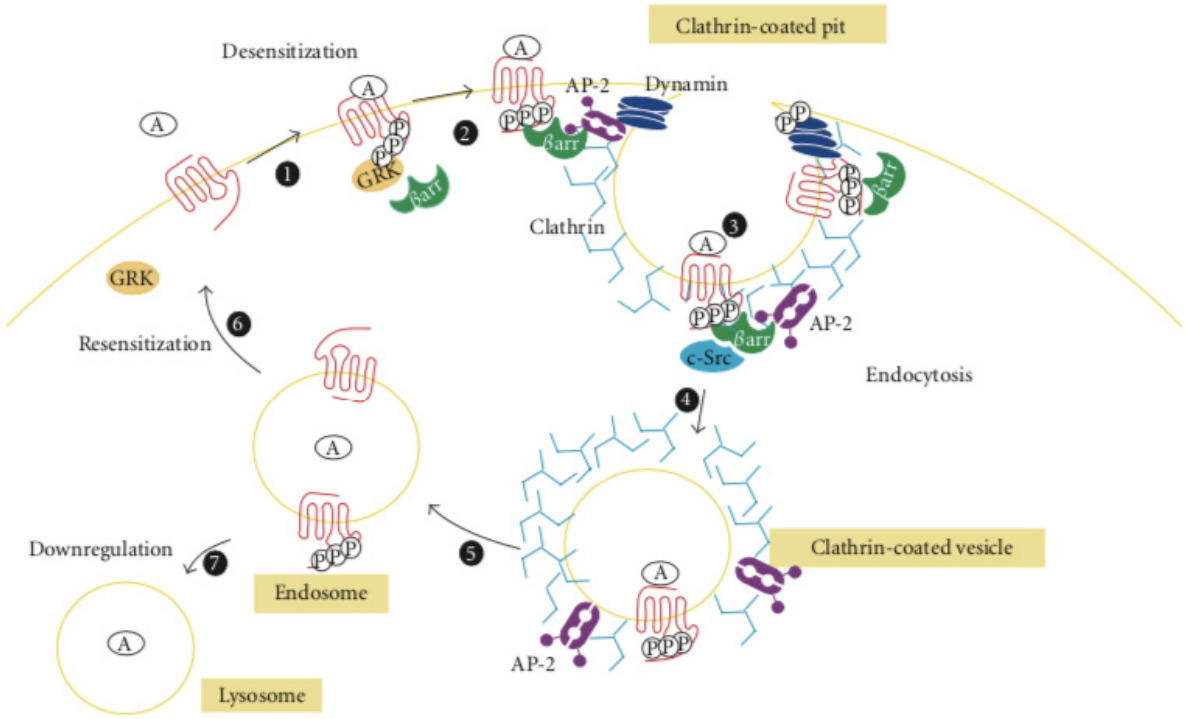


**Figure 1.2. Steps involved in GPCR trafficking: desensitization, endocytosis, resensitization and downregulation.** Upon agonist (A) binding, receptors are phosphorylated (P) by GRKs leading to the recruitment of β-arrestins (step 1). β-arrestins, through their interaction with clathrin, AP-2, Arf6, c-Src, target the receptor/arrestin complexes to clathrin-coated pits (steps 2 and 3). Dynamin regulates the pinching off of CCPs from the cell surface (steps 3). Once clathrin-coated vesicles are formed (step 4), the receptor is then internalized into endosomes (step 5), dephosphorylated before returning to the cell surface (step 6), or the receptor is degraded to lysosomes (step 7). Figure used and text adapted with permission from Creative Commons Attribution License (Delom & Fessart, 2011).

1.5.1. β-arrestins and their interacting endocytic proteins

β-arrestins are members of the arrestin family of proteins (arrestin1-4). Arrestin1 and arrestin4 (visual arrestins) are uniquely found in retinal rods and cones for phototransduction, whereas arrestin2 and arrestin3 (nonvisual arrestins) are ubiquitously expressed (Pierce et al., 2002). These latter two somatic forms, βarrestin1 (arrestin 2) and βarrestin2 (arrestin 3) have highly homologous structures, sharing 78% amino acid identity and regulate signaling as well as internalization of different GPCRs (Sterne-Marr & Benovic, 1995).

As endocytic adaptor proteins, β-arrestins target the desensitized receptors for internalization via CCPs by interacting directly with clathrin and the β2 subunit of adaptor-protein 2 (AP-2) (Goodman et al., 1996; Laporte, Oakley, Holt, Barak, & Caron, 2000; Laporte et al., 1999). AP-2 belongs to a highly conserved heterotetrameric assembly polypeptide family with three other members: AP-1, AP-3, and AP-4. AP-2 binds clathrin via its β2 chain (Shih, Gallusser, & Kirchhausen, 1995) and interacts with dynamin via its α chain (Laporte et al., 1999). β-arrestins also recruit the small GTPase Arf6 and its GEF Arf nucleotide binding site opener (ARNO) to initiate the assembly of clathrin cages and formation of CCVs (Claing et al., 2001; Claing, Laporte, Caron, & Lefkowitz, 2002). Arf6 regulates the recruitment of AP-2 and clathrin to activated receptors during the endocytic process (Poupart, Fessart, Cotton, Laporte, & Claing, 2007). Furthermore, β-arrestins recruit and activate the Src family of non-receptor tyrosine kinases. In particular, Src is recruited to the β-arrestin/receptor complex to phosphorylate dynamin (Miller et al., 2000), clathrin and the β2 subunit of the AP-2, permitting CCV endocytosis (Ahn, Maudsley, Luttrell, Lefkowitz, & Daaka, 1999; Zimmerman, Simaan, Lee, Luttrell, & Laporte, 2009).

GPCRs can be divided into class A and B depending on their β-arrestin-binding profile. Previous groups have generated β-arrestin1 and β-arrestin2 knockout (KO) mouse embryonic fibroblast (MEF) cell lines and used RNA interference to show the differential regulation of β-arrestin1 and 2 in the desensitization, internalization and signaling of receptors (Ahn, Nelson, Garrison, Miller, & Lefkowitz, 2003; Kohout, Lin, Perry, Conner, & Lefkowitz, 2001). Class A GPCRs, such as the β2-adrenergic, μ-opioid, endothelin ETA and dopamine D1 receptors, interact weakly with β-arrestins in a transient fashion since they are dephosphorylated in early endosomes, dissociate from β-arrestins and rapidly recycle back to the plasma membrane following internalization. They also have a higher affinity for β-arrestin2 than β-arrestin1. Conversely, Class B GPCRs, such as the neurotensin 1, AT1, vasopressin V2, and bradykinin B2 receptors, tightly bind both β-arrestin1 and β-arrestin2 with the same affinity, leading to a prolonged half-life of the complex in endosomes and preferential trafficking to late endosomes and lysosomes (Maurice et al., 2011; Oakley, Laporte, Holt, Caron, & Barak, 2000). Another level of complexity is added when taking into account that some receptors form an intermediate between class A and class B (i.e. class C). These receptors internalize with β-arrestin into endosomes, like class A receptors, which suggests they have a high avidity for β-arrestin. However, like class B receptors, β-arrestin dissociates rapidly from the receptors in the endosomes and they are recycled back to the plasma membrane (Simaan, Bedard-Goulet, Fessart, Gratton, & Laporte, 2005).

Since the discovery of β-arrestins as proteins that desensitize receptor-dependent second messenger signaling, several new roles for β-arrestins have been identified, as well as other β-arrestin interacting proteins (Pierce & Lefkowitz, 2001). For example, they have shown to also

bind other cellular components involved in the modulation of vesicular trafficking, such as the ATPase protein NSF (McDonald et al., 1999). The discovery of β-arrestin binding to the E3 ubiquitin ligase Mdm2 to mediate the ubiquitination of receptors provides another way of targeting GPCRs for internalization and degradation (Shenoy, McDonald, Kohout, & Lefkowitz, 2001).

### 1.5.2. β-arrestin and cell signaling

β-arrestins are ubiquitous multifunctional proteins that "arrest" downstream G protein signaling, such as activation of ERK1/2, and promote GPCR desensitization and internalization (Daaka et al., 1998; Shenoy & Lefkowitz, 2011). The recruitment of β-arrestins to activated GPCRs results in the assembly of protein complexes, where β-arrestins serve as scaffolds for the activation of a number of signaling pathways, including ERK1/2, JNK, p38, and Akt (DeWire, Ahn, Lefkowitz, & Shenoy, 2007; Peterson & Luttrell, 2017). The first hint that β-arrestins might regulate GPCR signalling beyond their roles in desensitization and internalization came with the discovery that β-arrestin1 interacts with Src to activate MAPK (Luttrell et al., 1999). The MAP kinases are a conserved family of proteins which phosphorylate serine and threonine residues and are involved in the transduction of signals regulating cell growth, division, differentiation and apoptosis. They can be grouped into three main families: extracellular-signal-regulated kinases (ERKs), Jun amino-terminal kinases (JNKs), and stress-activated protein kinases (p38/SAPKs) (Seger & Krebs, 1995).

The classic ERK1/2 MAPK cascade responds primarily to growth factors and mitogens to induce cell growth and differentiation. Important upstream regulators of ERK1/2 include cell

surface receptors, such as receptor tyrosine kinases (RTKs), GPCRs, and integrins, as well as the small GTPase Ras (Morrison, 2012). Receptor activation results in an increase in tyrosine phosphorylation of the adaptor protein Shc and recruitment of the adaptor protein growth factor receptor-bound protein 2 (Grb2) and the Ras GEF, Son of sevenless (SOS), which binds to the SH3 domains of Grb2, to the plasma membrane. SOS stimulates the exchange of GDP bound to Ras for GTP (Downward, 1996), which leads to the recruitment of Raf into complex with activated Ras. The subsequent signal transduction of the MAPK cascade involves the sequential phosphorylation of the MEK and ERK1/2 kinases. The Raf serine/threonine kinase phosphorylates and activates MEK at Ser218 and Ser222, which phosphorylates the Thr202 and Tyr204 sites of ERK1/2, activating ERK1/2 and promoting its translocation to the nucleus for cell proliferation (Figure 1.3) (Seger & Krebs, 1995).

It was first determined that ERK1/2 activation by GPCRs, such as AT1R, was via $G_i$ and $G_q$ signaling pathways. Receptors signaling through $G\alpha_i$ proteins activate the MAPK cascade by a $G_i$-dependent $G\beta\gamma$-mediated mechanism of Ras activation, which phosphorylates Raf to initiate the ERK cascade, independent of PKC (Chiloeches et al., 1999). Through $G\alpha_q$ proteins, AT1R activates PLCβ to generate inositol trisphosphates and diacylglycerol, which in turn will release calcium from intracellular calcium store sites and activate PKC, respectively. PKC then recruits Src and phosphorylates Raf to initiate the ERK cascade from here, independent of Ras (Figure 1.3) (Hawes, van Biesen, Koch, Luttrell, & Lefkowitz, 1995; Seta, Nanamori, Modrall, Neubig, & Sadoshima, 2002).

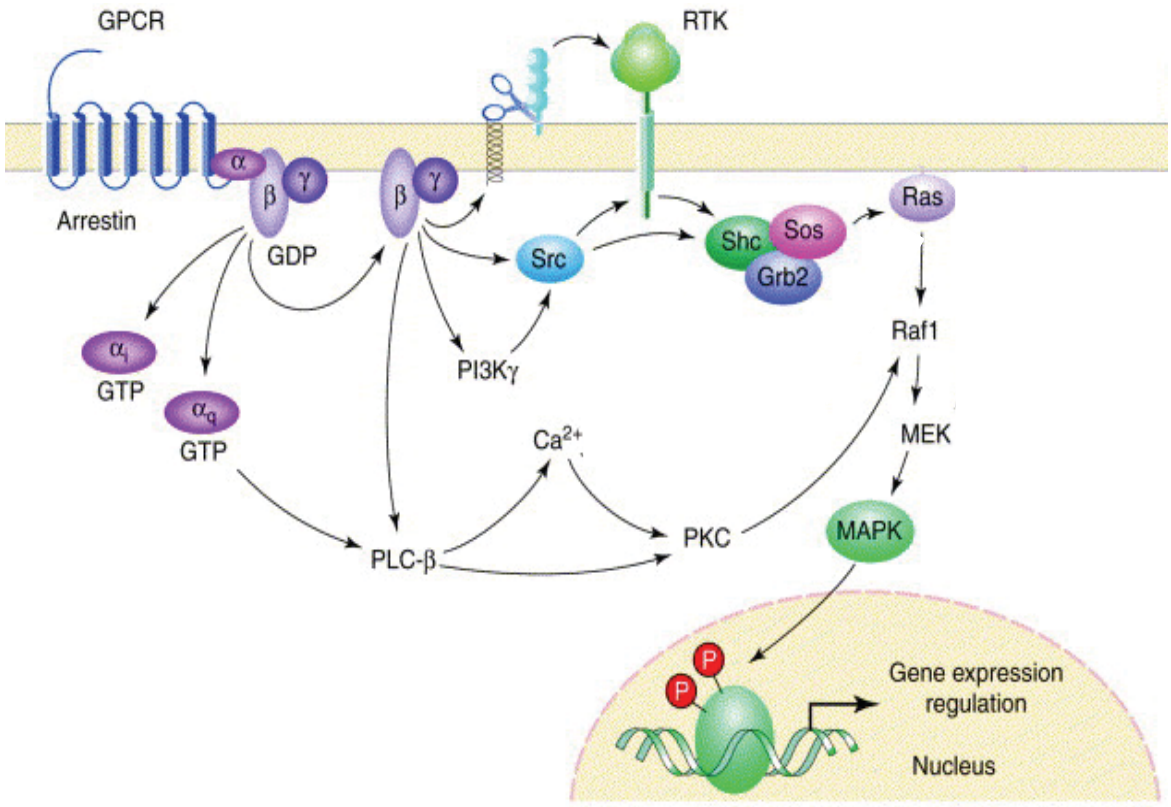


**Figure 1.3. Activation pathways of MAPK by GPCRs and RTKs.** GPCR-activated βγ-subunits and RTK activation results in the recruitment of SOS to the membrane and the stimulation of Ras-Raf1-MEK-MAPK pathway. GPCR-activated $G\alpha_q$ can stimulate Ras and Raf1 through phospholipase C-β (PLC-β) and protein kinase C (PKC), respectively. Activated MAPK translocates to the nucleus and phosphorylates nuclear proteins, such as transcription factors, thereby regulating gene expression. Figure and text adapted with permission from Elsevier (Marinissen & Gutkind, 2001).

β-arrestin can also mediate AT1R activation of MAPK via clathrin-dependent GPCR endocytosis. Once the class B receptor/β-arrestin complex internalizes, β-arrestins retain activated kinases within the cytosol in endosomes rather than allowing them to translocate to the nucleus where they would normally stimulate gene transcription (Wei et al., 2003). Here, β-arrestins act as scaffold proteins binding to Raf-1, MEK1/2 and ERK1/2, forming a complex with AT1R and activating ERK1/2 and JNK3 in the endosomes (Figure 1.4) (Luttrell et al., 2001; P. H. McDonald et al., 2000). In addition, β-arrestin2 and G proteins have different spatiotemporal patterns of ERK1/2 activation by AT1R. $G\alpha_{q/11}$ protein-dependent activation is rapid (peak <2 min), quite transient and leads to nuclear translocation of the activated ERK1/2. In contrast, β-arrestin2-dependent activation is slower (peak 5-10 min), quite persistent, and ERK1/2 is entirely confined in cytoplasmic endosomal vesicles that also contains the internalized receptors and β-arrestin (Ahn, Shenoy, Wei, & Lefkowitz, 2004). Here, β-arrestin1/2-bound ERK1/2 has a prolonged activation because it is protected from rapid dephosphorylation by nuclear and cytosolic MAPK phosphatases (Wei, Ahn, Barnes, & Lefkowitz, 2004). Recent studies using CRISPR/Cas9 to delete β-arrestin1/2 and G proteins suggest that β-arrestin1/2 functions as a regulatory hub, determining the balance between the different GPCR-mediated pathways that activate ERK1/2 (Luttrell et al., 2018). β-arrestin has also been shown to drive MAPK signaling directly from clathrin-coated structures at the plasma membrane without forming endosomes, after dissociating from its activated GPCR (Eichel, Jullie, & von Zastrow, 2016).

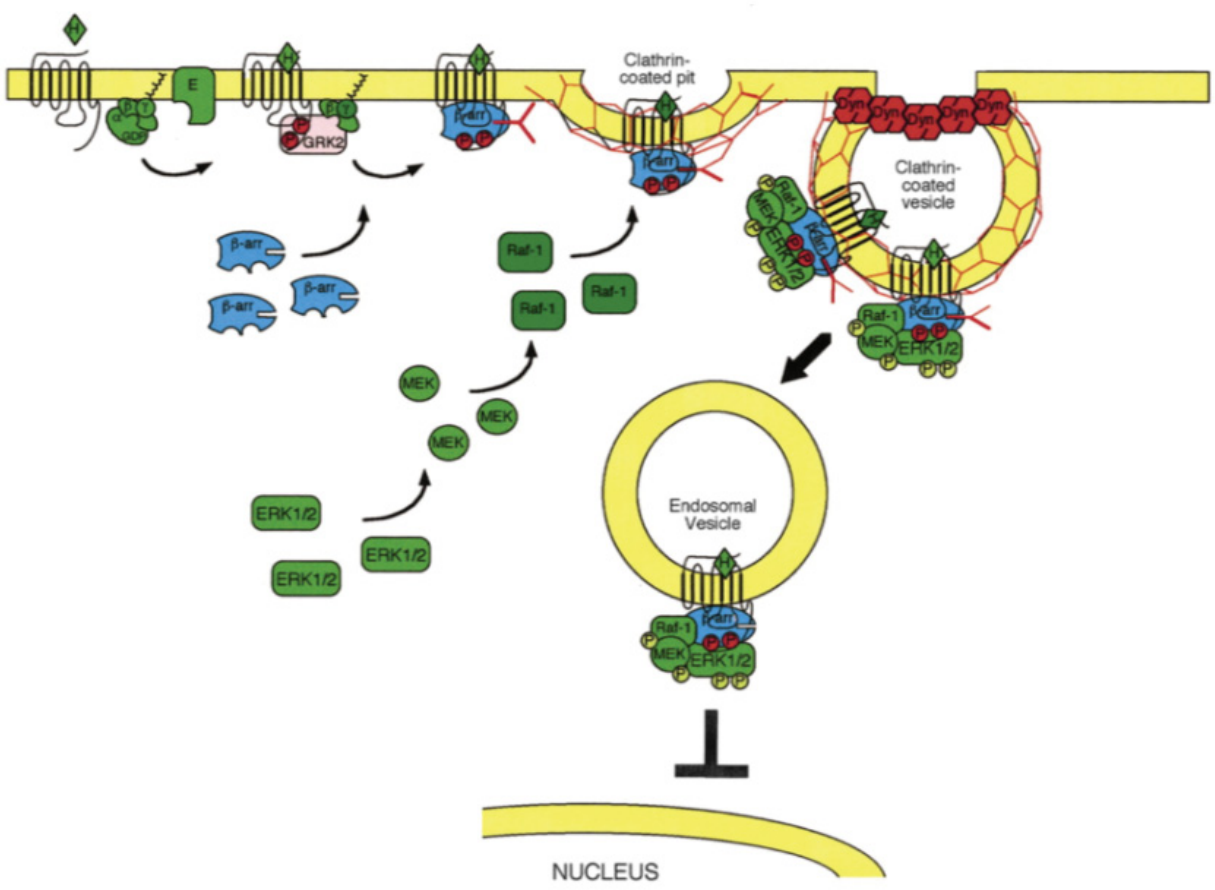


**Figure 1.4. Role of β-arrestins in the activation and targeting of MAP kinases.** The binding of β-arrestins to agonist-occupied GPCRs triggers the assembly of a MAP kinase activation complex using β-arrestin as a scaffold, with subsequent activation of a β-arrestin-bound pool of ERK1/2 at the plasma membrane and endosomes. The ERK1/2 signaling from the plasma membrane is activated by β-arrestin after dissociating from its activated GPCR. The ERK1/2 activated by the formation of receptor-β-arrestin-ERK complexes in endosomal vesicles does not result in nuclear translocation of ERK1/2 or stimulation of cell proliferation. Figure and text adapted with permission from The Company of Biologists Limited (Luttrell & Lefkowitz, 2002).

As a positive feedback mechanism, MAPK activity at a regulatory site in the β-arrestin2 hinge domain was determined to increase the avidity of the β-arrestin2/receptor complex and promote slower recycling of the receptor to the plasma membrane (Khoury, Nikolajev, Simaan, Namkung, & Laporte, 2014). ERK1/2 phosphorylation of β-arrestin-2 on Ser14 and Thr276 can lead to a reduction in the steady-state cell-surface expression of many GPCRs. This intracellular sequestration results in the dampening of cell responsiveness to GPCRs' ligand-mediated activation, making ERK1/2 both a downstream effector and a negative regulator of GPCRs (Paradis et al., 2015).

β-arrestins also play a role in the transduction of signals regulating protein synthesis and cell survival through its involvement in the Akt pathway. Akt, also known as protein kinase B (PKB), is a serine/threonine kinase that contains a pleckstrin-homology (PH) domain that allows it to interact with other proteins. Akt is activated in response to a wide variety of growth stimuli, including GPCRs, epidermal growth factor (EGF), platelet derived growth factor (PDGF) and insulin by different mechanisms all involving PI3K. β-arrestin-mediated GPCR activation of Akt involves the scaffolding of protein complexes containing protein phosphatase 2 (PP2A) and Akt, as shown for the D2R (Beaulieu et al., 2005). AT1R-mediated phosphorylation of the PP2A inhibitor, I2PP2A, transiently inhibits β-arrestin2-bound PP2A in the signalsome complex, permitting the phosphorylation of Akt by PI3K and increasing its activity (Kendall et al., 2011). Upon RTK activation, Ras binds the catalytic p110 subunit of PI3K. PI3K activation converts phosphatidylinositol (4,5)-bisphosphate (PIP2) to phosphatidylinositol (3,4,5)-trisphosphate (PIP3), which results in the subsequent plasma membrane production of PIP3 and binding to the PH domain of Akt. Here, Akt becomes phosphorylated at two major sites, Thr308 in the kinase

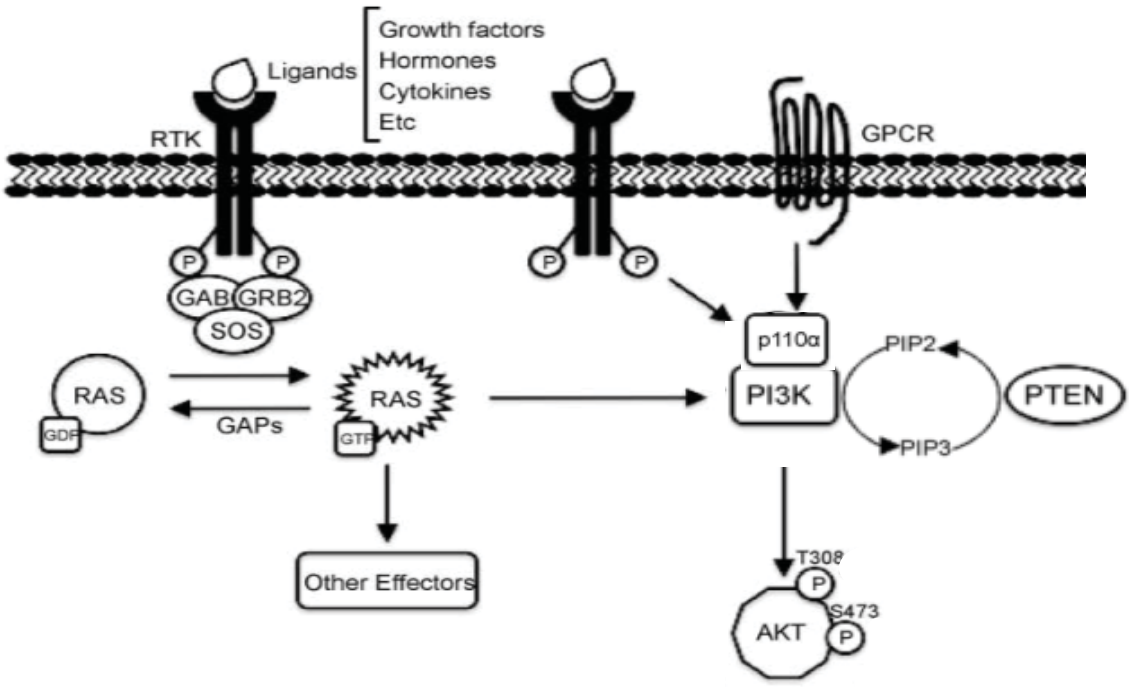


**Figure 1.5. Regulation of Akt signaling by RTKs and GPCRs.** Ligand-activated RTK recruits SOS to the membrane and leads to the exchange of GDP for GTP bound to Ras. GPCR- and RTK-activated Ras binds the p110 subunit of PI3K, which promotes the conversion of PIP2 to PIP3 at the plasma membrane. This leads to the recruitment of the PH domain of Akt to PIP3 and PI3K phosphorylation of Akt for its activation. PTEN negatively regulates PI3K activity. Figure adapted with permission from PubMed Central (Castellano & Downward, 2011).

domain and Ser473 in the carboxy-terminal tail, leading to its activation (Figure 1.5) (Marte & Downward, 1997). Upon $G_q$- and $G_i$-coupled GPCR activation, both Gβγ complexes and Gα subunits can effectively promote Akt activation in a PI3K-dependent manner, through its regulatory p110 subunit (Figure 1.5) (Murga, Laguinge, Wetzker, Cuadrado, & Gutkind, 1998).

## 1.6. GPCR resensitization

GPCR resensitization protects cells against prolonged receptor unresponsiveness. It requires agonist-dependent internalization and receptor sequestration via the β-arrestin-dependent targeting of receptors to CCVs and their endocytosis to endosomes (Ferguson et al., 1996). Here, β-arrestin dissociates from the receptor so that it may be exposed to protein phosphatase 2 (PP2A) for receptor dephosphorylation (Pitcher, Payne, Csortos, DePaoli-Roach, & Lefkowitz, 1995). However, association of PP2A with the receptor requires the acidification of the receptor in the endosomes (Anborgh, Seachrist, Dale, & Ferguson, 2000; Krueger, Daaka, Pitcher, & Lefkowitz, 1997). Furthermore, the fate of GPCRs is also regulated by the small GTPase Rab family (described in Chapter 1.7.4), which will traffic the dephosphorylated receptor to recycling endosomes and back to the cell surface to be available for a new round of agonist activation or to late endosomes to be degraded in lysosomes (Seachrist, Anborgh, & Ferguson, 2000).

## 1.7. Small G proteins

Small G proteins are typically 20–30 kDa in size and act as biological switches to regulate the downstream signaling of various plasma membrane receptors, such as the RTKs epidermal growth factor receptor (EGFR) or platelet derived growth factor receptor (PDGFR) and GPCRs.

They cycle between a GTP-bound form (the active state) and a GDP-bound form (the inactive state). The switch-ON process is reversible and involves the exchange of GDP for GTP by GEFs, resulting in the formation of the GTP-bound active protein in the cytosol, where GTP levels are relatively high. The binding of GTP induces conformational changes in two regions of the GTPase known as switch I and switch II, enabling the active GTPase to bind to specific effector proteins and initiate signaling events through them. The switch-OFF process involves the irreversible hydrolysis of GTP to GDP by GAPs, resulting in the GTPase conversion to the inactive GDP state. The GDP/GTP exchange reactions of Rho/Rac/Cdc42 and Rab subfamily proteins are furthermore regulated by guanine nucleotide–dissociation inhibitors (GDIs). They inhibit GEF-stimulated dissociation of GDP from the GDP-bound form and keep the small G protein in the GDP-bound form, preventing their interaction with regulatory and effector molecules. This inhibitory action of GDIs requires that they be dissociated from their partner GTPases for the GTPases to become activated and elicit their biological effects. GDIs also regulate membrane-to-cytosol cycling of Rho and Rab family GTPases by extracting them from the membrane and sequestering the inactive GTPase in the cytosol (Figure 1.6) (DerMardirossian & Bokoch, 2005; Takai, Sasaki, & Matozaki, 2001; Vetter & Wittinghofer, 2001).

The human genome contains approximately 150 small G proteins (Ras superfamily) that are structurally classified into five families: Ras, Arf, Rho, Rab and Ran families. They are conserved in primary structures and are 30-55% homologous to each other. Like other G proteins, all small G proteins have consensus amino acid sequences responsible for interacting with GEFs and GAPs, including the binding of guanine nucleotide (GDP or GTP) at the phosphate-binding loop (residues 10–17) and two switch loop regions (switch 1, residues 25–40, and switch 2,

residues 57–75). Moreover, Asp57, Thr35 and Gly60 interact with catalytic $Mg^{2+}$ ions, which are essential for GTP hydrolysis and are, therefore, conserved throughout the superfamily of GTPases. Conformational changes in these residues induced by GDP/GTP determines the inactive/active state of the GTPase (Bourne, Sanders, & McCormick, 1991; A. Hall, 1990). In addition, small G proteins belonging to Ras, Rho/Rac/Cdc42 and Rab proteins have sequences at their C-termini that undergo posttranslational modifications with lipid, such as farnesyl, geranylgeranyl, palmitoyl, and methyl moieties, and proteolysis. Arf proteins have an N-terminal Gly residue that is modified with myristic acid. Ran do not have such sequences to direct posttranslational modifications. Moreover, they have a region interacting with downstream effectors, which is specific to each GTPase-effector pair and determines which cellular functions they control. The Ras family regulates gene expression, cell proliferation and survival, the Rho family regulates cytoskeletal reorganization, the Rab and Arf families regulate membrane and vesicle trafficking, and the Ran family regulates nucleocytoplasmic transport. However, there exists cross-talk between small G proteins to regulate various cellular functions in a cooperative manner (Takai et al., 2001). These five GTPase subfamilies are described individually in more detail below.

### 1.7.1. Ras GTPase family

Ras proteins, the first members of the entire superfamily were discovered on the basis of their homology to rat sarcoma (Ras) virus genes. The human genome encodes three Ras isoforms: H-Ras, N-Ras and two forms of K-Ras (K-Ras-4A and -4B), which are generated through alternative splicing of the fourth coding exon. These three members are very closely related, having 85% amino acid sequence identity but have different molecular functions (Downward, 2003).

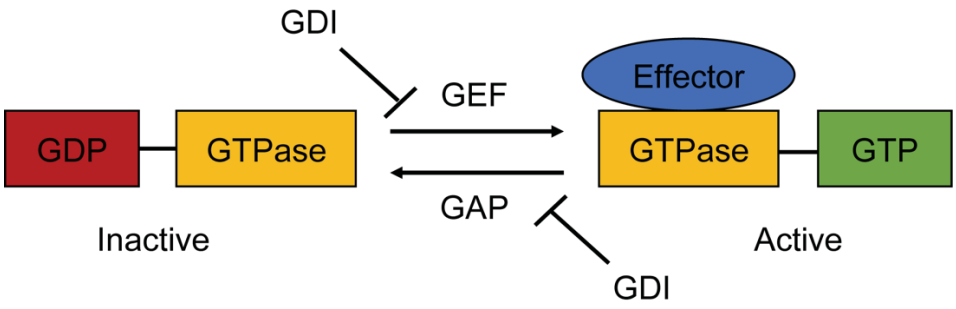


**Figure 1.6. GTPases act as molecular switches to regulate downstream biological responses.** They cycle between GDP-bound inactive states and GTP-bound active states. This regulatory cycle of GTP binding and hydrolysis is controlled overall through the action of three classes of regulatory proteins. Guanine nucleotide exchange factors (GEFs) catalyze the release of bound GDP, resulting in the formation of the GTP-bound active protein. GTPase-activating proteins (GAPs) stimulate the intrinsically low GTP hydrolytic activity of the GTPases, resulting in their conversion to the inactive GDP state. GDP dissociation inhibitors (Rho and Rab GDIs) sequester the inactive GTPase, preventing the dissociation of GDP and interactions with regulatory and effector molecules. Figure and text adapted with permission from Elsevier (DerMardirossian & Bokoch, 2005).

Mutations in codon 12, 13, or 61 of one of the three Ras genes, H-Ras, K-Ras, or N-Ras, convert these genes into active oncogenes. High rates of Ras-activating missense mutations have been detected in non–small cell lung cancer (30%), colon adenomas (50%), thyroid tumors (50%) and pancreatic adenocarcinomas (95%), making it the single most common mutationally activated human oncoprotein (Bos, 1989). In addition to mutational activation, Ras genes are amplified or overexpressed in some tumors. In the case of breast cancer, the incidence of Ras-activating mutations is low, but Ras activity is elevated due in part to increased upstream signaling from the RTKs EGFR and ERBB2 (also called Her2) (Colicelli, 2004).

Two known Ras effector proteins are the Raf-1 family (A-Raf, B-Raf and C-Raf) and PI3K (Rodriguez-Viciana et al., 1994; Vojtek, Hollenberg, & Cooper, 1993). GTP-bound Ras binds with high affinity to the Raf-like Ras-binding domain (Raf-RBD) (Herrmann, Martin, & Wittinghofer, 1995), as well as an adjacent cysteine-rich domain, and leads to activation of the kinase activity of Raf-1 and initiation of the MEK-ERK MAPK cascade (Takai et al., 2001) (described in Chapter 1.5.2). Similarly, GTP-bound Ras binds to at least four different isoforms of the catalytic p110 subunit of PI3K Ras-binding domain (PI3K-RBD), which in turn activates the PI3K/Akt cascade (described in Chapter 1.5.2) (Downward, 1998). PI3K has an important role in mediating the pro-survival and proliferative functions of Ras. As a negative regulator of PI3K, the loss of the PTEN tumor suppressor in cancer cells supports the important contribution of PI3K hyperactivation in cancer development (Figure 1.7) (Repasky, Chenette, & Der, 2004).

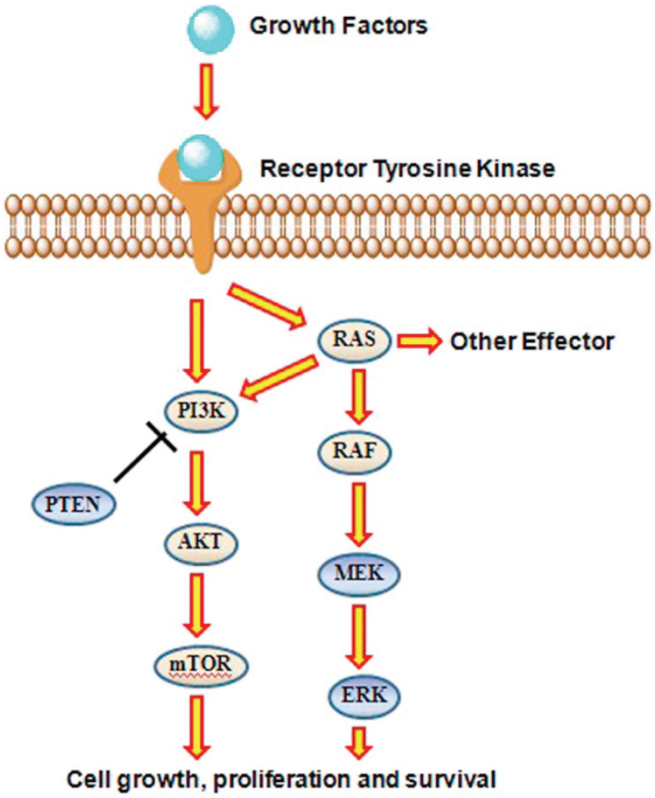


**Figure 1.7. Ras regulation of cell growth, proliferation and survival.** RTK-activated Ras binds and stimulates PI3K and RAF kinases to mediate both the Akt/mTOR and MEK/ERK signaling pathways, respectively. PTEN negatively regulates PI3K. Figure adapted with permission from Elsevier (Asati, Mahapatra, & Bharti, 2016).

Ras's tight interactions with GDP/GTP nucleotides are governed by its GEFs, including SOS. The insertion of an α-helix from SOS into Ras results in the displacement of the switch I region of Ras, opening up the nucleotide-binding site. Side chains of this helix and the resulting distorted conformation of the switch II region of Ras alter the chemical environment of the binding site for the phosphate groups of the nucleotide and the associated magnesium ion, so that their binding is no longer favoured. Overall, the Ras–SOS complex adopts a conformational structure that allows nucleotide release and rebinding for the activation or inactivation of Ras (Boriack-Sjodin, Margarit, Bar-Sagi, & Kuriyan, 1998).

### 1.7.2. Rho GTPase family

Members of the Ras homologous (Rho) family are primarily involved in the organization of cell polarity, shape and motility, via regulation of the actin cytoskeleton. More than twenty members have been identified, with Rho (A, B and C isoforms), Rac (1, 2 and 3 isoforms) and Cdc42 (Cdc42Hs and G25K isoforms) being the best characterized. Rho promotes actin stress fiber formation and focal adhesion assembly; Rac promotes lamellipodium formation, membrane ruffling and regulates the superoxide-producing NADPH oxidase of phagocytes; and Cdc42 promotes actin microspikes and filopodium formation (A. Hall, 1994; Mackay & Hall, 1998).

About 30 effector proteins have been identified that interact with members of the Rho family. For example, downstream of Rho activation are the two Rho effectors, Rho-associated serine-threonine protein kinases ROCK1 and ROCK2, which phosphorylate myosin light chain (MLC) phosphatase and MLC, inducing the formation of actin stress fibers and smooth muscle cell contraction. Other Rho effectors include the Rho-binding proteins Rhophilin, Rhophilin2, and

Rhotekin. Protein kinase N (PKN) was identified as a Rho effector through its homology to Rhophilin. Rho proteins bind to and activate protein kinase N (PKN) proteins, which are serine/threonine kinases that translocate from the cytosol to the plasma membrane upon Rho activation. Ras-related C3 botulinum toxin substrate (Rac) proteins function primarily through the direct activation of the serine/threonine kinases p21-associated protein kinase (PAK) family through their 18-amino acid Cdc42/Rac interactive binding (CRIB) motif. PAKs may mediate the effects on the cytoskeleton induced by Rac/Cdc42 proteins, which are different from their direct effects on actin reorganization. Other Rac/Cdc42 effectors were identified solely on the basis of having a CRIB domain similar to PAK. Furthermore, Cdc42 interacts with effector Wiscott-Aldrich syndrome protein (WASP) to mediate actin polymerization (Bishop & Hall, 2000; Ridley, 2001; Takai et al., 2001).

As previously mentioned in Chapter 1.3.1.4, the Rho GEFs p115RhoGEF, PDZ-RhoGEF, and LARG provide a direct link between $G\alpha_{12/13}$-coupled GPCRs and Rho activation. These GPCRs, such as AT1R, activate $G\alpha_{12}$ and/or $G\alpha_{13}$, which, in turn, will interact directly with Rho-GEFs containing a $G\alpha_{12}/G\alpha_{13}$-binding region, such as the PDZ and LH domains, thereby stimulating the activity of Rho-dependent pathways (Fukuhara et al., 1999). RhoA activation induced by receptor agonists via $G\alpha_{12/13}$ occurs with higher potency than RhoA activation via $G\alpha_{q/11}$. $G\alpha_{q/11}$-mediated RhoA activation occurs independently of phospholipase C-β (PLCβ) and involves LARG and p63 Rho-GEFs (Chikumi, Vazquez-Prado, Servitja, Miyazaki, & Gutkind, 2002; Lutz et al., 2007; Rojas et al., 2007; Vogt, Grosse, Schultz, & Offermanns, 2003). Whereas, Rac is activated by $G\alpha_{q/11}$-dependent activation of PLCβ (Harden, Waldo, Hicks, & Sondek,

2011). AT1R can also activate Rac1 through its interaction with Arf6, which forms a complex that regulates membrane ruffling (Cotton et al., 2007). Cdc42 is activated by $G\alpha_i$-dependent activation of PI3K, notably activated by lysophosphatidic acid (LPA) agonist acting through the LPA1 receptor (Kedziora et al., 2016). Moreover, growth factors, such as PDGF, insulin and EGF, activate PLCγ, Src kinase and PI3K, which activate Rac/Cdc42 to induce the formation of actin polymerization and membrane ruffling (Dise, Frey, Whitehead, & Polk, 2008; Mackay & Hall, 1998; Ridley, 2001).

### 1.7.3. Arf GTPase family

Although ADP-ribosylation factor (Arf) proteins were originally identified and named for their ability to act as cofactors during cholera toxin-catalyzed ADP-ribosylation of $G\alpha_s$, they are now better known to regulate the vesicular trafficking of intracellular proteins and membranes, as well as the remodeling of the actin cytoskeleton. Based on amino-acid sequence homology, the six mammalian Arf proteins can be categorized into three classes. Class I Arf proteins (Arf1, Arf2 and Arf3) share more than 96% similarity, regulate the assembly of different types of coat complexes during vesicle budding at the Golgi, and activate lipid-modifying enzymes. The functions of the class II Arf proteins (Arf4 and Arf5) in regulating early Golgi transport and in recruiting coat components to trans-Golgi network (TGN) membranes still remain unclear. Arf6, which is the sole member of class III, regulates endosomal membrane trafficking and the structural organization of the plasma membrane. Arfs 1-5 reversibly associate with the Golgi complex and cycle into the cytosol during GTP-binding and GTP-hydrolysis, respectively. Arf6, on the other hand, appears

to spend more time associated with membranes while GDP-bound (D'Souza-Schorey & Chavrier, 2006; Donaldson & Jackson, 2011).

The best studied Arf protein, Arf1, recruits the coat protein complex I (COPI) to budding transport vesicles for transport of proteins and lipids from the Golgi to the endoplasmic reticulum (ER) and between Golgi cisternae. Arf1-GTP also regulates the recruitment of clathrin to late Golgi and endosome compartments through the recruitment of the heterotetrameric adaptor-protein (AP-1, AP-3 and AP-4) complexes, as well as monomeric Golgi-localized gamma-ear-containing ARF-binding (GGA) effector proteins (D'Souza-Schorey & Chavrier, 2006; Donaldson & Jackson, 2000).

Similar to Arf1, Arf6-GTP recruits adaptor proteins and GGA3 for vesicular transport, but exclusively in the endosomal-plasma membrane system. Arf6 regulates endocytosis by interacting with β-arrestin, AP-2 and clathrin in CCV complex formation for vesicular invagination at the cell surface and endosomal recycling back to the plasma membrane (Poupart et al., 2007). Through its metabolic effects on phosphatidylinositol-4-phosphate 5-kinase (PIP5K) and phospholipase D (PLD), and the production of phosphatidylinositol 4,5-bisphosphate (PIP2), Arf6 can also modulate the actin cytoskeleton, change cell membrane morphology and facilitate clathrin-dependent and clathrin-independent internalization of ligands and receptors (D'Souza-Schorey & Chavrier, 2006; Donaldson & Jackson, 2000; Houndolo, Boulay, & Claing, 2005). $G\alpha_q$-coupled GPCRs, such as AT1R, activate Arf6 through a mechanism independent of PLCβ and PKC activation, where $G\alpha_q$ forms molecular complexes directly with ARNO and Arf6 proteins (Giguere et al., 2006). Furthermore, the enhanced expression of Arf1 and Arf6 seen in triple

negative breast cancer cell lines provides a role for these small G proteins in cancer cell invasion (Schlienger, Campbell, Pasquin, Gaboury, & Claing, 2016).

The active and inactive states of Arfs differ mainly by the conformation of switch I and switch II, which constitute a major site of interaction with GEFs. The Arf GEFs of the Gea/GBF and Sec7/BIG subfamilies function in the ER-Golgi system, whereas the ARNO/cytohesin/GRP and EFA6 subfamilies function primarily in the endosomal-PM system (Donaldson & Jackson, 2000; Takai et al., 2001). ARNO exchange activity on Arfs 1 and 6 is localized to the catalytic Sec7 domain and mediated through its PH domain specifically interacting with inositol phospholipids at the PM (Chardin et al., 1996; Frank, Upender, Hansen, & Casanova, 1998; Santy, Frank, Hatfield, & Casanova, 1999). The Sec7 domain of ARNO contains an elongated α-helical protein with a conserved hydrophobic groove that engages the switch regions of Arfs. A shift in the position of switch I opens the GTPase active site and allows the binding of a critical glutamate residue (at position 97) from the Sec7 domain into the Arf. The resulting steric and electrostatic repulsion of the β-phosphate and magnesium ion on Arf1/6 promotes nucleotide dissociation (Goldberg, 1998; Mossessova, Gulbis, & Goldberg, 1998).

### 1.7.4. Rab GTPase family

There are more than 60 members of the Ras-like proteins in brain (Rab) family that regulate intracellular vesicular transport and the trafficking of proteins between different organelles of the endocytic and secretory pathways. Rab proteins facilitate vesicle formation and budding from the donor compartment, transport to the acceptor compartment, and vesicle fusion and release of the vesicle content into the acceptor compartment through the coordinated recruitment of 20 different

effector proteins, such as sorting adaptors, tethering factors, kinases, and phosphatases (Zerial & McBride, 2001).

Rab proteins localize to specific intracellular compartments consistent with their function in distinct vesicular transport processes. This localization is dependent on prenylation and specificity is dictated by divergent C-terminal sequences. To list a few, Rab1, Rab2, and Rab6 are localized at the endoplasmic reticulum and the Golgi apparatus to regulate ER-to-Golgi transport along the biosynthetic/secretory pathway; Rab3 is localized on secretory granules including synaptic vesicles and is involved in calcium-dependent exocytosis; Rab4 is present on early endosomes to mediate endocytic recycling directly from the early endosomes to the plasma membrane; Rab5 is localized to early endosomes and the plasma membrane to mediate endocytosis and endosome fusion of clathrin-coated vesicles (CCVs) from the plasma membrane to early endosomes; Rab7 and Rab9 are present on late endosomes to mediate trafficking to lysosomes and the TGN, respectively; Rab11 is localized to recycling endosomes to mediate endocytic trafficking from the recycling endosome and to the plasma membrane (Stenmark, 2009; Zerial & McBride, 2001).

Phagocytosis also requires the coordinated actions of several endocytic Rab GTPases, in particular Rab5, which is known to associate with early phagosomes, and Rab7, which associates after phagosome maturation and is a prerequisite for their eventual fusion with lysosomes to yield degradative phagolysosomes (Stenmark, 2009).

### 1.7.5. Ran GTPase

There is only one Ras-like nuclear protein (Ran) and it was originally cloned on the basis of its homology to Ras proteins. It is now clear that Ran regulates the cycle of nuclear import and export. Unlike the other four small GTPase families, Ran function is dependent on a spatial gradient of the GTP-bound form of Ran. It is regulated by Ran-specific nuclear GEF and cytoplasmic GAP activities. This results in a high concentration of Ran-GTP in the nucleus, which facilitates the directionality of nuclear import and export, and a high concentration of Ran-GDP outside the nucleus. Nuclear Ran-GTP interacts with importin to promote cargo release, and with exportin-complexed cargo to facilitate nuclear import and export of cargo, respectively. Importins bind their substrates in the absence of Ran in the cytoplasm and release them upon Ran-GTP binding in the nucleus. The cargo-free importin-Ran-GTP complex then rapidly recycles back to the cytoplasm. In contrast, exportins can bind to their cargo only in the presence of Ran-GTP and thus associate with their substrates exclusively in the nucleus. Upon export to the cytoplasm, the trimeric exportin/Ran-GTP/cargo complex is disassembled by Ran-GTP hydrolysis induced by Ran-GAP and RanBP1/2. By a similar mechanism, during cell division Ran GDP/GTP cycling also regulates mitotic spindle assembly, DNA replication and nuclear envelope assembly. Importin β was identified as a potential downstream effector of Ran in nuclear envelope formation, but its role in this pathway appears to be distinct from its function in spindle assembly (H. Y. Li, Cao, & Zheng, 2003; Takai et al., 2001; Weis, 2003).

## 1.8. Bioluminescence Resonance Energy Transfer (BRET)

Bioluminescence resonance energy transfer (BRET) is a process in which a non-radiative transfer of energy occurs between an excited bioluminescent enzyme/substrate donor, such as *Renilla reniformis* luciferase (Rluc), and a fluorescent molecular acceptor, like green fluorescent proteins (GFPs) (Pfleger & Eidne, 2006). Energy transfer depends on (1) the overlap between the emission spectra of the donor and excitation spectra of the acceptor, (2) the relative orientation of donor and acceptor, and (3) their relative distance; resonance energy transfer (RET) occurs when the donor and the acceptor are separated by less than 100 Å (Devost et al., 2016). Cleavage of a luminescent substrate, such as coelenterazine, by Rluc excites the GFP which in turn emits fluorescence. RET techniques such as fluorescence resonance energy transfer (FRET) and BRET have become experimental techniques of choice for measuring constitutive and dynamic protein–protein interactions and interrogating changes in the activity of many biochemical signaling pathways. Although FRET has the advantage of allowing cellular localization of the biological interaction that is studied, this method is semi-quantitative. On the other hand, BRET has advantage over FRET since it does not require an external illumination to initiate the energy transfer, which may lead to high background noise resulting from direct excitation of the acceptor or photobleaching. BRET experiments much like FRET can be conducted under conditions that more closely reflect the biochemical environments occurring in living organisms (Salahpour et al., 2012). As such, several studies have applied BRET for the study of protein–protein interactions (Angers et al., 2000; Hamdan, Percherancier, Breton, & Bouvier, 2006; Hamdan et al., 2007), receptor signalling pathways (Gales et al., 2005; Namkung et al., 2018; Namkung, Radresa, et al., 2016), receptor trafficking (Namkung, Le Gouill, et al., 2016), as well as the dynamics of cellular

processes or interaction of two proteins following a pharmacological treatment (Salahpour et al., 2012).

More recently, the natural combination of luciferase and GFP from the same *Renilla reniformis* species (Rluc and rGFP), which self-associate with moderate affinity and optimally transfer energy (Anderson & Cormier, 1973; Molinari, Casella, & Costa, 2008; Titushin, Feng, Lee, Vysotski, & Liu, 2011), has been used as enhanced bystander BRET (ebBRET) pair to improve the recording of signals between proteins interacting in the same or different compartments of the cell. EbBRET relies on the stochastic interaction of the donor and the acceptor in one cell compartment and changes in BRET signal comes from the relocalization of the donor- or acceptor-tagged proteins rather than the direct protein-protein interaction. For example, ebBRET has been used to monitor GPCR trafficking from PM to endosomes. BRET sensors were developed by anchoring rGFP in endosomes to generate BRET signals on ligand-promoted sequestration of RLuc-tagged proteins located at the PM, reflected by an accumulation of proteins in endosomes (Namkung, Le Gouill, et al., 2016).

# CHAPTER 2: RATIONALE AND OBJECTIVES

## 2.1. Rationale

The overall aim of this thesis is to advance the understanding of the molecular and cellular mechanisms regulating G protein-coupled receptor internalization and signaling, in particular, how receptor trafficking regulates the signaling scaffolding role of β-arrestins. It is well-established that β-arrestins function as endocytic proteins to "arrest" downstream G protein signaling, such as ERK1/2 activation, and promote GPCR desensitization and internalization. Spatiotemporal differences between β-arrestin- and G protein-mediated ERK1/2 activation by AT1R have been identified, whereas, the role of β-arrestins in activating specific pools of ERK1/2 at the plasma membrane and in endosomes after receptor endocytosis has not been fully elucidated due to the dearth of selective tools. Therefore, we previously characterized a small molecule that we named Barbadin as a selective β-arrestin/AP-2 inhibitor that blocks vasopressin V2 receptor internalization and signaling but does not affect its desensitization (Beautrait et al., 2017). However, its role on AT1R and other GPCRs is not known and despite the fact that Barbadin can potentially be used to study the early stages of internalization and signaling at the PM, it still would not address how and whether receptor/β-arrestin complexes regulate MAPK signaling in endosomes.

With the goal of discovering new pharmacological tools to study the mechanisms regulating the internalization and spatiotemporal signaling of GPCRs, a phenotypic high-throughput screen (HTS) was performed in a heterologous system such as HEK293 cells to identify modulators of GPCR trafficking (Figure 2.1A). The prototypical $G\alpha_q$-coupled (class B) GPCR, AT1R, which signals to MAPK and internalizes in a β-arrestin-dependent manner (Ahn et al., 2004; Luttrell et al., 2001; P. McDonald et al., 2000; Tohgo et al., 2003) was used for the primary

screening of commercially available libraries of ~115,000 compounds. The BRET trafficking sensors described in (Namkung, Le Gouill, et al., 2016) were used to quantitatively monitor the translocation of the *Renilla* luciferase-tagged AT1R (AT1R-RlucII) from the PM into endosomes that have the endofin-FYVE domain tagged with *Renilla* GFP (rGFP-FYVE). Since the assay is based on fluorescence measurement, ~6,610 compounds that quenched more than 50% the fluorescence of RlucII and/or rGFP were excluded. Following the primary screen, only compounds blocking more than 40% of receptor internalization or potentiating more than 100% (normalized to vehicle) were considered hits. These 943 compounds were then validated a second time on AT1R and on another class B GPCR, the bradykinin B2 receptor (B2R), where 40 active hits on AT1R (20 inhibitors and 20 potentiators) were similarly active on B2R. Using confocal microscopy, the 40 compounds were tested for their toxicity by looking at morphological changes, such as rounding up of cells following treatment with 50 μM of the compounds, which is an indication of cell death. One inhibitor, compound #21, was selected as a lead molecule based on its apparent lower cell toxicity, solubility properties, chemistry and availability of analogues (Figure 2.1B). The HTS results showed that Comp#21 inhibited by 54% (primary screen) and 60% (secondary screen) AT1R internalization and 67% B2R internalization. To validate Comp#21's effects on AT1R and B2R internalization, cellular imaging was used to follow the trafficking of these receptors into endosomes. HEK293 cells were transfected with YFP-tagged AT1R or B2R and pretreated with vehicle or Comp#21 (Figure 2.1C). In the absence of ligand (control conditions; top panels), AT1R and B2R were restricted to the plasma membrane for both vehicle and Comp#21 treated cells. After 15 min of AngII or BK, in vehicle conditions, AT1R and B2R trafficked from the plasma membrane into endosomes; whereas Comp#21 kept the YFP-tagged

AT1R and B2R at the plasma membrane after receptor stimulation, as fewer endosomes are seen. This new endocytic inhibitor could be a used as a tool compound to further study the mechanisms regulating receptor internalization and its related signaling pathways.

## 2.2. Objectives

The objectives of the work presented in this thesis are:

1. Develop new BRET-based sensors to study the activity of small G proteins and kinases
2. Characterize the mechanism of action of Comp#21 (Rasarfin)
3. Identify functionally selective analogs of Rasarfin

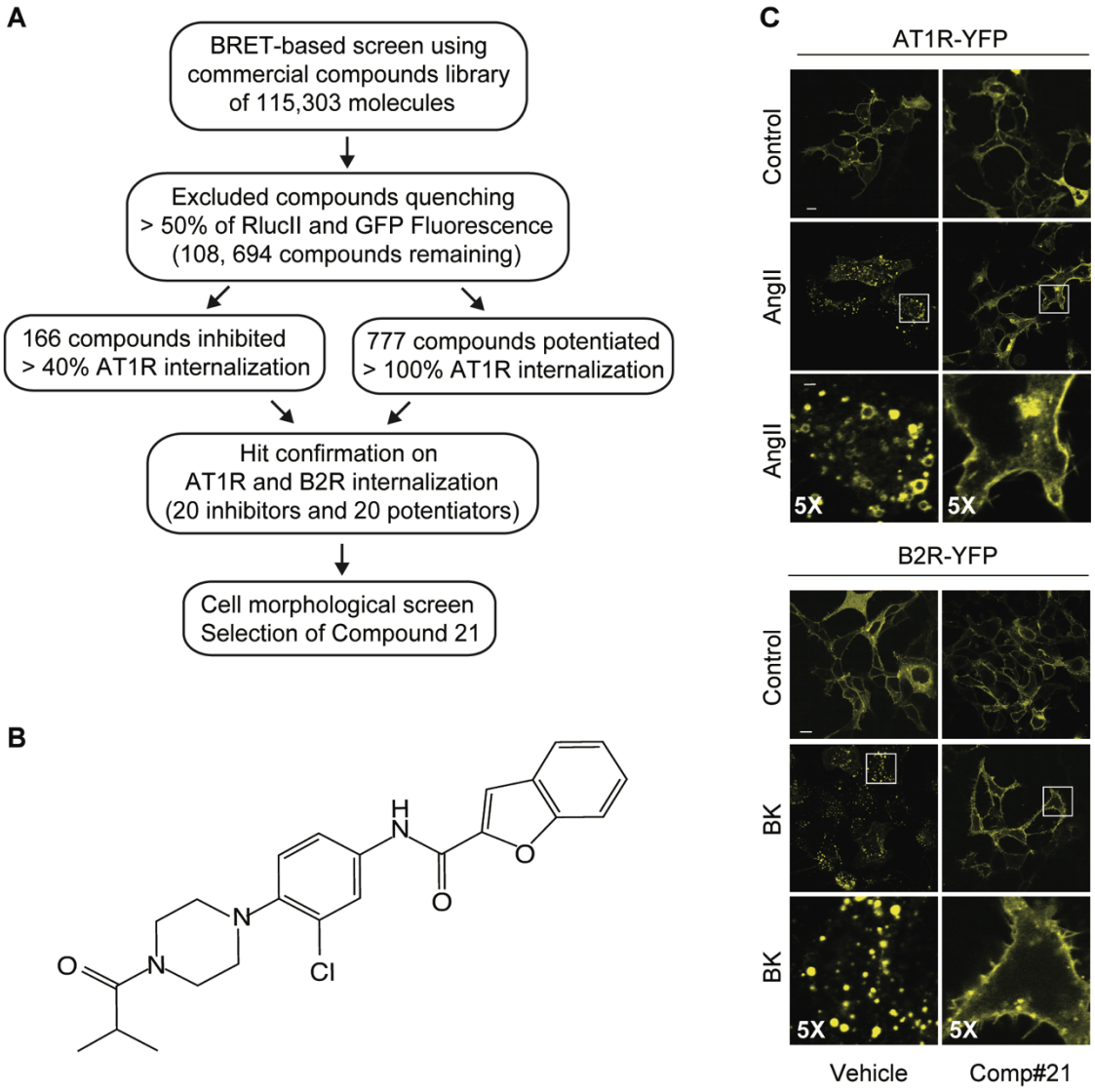


**Figure 2.1. High-throughput screening identifies Comp#21 as an inhibitor of AT1R and B2R internalization. (A)** Schematic of the screening of compounds and filters used for the selection of hits to the lead compound. **(B)** Structure of the selected compound (Comp#21). **(C)** Confocal microscopy images of YFP-tagged ATIR and B2R internalization. Transfected HEK293 cells were serum starved, pretreated with vehicle (DMSO) or Comp#21 (50 µM) for 30 min and stimulated or not with 100 nM Angiotensin II (AngII) or Bradykinin (BK) for 15 min. Scale bar, 10 µm.

# CHAPTER 3. MATERIALS AND METHODS

3.1. Compounds acquisition

Rasarfin (CID: 1396167; Catalogue #001-728-363), **21.1** (CID: 2236635; Catalogue #001-615-578), **21.2** (CID: 2238454; Catalogue #001-009-312), **21.3** (CID: 2968266; Catalogue #001-728-365), **21.4** (CID: 1087127; Catalogue #001-728-361), **21.5** (CID: 1088362; Catalogue #001-629-834), **21.6** (CID: 1088375; Catalogue #001-629-837), **21.7** (CID: 2997077; Catalogue #002-020-863) and **21.8** (CID: 2944643; Catalogue #001-728-355) were purchased from MolPort and solubilized in 100% DMSO at a final stock concentration of 50 mM.

3.2. Chemicals and reagents

Human AngiotensinII (AngII), Bradykinin (BK), Isoproterenol (ISO), epidermal growth factor (EGF), PD184352, Wortmannin, poly-L-lysine hydrobromide and poly-L-ornithine hydrochloride were purchased from Sigma Aldrich. UBO-QIC from Cedarlane. Dulbecco's modified Eagles medium (DMEM), fetal bovine serum (FBS), Phosphate Buffered Saline (PBS) and gentamicin were purchased from Gibco, Life Technologies. Coelenterazine 400a (DeepBlue C) and Coelenterazine H were purchased from Nanolight Technology. Dimethyl sulfoxide (DMSO), Phenylmethyl-sulfonyl fluoride (PMSF), leupeptin, aprotinin, pepstatin A, NaF and EDTA were from BioShop. Glutathione Sepharose™ 4B was from GE healthcare. Linear polyethylenimine 25-kDa (PEI) was from Polysciences. The phospho-p44/42 MAPK (ERK1/2) (Thr202/Tyr204) (E10) (#9106), p44/42 MAPK (ERK1/2) (#9102), phospho-Akt (Thr308) (#9275), Akt (pan) (C67E7) (#4691), Ras (#3965) and RhoA (#2117) antibodies were purchased from Cell Signaling Technology. The anti-HA-Peroxidase (3F10) (#12013819001), anti-FLAG (#F7425) and anti-c-Myc (clone 9E10) (#M4439) antibodies were purchased from Sigma Aldrich.

Anti-mouse and anti-rabbit IgG HRP from BioRad. The β-actin (C4) antibody (#sc-47778) was from Santa Cruz Biotechnology. SOS1 Protein (ExD Exchange Domain, aa564-1049, 6xHis tag) (#CS-GE02) and Mant-GTP exchange buffer (2X) (#EB01 from BK100 kit) were purchased from Cytoskeleton Inc.

3.3. Plasmids and constructs

Plasmids encoding β-arrestin1-RlucII, AT1R-YFP (Zimmerman et al., 2012), signal peptide-Flag tagged human AT1R (sp-Flag-AT1R) (Goupil et al., 2015), β-arrestin2-YFP, HA-B2R, B2R-YFP (Simaan et al., 2005), AT1R-RlucII, B2R-RlucII, β2AR-RlucII, HA-β2AR, rGFP-CAAX, rGFP-FYVE (Namkung, Le Gouill, et al., 2016), β-arrestin2-RlucII, $G\alpha_{i3}$-RlucII (Quoyer et al., 2013), Polycistronic $G\alpha_q$ sensor, Flag-$G\beta_1$ (Namkung, Radresa, et al., 2016), GFP10-$G\gamma_1$ (Urizar et al., 2005), PKC and Rho sensors (Namkung et al., 2018), β-arrestin/AP-2 sensor (Hamdan et al., 2007) and GST-Rhotekin-RBD (Ren & Schwartz, 2000) were previously described. FLAG-K-Ras-WT, FLAG-K-Ras-G12V, FLAG-SOS1$^{cat}$-CAAX were kindly provided by Dr. Matthew Smith (Université de Montréal, Qc). GST-Raf1-RBD, GST-GGA3-PBD, HA-ARF6-WT and HA-ARF6-T27N were kindly provided by Dr. Audrey Claing (Université de Montréal, Qc). Myc-Rac1-WT, Myc-Rac1-Q61L, Myc-Rac1-T17N were kindly provided by Dr. Serge Lemay (McGill University, Qc).

To generate RlucII-tagged GGA3 (1-316) domain, the GGA3 (1-316) cDNA was amplified by PCR primers using GST-GGA3(1-316) DNA as a template. The PCR product was subcloned into the NheI/HindIII sites of RlucII containing vector (βarr2-RlucII, (Paradis et al., 2015)) using Gibson assembly (New England Biolabs). Partial cDNAs of Raf and PAK were obtained by RT-

PCR of HEK293 total RNA. For subcloning of the Ras-binding domain (RBD) of Raf, the RasBD was PCR amplified using the partial cDNA of Raf as a template and assembled into the NheI/HindIII sites of RlucII containing vector (βarr2-RlucII, (Paradis et al., 2015)) using Gibson assembly. The CRIB domain of PAK1 was PCR amplified using the partial cDNA of PAK1 as a template and subcloned into the KpnI/AgeI sites of RlucII containing vector (PKN-RBD-RlucII, (Namkung et al., 2018)) using Gibson assembly.

To generate the fluorescently tagged GTPase effectors GGA3(1-316)-PBD-YFP, Raf-RBD-YFP and PAK-CRIB-YFP used for microscopy experiments, the DNA from the RlucII versions above were digested with NheI and HindIII and subcloned into the pEYFP-N1 vector (Invitrogen) by using NheI and HindIII sites and Gibson assembly. For the Akt sensor, the PH domain of Akt was PCR amplified from HEK293SL cell's cDNA as a template. The PCR product was reamplified with flanking sequences for the Gibson assembly. The final PCR product was assembled into NheI/HindIII sites of RlucII containing vector (βarr2-RlucII, (Paradis et al., 2015)).

To generate pGEX-6P-1-H-Ras, the cDNA of H-Ras (full length) was obtained by RT-PCR of HEK293SL cells total RNA. PCR product was then re-amplified with flanking sequences for the Gibson assembly. The final PCR product was subcloned into the pGEX-6P-1 vector, kindly provided by Dr. Matthew Smith (Université de Montréal, Qc), into the BamHI and NotI sites using Gibson assembly.

The S17N, Y32A and Y40A substitutions in FLAG-K-Ras was generated by complementation PCR reaction, whereas the Y32A/Y40A substitution was generated by overlapping PCR amplification using the two PCR products for Y32A and Y40A as templates. All the final PCR products from the amplified complementing fragments were subcloned into

XhoI/HindIII sites of FLAG-K-Ras vector using Gibson assembly. For generating the pGEX-6P-1-FLAG-K-Ras-WT and pGEX-6P-1-FLAG-K-Ras-Y32A, K-Ras-WT and K-Ras-Y32A DNA were PCR amplified and assembled into the BamHI/NotI sites of pGEX-6P-1 vector using Gibson assembly. All constructs were verified by DNA sequencing before use (McGill Genome Center).

3.4. Cell culture

HEK293SL cells, characterized in (Namkung, Le Gouill, et al., 2016), are a subclone derived from regular HEK293 cells (Ad5 transformed) selected in our lab and have been used in all experiments. These cells have a cobblestone appearance and show better adherence as compared with regular HEK293 and HEK293T cells, making them more amenable to microscopy and BRET experiments. These cells were regularly tested for mycoplasma contamination (PCR Mycoplasma Detection kit, abm, BC, Canada) and cultured in DMEM supplemented with 10% FBS and 20 μg/ml of gentamycin. Cells were transiently transfected using calcium phosphate methods (Kwon & Firestein, 2013) or 25-kDa linear PEI (2:1 PEI/DNA ratio) (Baker et al., 1997).

3.5. Live cell imaging/confocal microscopy

One day before transfection, cells were seeded in 35-mm glass-bottom dishes (MatTek Corporation) at a density of $1x10^5$ cells per dish. For the recordings of receptor internalization, HEK293 SL cells were transfected with 2 μg of AT1R-YFP. For the recordings of β-arrestin-2 recruitment to the receptor, HEK293SL cells were transfected with 50 ng of β-arrestin2-YFP and 250 ng of Flag-AT1R or HA-B2R. Forty-eight hours post-transfection, cells were serum starved, preincubated with DMSO (0.1% final concentration) or Rasarfin (50 μM) for 30 min at 37 °C.

AT1R-expressing cells were stimulated with angiotensinII (AngII; 100 nM) and B2R-expressing cells were stimulated with bradykinin (BK; 1 uM) for 30 min (receptor-YFP) or 15 min (β-arrestin2-YFP). Cells were imaged with Zeiss LSM-510 laser scanning confocal microscope. To detect YFP, UV laser was used with 405 nm excitation and BP 505-550 nm emission filter. Images (2048 x 2048) were collected using a 63x oil immersion lens. For the recordings of GTPase effector proteins to PM, HEK293SL cells were transfected with 1μg of Flag-AT1R and 600 ng of either GGA3(1-316)-PBD-YFP (and 300ng HA-Arf6), Raf1-RBD-YFP or PAK-CRIB-YFP. Forty-eight hours post-transfection, cells were serum starved and stimulated with 1 uM AngII for 10 min, 2 min or 5 min, respectively, at 37 °C. Cells were imaged (1048 x 1048 pixels) using a Zeiss LSM-780 laser scanning confocal microscope with a 63x oil immersion lens (RI-MUHC Molecular Imaging Facility). To detect YFP, an Argon laser was used with 514 nm excitation and BP 530-600 nm emission filter sets.

3.6. BRET measurements

HEK293SL cells were seeded at a density of 7.5 x $10^5$ cells per 100-mm dish and 24 hours later, transiently transfected as such. For receptor internalization experiments, cells were transfected with 0.12 μg AT1R-RlucII, B2R-RlucII or β2AR-RlucII and 0.48 μg of either rGFP-CAAX or rGFP-FYVE. For β-arrestin recruitment assays, cells were transfected with 0.48 μg of receptor-YFP along with 0.12 μg of β-arrestin-RlucII. For β-arrestin/AP-2 binding experiments, cells were transfected with 1 μg Flag-AT1R, 1 μg β2-Adaptin-YFP and 0.12 μg β-arrestin2-RlucII. For G protein activation, cells were transfected with 3 μg of sp-Flag-AT1R along with either 4.5 μg of the $G\alpha_q$-polycistronic BRET sensor or 0.24 μg of the $G\alpha_{i3}$-RlucII and 0.6 μg of GFP10-

$G\gamma_2$ and $G\beta_1$ sensors or 0.12 μg PKN-RBD-RlucII and 0.48 μg of rGFP-CAAX. For PKC activation, cells were transfected with 3 μg of sp-Flag-AT1R and 0.18 μg of the PKC sensor. For GTPase activation experiments, cells were transfected with 1 μg Flag-AT1R, 0.48 μg of rGFP-CAAX and either 0.12 μg of GGA3-PBD-RlucII, PAK-CRIB-RlucII or Raf-RBD-RlucII. For biosensor validation experiments, cells were additionally transfected with 500 ng FLAG-K-Ras-WT, Flag-KRas-G12V, Flag-KRas-SOS-CAAX, HA-Arf6-WT, HA-Arf6-T27N, Myc-Rac1-WT, Myc-Rac1-Q61L or Myc-Rac1-T17N. For PI3K/Akt activation experiments, cells were transfected with 0.48 μg of rGFP-CAAX and 0.12 μg of Akt(PH)-RlucII. After 18 h of transfection, the media was replaced and cells were divided for subsequent experiments. Cells were detached and seeded onto poly-L-ornithine-coated 96-well flat white bottom plates (BrandTech Scientific) at a density of $2.5x10^4$ cells per well in media. The next day, cells were washed once with Tyrode's buffer (140 mM NaCl, 2.7 mM KCl, 1 mM $CaCl_2$, 12 mM $NaHCO_3$, 5.6 mM D-glucose, 0.5 mM $MgCl_2$, 0.37 mM $NaH_2PO_4$, 25 mM HEPES, pH 7.4) and left in Tyrode's buffer. For kinetics of β-arrestin binding to receptor and AP-2 experiments, cells were serum starved, pretreated with compounds for 30 min and BRET signals were monitored at indicated times using a Victor X Light plate reader (PerkinElmer). Coelenterazine H (final concentrations of 5 μM) was added 3-5 min prior to BRET measurements. Filter set was 460/80 nm and 535/30 nm for detecting the RlucII *Renilla* luciferase (donor) and YFP (acceptor) light emissions, respectively. The BRET ratio was determined by calculating the ratio of the light emitted by YFP over the light emitted by the RlucII. For G protein activation, cells were serum starved, pretreated with compounds for 30 min, stimulated with AngII for 2 min ($G\alpha_q$, $G\alpha_{i3}$ and Rho sensors) or 5 min (PKC sensor). For the kinetics of GTPase and PI3K/Akt activation, cells were serum starved, pretreated with compounds

for 30 min, stimulated with ligand at indicated times. For concentration-response curves, cells were serum-starved, pretreated with various concentrations of compounds and stimulated with ligand in Tyrode's buffer for 30 min for receptor internalization, 10 min for Arf6, 2 min for Rac and Rho activation and 5 min for Ras activation and PI3K/Akt activation. BRET signals were monitored using a Synergy2 (BioTek) microplate reader and coelenterazine 400a (final concentrations of 5 µM) added 3-5 min prior to BRET measurements. Filter set was 410/80 nm and 515/30 nm for detecting the RlucII *Renilla* luciferase (donor) and rGFP (acceptor) light emissions, respectively. The BRET ratio was determined by calculating the ratio of the light emitted by rGFP over the light emitted by the RlucII.

3.7. Western blot analysis

HEK293SL cells ($10^5$ cells per well) were seeded in a poly-L-lysine-coated 6-well plate and transiently transfected with 3 µg Flag-AT1R, HA-B2R or HA-β2AR and/or 500 ng Flag-MEK1-WT, Flag-MEK1-DD, Flag-BRAF-WT, Flag-BRAF-V600E, Flag-K-Ras-WT, Flag-K-Ras-G12V, HA-Arf6-WT or HA-Arf6-T27N. Forty-eight hours post transfection, in a 37 °C water bath, cells were serum-starved for 30 min, pretreated with DMSO or Rasarfin (at indicated concentrations) for 30 min, then stimulated or not with the indicated ligand [Angiotensin II (1 µM), Bradykinin (1 µM), Isoproterenol (10 µM) or epidermal growth factor (EGF, 100 ng/ml)] at indicated times. Cells were put on ice, washed with PBS and solubilized in 2x laemmli buffer (250 mM Tris–HCl pH 6.8, 2% SDS (w/v), 10% glycerol (v/v), 0.01% bromophenol blue (w/v) and 5% b-mercaptoethanol (v/v)) by heating at 65 °C for 15 min. Lysates were resolved on 10% or 14% SDS-PAGE, transferred to nitrocellulose membranes and immunoblotted for p-ERK1/2, ERK1/2,

p-Akt, Akt, HA or FLAG. ImageLab 5.2 software was used to quantify the digital blots as fold of the phosphorylated protein over total protein, which were then normalized as indicated in the figure legends.

3.8. Purification of recombinant proteins

GST, GST-tagged Golgi Associated, Gamma Adaptin Ear Containing, ARF Binding Protein 3 Binding Domain (GST-GGA3-PBD), Raf1-Ras Binding Domain (GST-Raf1-RBD) and Rhotekin-Rho Binding Domain (GST-Rhotekin-RBD), as well as Ras proteins (pGEX-6P-1-H-Ras, pGEX-6P-1-K-Ras-WT and pGEX-6P-1-K-Ras-Y32A) were expressed in E. coli BL21 cells grown in LB medium and induced with isopropyl β-D-1-thiogalactopyranoside (IPTG) under the respective conditions: 1mM for 1 hour at 37 °C (GST and GST-Raf1-BD), 0.6 mM for 3-4 hours at 30 °C (GST-Rhotekin-RBD and GST-GGA3-PBD) or 0.12 mM for 16 hours at 15 °C (pGEX-6P-1-H-Ras, pGEX-6P-1-K-Ras-WT and pGEX-6P-1-K-Ras-Y32A). The GST fusion proteins were purified using Glutathione Sepharose 4B as previously described by (Vikis & Guan, 2004).

3.9. Glutathione S-transferase (GST) pull-down assays

Activation of Arf1, Arf6, Ras, and Rho were assessed by using GST pull-down assays. HEK293SL cells were transiently transfected with 3µg AT1R-flag only (Ras and Rho) or along with 500 ng HA-Arf6 (Arf6) or HA-Arf1 (Arf1). Forty-eight hours later, the cells were serum-starved for 4 hours with DMEM containing 20 mM HEPES then pretreated with DMSO or Rasarfin (50 µM) for 30 min. Cells were then stimulated with 1 µM AngII or 100 ng/ml EGF (Ras) for 0 and 5 min. Cells were then washed once with ice-cold PBS and lysed for 30 min at 4 °C in

300 µL of lysis buffer (pH 7.5, 50 mM Tris-HCl, 140 mM NaCl, 5 mM $MgCl_2$, 10% glycerol, 1% Nonidet P-40, 1 mM dithiothreitol) supplemented with protease inhibitors (1 mM phenylmethyl-sulfonyl fluoride (PMSF), 10 µg/ml leupeptin, 5 µg/ml aprotinin, 1 µg/ml pepstatin A) and phosphatase inhibitors (20 mM NaF, 0.025 mM sodium pervanadate). The samples were cleared by centrifugation and 30 µL (cell lysates) was kept for assesing total protein contents. The remaining was transferred to fresh tubes with 20 µg of either GST, GST-GGA3-PBD, GST-Raf1-RBD or GST-Rhotekin-RBD coupled to glutathione resin and rotated for 1-2 h at 4 °C. Beads were washed twice with lysis buffer and proteins were eluted in 25 µl 2x laemmli buffer by heating at 65 °C for 15 min. Proteins were resolved on 14% SDS-PAGE, transferred to nitrocellulose membranes and immunoblotted for HA, Ras or RhoA. ImageLab 5.2 software was used to quantify the digital blots as fold of the amount of pulled down protein over total protein.

3.10. Mant GTP Exchange Factor (GEF) assay

Ras activity was assessed in a 384-well black bottom plate using the mant-GTP exchange factor assay that measures the uptake of the fluorescent nucleotide analog N-methylanthraniloyl-GTP (mant-GTP) into GTPases. For Ras activation, 2X exchange buffer, 1.66 µg of purified pGEX-6P-1-H-Ras or pGEX-6P-1-K-Ras-WT or pGEX-6P-1-K-Ras-Y32A were added per well in presence of DMSO, different concentrations of Rasarfin (as indicated) or 50 µM of Compounds 4, 7 or 8. Using the Infinite 200 Pro plate reader (Tecan) with filters set at 360 nm and 440 nm for detecting the excitation and emissions, respectively, and temperature set at 20 °C, 5 readings were recorded every 5 sec before the addition of either $H_2O$, 40 mM EDTA or 0.66 µg purified SOS1. The fluoresence of mant-GTP uptake was measured every 30 sec for 30 min and quantified as the

delta relative florescence units (RFU), which was calculated as the RFU post-addition minus the 5 averaged RFU pre-addition, per condition.

### 3.11. Computational studies

For the flexible docking of compounds into the SOS-Ras X-ray structure (PDB 1BKD), the SOS1 (chain S) and water molecules were first deleted. The Ras-structure (chain R) was then protonated and charged accordingly using Structure Preparation in Molecular Operating Environment (MOE; Chemical Computing Group). The Site Finder Tool in MOE suggests a binding site of 47 side chain contact atoms on the protein. The selected binding site has a propensity of ligand binding (PLB) of 1.77 and displays 25 hydrophobic contact atoms on the protein (Soga, Shirai, Kobori, & Hirayama, 2007). Dummy atoms were used as a binding site reference for the flexible protein docking. Triangle Placement was carried out using Triangle Matcher, which allows 300 seconds for compound placement and a maximum output of 1000 compound-protein poses. London dG was used for the Scoring as it estimates the free Energy of binding for each pose. Post-placement refinement was carried out using Induced Fit of the Receptor, and the Force Field based Scoring Function GBVI/WSA dG for final Scoring, which produced 5 poses of the compound docked into the protein.

For the Molecular Dynamics (MD) simulations, the output of the docking was used as the starting point. A cubic water box was used with a margin of 12 and the protein-compound system centered. 12027 water molecules and 8 Na ions were added for Rasarfin simulations, while 12046 water molecules and 8 Na ions were added for the Compound 4 simulations. NAMD 2.12 was employed for the Molecular Dynamics simulation, AMBER10 force field was employed for the

protein and ETH was employed for the compound. Checkpoint every 500 ps, Sample time was 0.25 ps and Time step was 2 fs. Particle Mesh Ewald implementation was enabled for periodic electrostatic. Cell periodicity and wrap all atoms was applied. System was minimized for 100 ps, equilibration was run for 200 ps at 300 K and production was run at 300 K. Rasarfin was simulated for a total of 200ns: one 100ns simulation and ten 10ns simulations. Five independent 10ns simulations were computed for Compound 4.

For the pharmacophore docking analysis, the starting coordinates and trajectories of protein and compound were imported into LigandScout (Inte:Ligand) (Wolber & Langer, 2005) using a stride of 50. The "MD Pharmacophores" tool was used to create dynamic pharmacophores to show protein-compound interaction patterns and calculate their frequency of interaction, which were based on the following distances and angles. Hydrophobic interactions were set at 1 - 5 Å and H-bond donor/acceptor at 2.5 – 3.8 Å. Angle tolerance of 180° for $sp^3$ hybridised atoms is an ideal hydrogen bond, which is broken when the angle difference exceeds 34° in either direction around the central position (angle tolerance of 50° is allowed for $sp^2$ hybridised atoms). Angle tolerance of 60° was set for pi-cation interactions. Angle tolerance of 20° was set for orthogonal pi-pi interactions and 20° for parallel pi-pi interactions. Aromatic interactions were set at 0.0 – 2.0 Å orthogonal/parallel center deviation (minimum and maximum distance of two orthogonal or parallel plane feature center points). Once docked, the final output displays the number of unique pharmacophores, appearance frequency and Feature Timeline of computed interactions between the compound and the protein.

3.12. Data analysis

Statistical analyses were performed using GraphPad Prism 6 software (GraphPad Software Inc.; La Jolla, CA) using either Student's *t*-tests, two-way ANOVAs, or Dunnett's comparisons tests, when appropriate and as indicted in the figure legends. Curves presented throughout this study were generated using GraphPad Prism software and represent the best fits, from which $IC_{50}$s were calculated. *P* values < 0.05 were considered significant.

# CHAPTER 4. RESULTS

# DEVELOPMENT OF NEW BRET-BASED SENSORS TO STUDY THE ACTIVITY OF GTPASES AND KINASES

## 4.1. Preface to Chapter 4

Small G proteins are also involved in regulating the signaling and trafficking of GPCRs, but this activation profile is not well-characterized. There is currently a panel of FRET and BRET sensors used to study the GPCR signaling nature of heterotrimeric G proteins, second messengers, protein kinases and ion channels, but there is a need to develop better tools to assess GTPase responses, as well as modulators of these processes. Here, having previously described the Rho and p63 RhoGEF BRET sensors in (Namkung et al., 2018), new BRET sensors were generated to quantitatively measure the signaling kinetics of Ras, Arf, Rac and PI3K as well as pharmacological parameters. Dr. Yoon Namkung designed and generated the four BRET sensor constructs. I contributed to the characterization of these sensors, performing and analyzing all experiments in this chapter.

## 4.2. Results

### 4.2.1. Generating the Arf, Ras and Rac/Cdc42 BRET sensors

The activation of GTPases by GPCRs and RTKs results in the recruitment of effector proteins to the PM, which in turn activate cascades of cellular signaling. Therefore, a RlucII tag was fused to the C-terminus of the binding domain of the effector protein for each respective GTPase: for Arf, the Protein-3 binding domain (PBD) of the golgi-associated, gamma adaptin ear containing, ARF binding protein 3 (GGA3) (GGA3-PBD- RlucII, Figure 4.1A); for Ras, the Ras binding domain of Raf1 (Raf1-RBD-RlucII, Figure 4.1B) and for Rac/Cdc42, the Cdc42- and Rac-interactive binding motif (CRIB) of p21 activated kinase 1 protein (PAK) (PAK-CRIB-RlucII, Figure 4.1C). Upon activation of the GTPase by receptors, the recruitment of the effector to the

PM was monitored by coexpressing effector-RlucII with an rGFP anchored at the PM through the prenylation of the CAAX domain of K-Ras (rGFP-CAAX), resulting in a bystander BRET response.

The functionality of the sensors was validated by confocal microscopy, where HEK293 cells were transfected with AT1R and a YFP-tagged version of the effector protein domains, and their translocation was monitored upon receptor stimulation. In control conditions, GGA3-PBD is localized mostly in the Golgi/ER and cytosol, Raf1-RBD in the cytosol and nucleus, and PAK-CRIB in the cytosol. When stimulated with AngII, they all translocate to the plasma membrane as seen by a better definition of the contour of the cell due to an accumulation of the fluorescence (arrows in Figure 4.1D-F). This is consistent with the notion that the activation of these GTPases by AT1R recruits effectors to the plasma membrane.

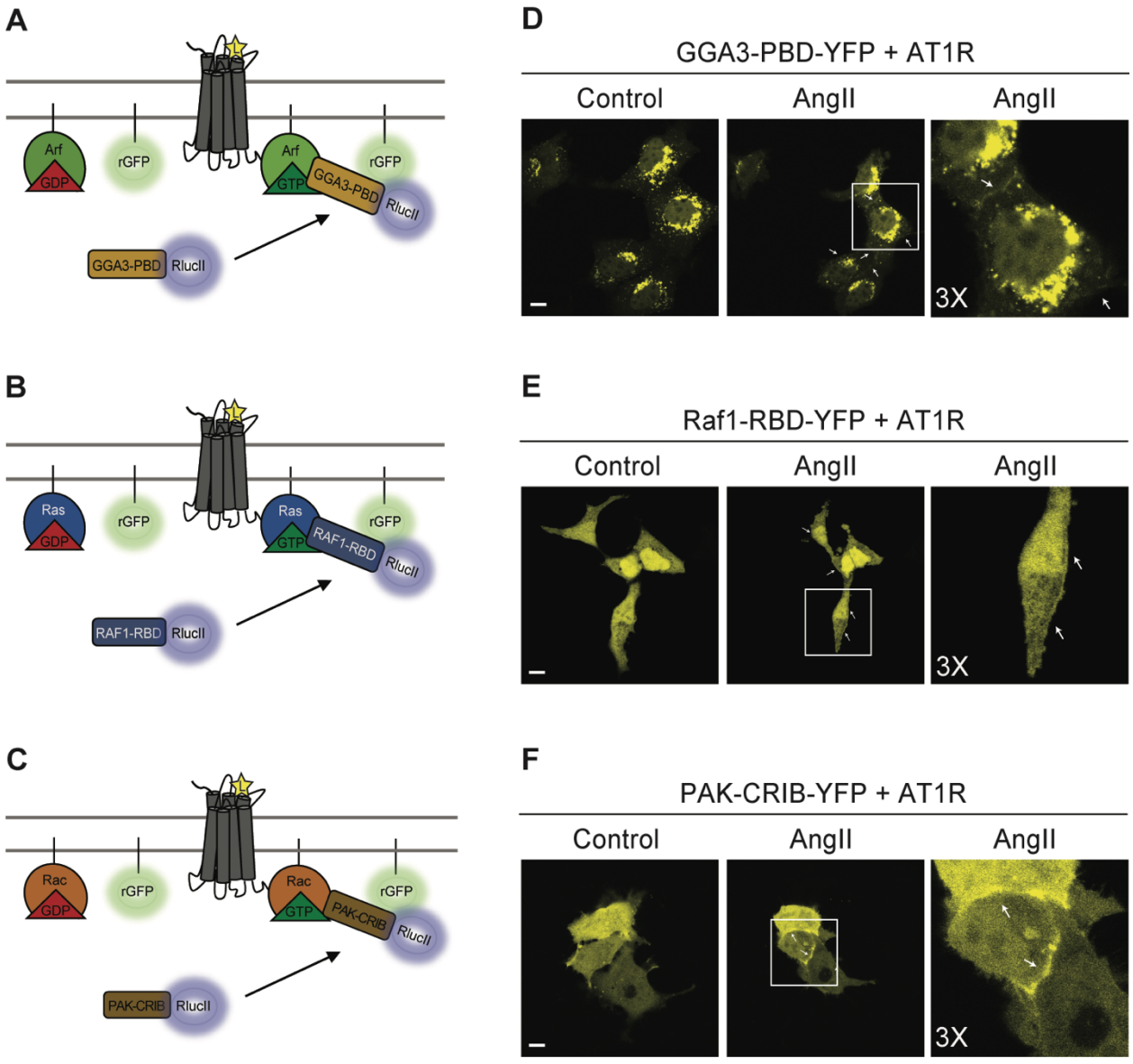
A
Arf
GDP
rGFP
Arf
GTP
GGA3-PBD
RlucII
rGFP
GGA3-PBD
RlucII
B
Ras
GDP
rGFP
Ras
GTP
RAF1-RBD
RlucII
rGFP
RAF1-RBD
RlucII
C
Rac
GDP
rGFP
Rac
GTP
PAK-CRIB
RlucII
rGFP
PAK-CRIB
RlucII
D
GGA3-PBD-YFP + AT1R
Control
AngII
AngII
3X
E
Raf1-RBD-YFP + AT1R
Control
AngII
AngII
3X
F
PAK-CRIB-YFP + AT1R
Control
AngII
AngII
3X

**Figure 4.1. Generation of Arf, Ras and Rac/Cdc42 BRET sensors. (A-C)** Schematic diagram of the Arf, Ras and Rac/Cdc42 BRET sensors. **(A)** The recruitment of GGA3-PBD-RlucII to the plasma membrane (rGFP-CAAX) after Arf activation by a receptor (GPCR) increases bystander BRET. **(B)** The recruitment of Raf1-RBD-RlucII to the PM (rGFP-CAAX) after Ras activation by a receptor increases bystander BRET. **(C)** The recruitment of PAK-CRIB-RlucII to the PM (rGFP-CAAX) after Rac/Cdc42 activation by a receptor increases bystander BRET. **(D-F)** Confocal microscopy images of the translocation of YFP-tagged effectors to the PM upon small G protein activation by AT1R. **(D)** HEK293 cells were transfected with GGA3-PBD-YFP, HA-Arf6 and Flag-AT1R, starved and stimulated with AngII for 10 min. **(E)** HEK293 cells were transfected with Raf1-RBD-YFP and Flag-AT1R, starved and stimulated with AngII for 2 min. **(F)** HEK293 cells were transfected with PAK-CRIB-YFP and Flag-AT1R, starved and stimulated with AngII for 5 min. Arrows show PM contour of cell. Insets are zoomed in 3X. Scale bar, 10 μm.

4.2.2. Validating the receptor-mediated activation of Arf, Ras and Rac/Cdc42 BRET sensors

The BRET sensors were next validated using receptors, such as AT1R and EGFR, which are known to promote the activity of these small G proteins. For the Arf sensor, AngII and EGF increased the BRET ratio within 5 min of agonist addition, and the maximum signal persisted up to 10 min (Figure 4.2A). Therefore, 10 min was chosen as the optimal stimulation time for subsequent Arf experiments. For the Ras sensor, AngII and EGF increased the BRET ratio within 2-5 min of agonist addition and the maximum signal persisted up to 10 min (Figure 4.2B). Therefore, 5 min was chosen as the optimal stimulation time for subsequent Ras experiments. For the Rac/Cdc42 sensor, AngII increased the BRET ratio within 1 min of agonist addition, while EGF increased the BRET ratio within 1-5 min of agonist addition. In both cases, the maximum signal persisted up to 10 min (Figure 4.2C). Therefore, 2 min was chosen as the optimal stimulation time for subsequent Rac/Cdc42 experiments.

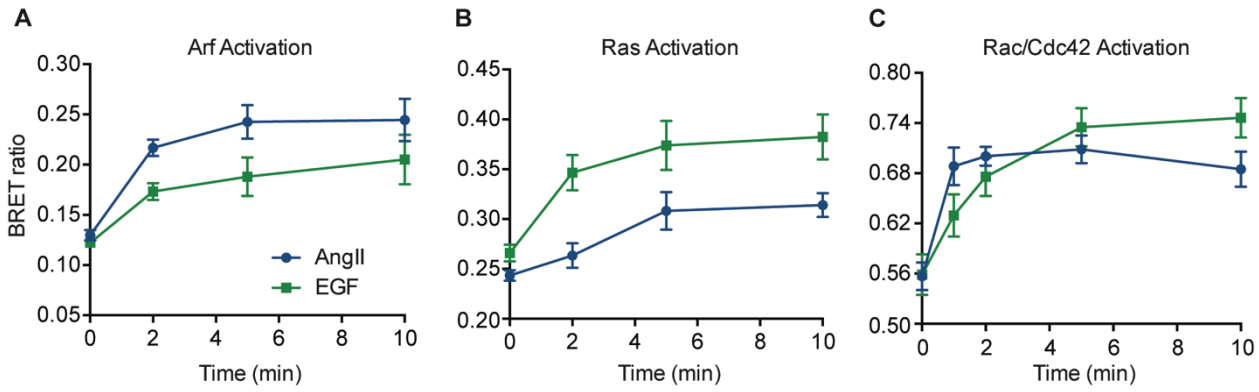


**Figure 4.2. Recording of the kinetics of Arf, Ras and Rac/Cdc42 BRET sensors activation by AT1R and EGFR. (A)** HEK293 cells expressing GGA3-PBD-RlucII and rGFP-CAAX along with Flag-AT1R were serum starved and stimulated or not with AngII or EGF at indicated times. **(B)** HEK293 cells expressing Raf1-RBD-RlucII and rGFP-CAAX along with Flag-AT1R were serum starved and stimulated or not with AngII or EGF at indicated times. **(C)** HEK293 cells expressing PAK-CRIB-RlucII and rGFP-CAAX along with Flag-AT1R were serum starved and stimulated or not with AngII or EGF at indicated times. Data represent means BRET ratio ± SEM of three independent experiments.

4.2.3. Characterizing the AT1R-mediated activation of Arf, Ras and Rac/Cdc42 BRET sensors using GTPase defective mutants

Each sensor was next characterized by overexpressing wild type, constitutively active, or dominant negative forms of the small G protein along with AT1R and the corresponding BRET sensor. Wild type Arf6 increased the basal BRET response by 1.3-fold as compared to mock cells, while the dominant negative Arf6-T27N decreased the basal response (compare black control bars in Figure 4.3A). AngII treatment promoted a 1.7-fold increase in BRET response compared to control in conditions expressing wild type Arf6. No significant agonist-mediated activation of the sensor was detected when Arf6-T27N was expressed. For the Ras sensor, cells expressing the wild type K-Ras increased the basal BRET response by 1.3-fold compared to mock cells and AngII treatment promoted a 1.4-fold increase in BRET response compared to control. Overexpression of the active form of Ras (K-Ras-G12V) or the catalytic domain of SOS that is constitutively present at the PM ($SOS^{cat}$-CAAX) substantially increased the basal BRET response of the sensor by 2.9-fold and 1.8-fold, respectively, compared to mock cells with no further agonist-mediated effects. On the other hand, expression of the dominant negative form of Ras (K-Ras-S17N) reduced its basal activity and blocked the AngII-mediated activation of the sensor (Figure 4.3B). For the Rac sensor, overexpression of wild type Rac1 increased the basal BRET response by 1.3-fold compared to mock cells and AngII treatment promoted a 1.4-fold increase in BRET response compared to control. Cells expressing constitutively active Rac1-Q61L increased the basal BRET response by 1.5-fold compared to mock cells and no further agonist-mediated effects on the Rac sensor's response were observed. The dominant negative Rac1-T17N did not reduce the basal BRET response, but prevented the AngII-mediated activation of the sensor (Figure 4.3C).

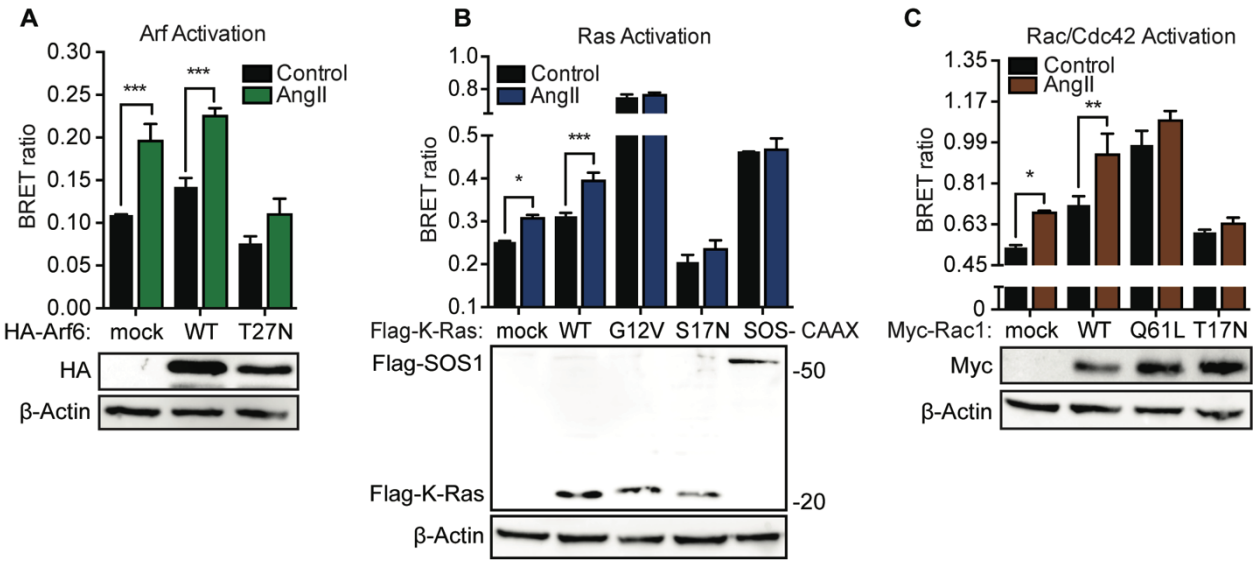


**Figure 4.3. Characterization of Arf, Ras and Rac/Cdc42 BRET sensors activation by AT1R.** **(A)** HEK293 cells expressing GGA3-PBD-RlucII, rGFP-CAAX, Flag-AT1R and either mock (pcDNA3.1), HA-Arf6-WT or HA-Arf6-T27N were serum starved and stimulated or not with 100 nM AngII for 10 min. Shown below are representative western blots of HA-tagged proteins and β-actin as a loading control. **(B)** HEK293 cells expressing Raf1-RBD-RlucII, rGFP-CAAX, Flag-AT1R and either mock (pcDNA3.1), Flag-K-Ras-WT, Flag-K-Ras-G12V, Flag-K-Ras-S17N or Flag-SOS$^{cat}$-CAAX were serum starved and stimulated or not with 100 nM AngII for 5 min. Shown below are representative blots of Flag-tagged proteins and β-actin. **(C)** HEK293 cells expressing PAK-CRIB-RlucII, rGFP-CAAX, Flag-AT1R and either mock (pcDNA3.1), Myc-Rac1-WT, Myc-Rac1-Q61L or Myc-Rac1-T17N were serum starved and stimulated or not with 100 nM AngII for 2 min. Shown below are representative blots of Myc-tagged proteins and β-actin. Data represent mean BRET ratio ± SEM of three independent experiments, *$p < 0.05$, **$p < 0.01$, ***$p < 0.005$, two-way ANOVA with Bonferroni correction.

4.2.4. Generating and validating a PI3K/Akt BRET sensor

As previously mentioned, PI3K functions in the plasma membrane where it phosphorylates $PIP_2$ to generate $PIP_3$, leading to the recruitment of the PH domain of Akt to $PIP_3$ at the plasma membrane. Therefore, a RlucII tag was fused to the C-terminus of the PH domain of Akt to generate a BRET sensor that would work in pair with rGFP-CAAX at the PM. Upon activation of PI3K by a hormone receptor such as a RTK, the PH domain within the Akt (PH)-RlucII construct is recruited to $PIP_3$ at the plasma membrane, which will bring it in close proximity to the rGFP-CAAX, resulting in a bystander BRET response (Figure 4.4A).

The kinetics of activation of the PI3K/Akt sensor was evaluated in HEK293 cells endogenously expressing EGFR and transfected with the sensor. EGF increased the BRET ratio within 2 min of agonist addition and the maximum signal persisted up to 5 min (Figure 4.4B). Therefore, 5 min was chosen as the optimal stimulation time for subsequent Akt experiments. This sensor was further characterized using the PI3K inhibitor, Wortmannin (Arcaro & Wymann, 1993). In vehicle conditions, EGF induced the activation of the sensor in a dose-dependent manner, while the BRET response was completely inhibited by blocking PI3K with Wortmannin (Figure 4.4C).

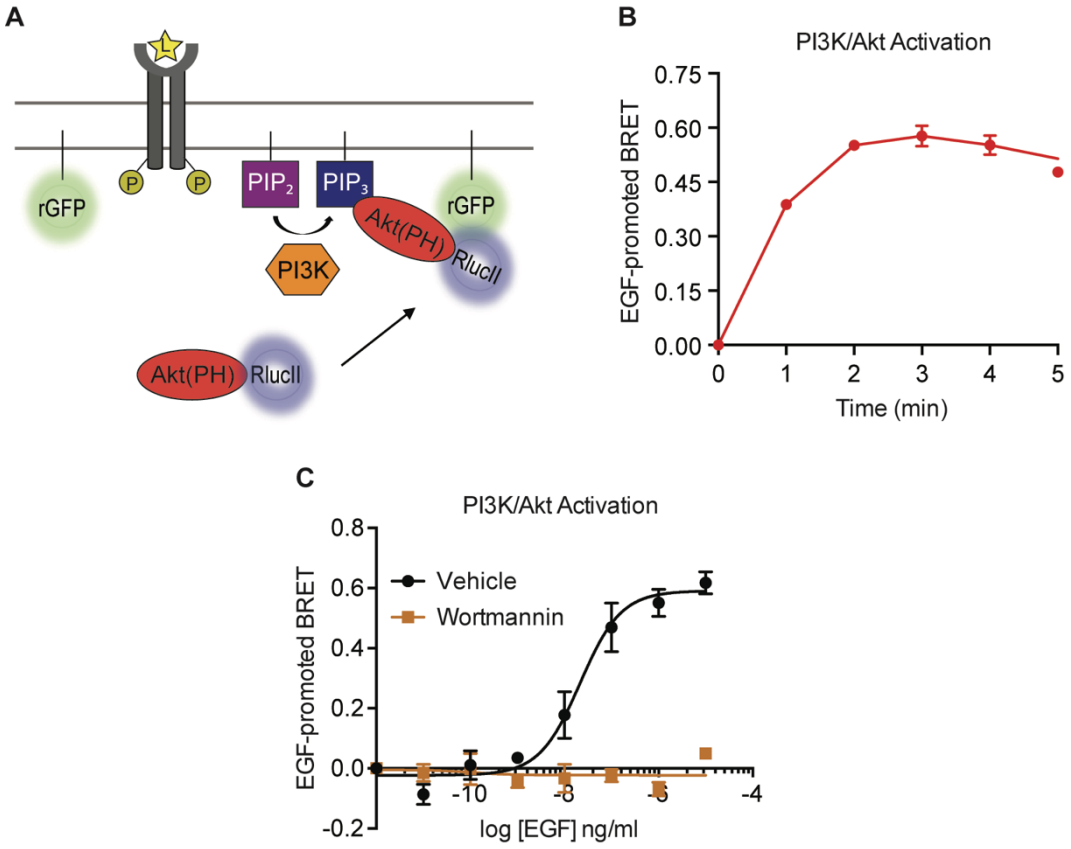


**Figure 4.4. Generation and validation of PI3K/Akt BRET sensor. (A)** Schematic diagram of PI3K/Akt BRET sensor. Upon activation of PI3K by a receptor (RTK), the recruitment of the RlucII-tagged PH domain of Akt (Akt(PH)-RlucII) to $PIP_3$ at the plasma membrane (rGFP-CAAX) increases bystander BRET. **(B)** BRET recording of the kinetics of PI3K/Akt activation by EGFR. HEK293 cells expressing Akt(PH)-RlucII and rGFP-CAAX were serum starved and stimulated or not with 100 ng/ml EGF at indicated times. **(C)** Validation of the PI3K/Akt BRET sensor. Transfected cells were pretreated with vehicle (DMSO) or Wortmannin (PI3K inhibitor, 200nM) for 30 min and stimulated or not with indicated concentrations of EGF for 5 min. Data were quantified as EGF-promoted BRET and represent means ± SEM of three independent experiments.

## 4.3. Summary

In this chapter, four new BRET sensors were generated, characterized and validated to sensitively measure the signaling kinetics of Ras, Arf and Rac/Cdc42 GTPases and Akt, as well as pharmacological parameters. These BRET sensors monitor the recruitment of surrogate effector proteins to the plasma membrane upon protein activation by receptors, which generates an enhanced bystander BRET signal. Overexpressing dominant negative or constitutively active forms of these small GTPases decreases or increases the basal and agonist-induced BRET responses, respectively. The sensors can also capture decreased kinase activity when cells are treated with inhibitors. Their use and further benchmarking against other classical biochemical assays will be described in Chapter 5, which relates to the discovery and characterization of new inhibitors of small G proteins.

# CHAPTER 5. RESULTS

## CHARACTERIZATION OF THE MECHANISM OF ACTION OF COMP#21 (RASARFIN)

## 5.1. Preface to Chapter 5

From the high-throughput screen for AT1R trafficking described in Chapter 2.1, Comp#21 was one of 20 inhibitors of both AT1R and B2R internalization, and whose mechanism of action will be further characterized in this chapter. Dr. Etienne Khoury designed and performed the microscopy experiments in Figure 5.1D and E. Dr. Doris A. Schuetz designed, performed and analyzed all of the computational data in Figure 5.10. Figures were used with their permission. I designed, performed and analyzed all other experiments.

## 5.2. Results

### 5.2.1. Comp#21 inhibits receptor trafficking

First, Comp#21's effects on receptor internalization were validated by transfecting cells with different GPCRs (AT1R, B2R, or $\beta_2$AR) and the same BRET trafficking sensor as the HTS (Namkung, Le Gouill, et al., 2016). As the RlucII-tagged receptor traffics from the PM into endosomes tagged with rGFP through its FYVE domain, an increase in BRET signal is recorded as these two chromophores are within the same compartment. HEK293 cells were pretreated with various concentrations of compound and the internalization of AT1R, B2R, and $\beta_2$AR was monitored after 30 minutes stimulation with AngII, BK or ISO, respectively. From the generated curves, Comp#21 inhibited the internalization of AT1R, B2R and $\beta_2$AR with similar potencies of 10 μM, 11 μM and 15 μM, respectively (Figure 5.1A). Therefore, Comp#21 is not specific to AT1R but inhibits the internalization of multiple GPCRs (classes A and B). As one of the first crucial steps in receptor endocytosis, the recruitment of β-arrestin to the receptor was assessed next using BRET sensors that monitor the trafficking of β-arrestin1 or β-arrestin2 to the receptor at the

PM. Cells were transfected with AT1R-YFP or B2R-YFP and β-arrestin2-RlucII or β-arrestin1-RlucII, then pretreated with vehicle (DMSO) or Comp#21 and subjected to kinetics experiments. Overall, Comp#21 did not affect the kinetics of β-arrestin1 or β-arrestin2 recruitment to AT1R (Figure 5.1B) nor β-arrestin2 recruitment to B2R (Figure 5.1C).

These receptors traffic/internalize with β-arrestin2 into endosomes, so it was hypothesized that if Comp#21 inhibits receptor internalization, it would also affect β-arrestin2 co-trafficking inside the cell. Therefore, cellular imaging was used to follow the trafficking of β-arrestin2-YFP into endosomes upon receptor stimulation. HEK293 cells were transfected with YFP-tagged β-arrestin2 and either Flag-AT1R or HA-B2R and pretreated with vehicle or Comp#21 for 30 min. As can be seen from the top panels, in the absence of ligand (control conditions), β-arrestin2 was restricted to the cytosol for both vehicle and Comp#21 treated cells. In the presence of vehicle, β-arrestin2 was recruited to the plasma membrane within the first 5 min of receptor stimulation (not shown) and after 15 min of AngII or BK, β-arrestin2 trafficked into endosomes. However, in the presence of Comp#21, β-arrestin2 was recruited to the plasma membrane but does not internalize after 15 min of receptor stimulation, as β-arrestin2 remains at the plasma membrane after AT1R (Figure 5.1D) and B2R stimulation (Figure 5.1E).

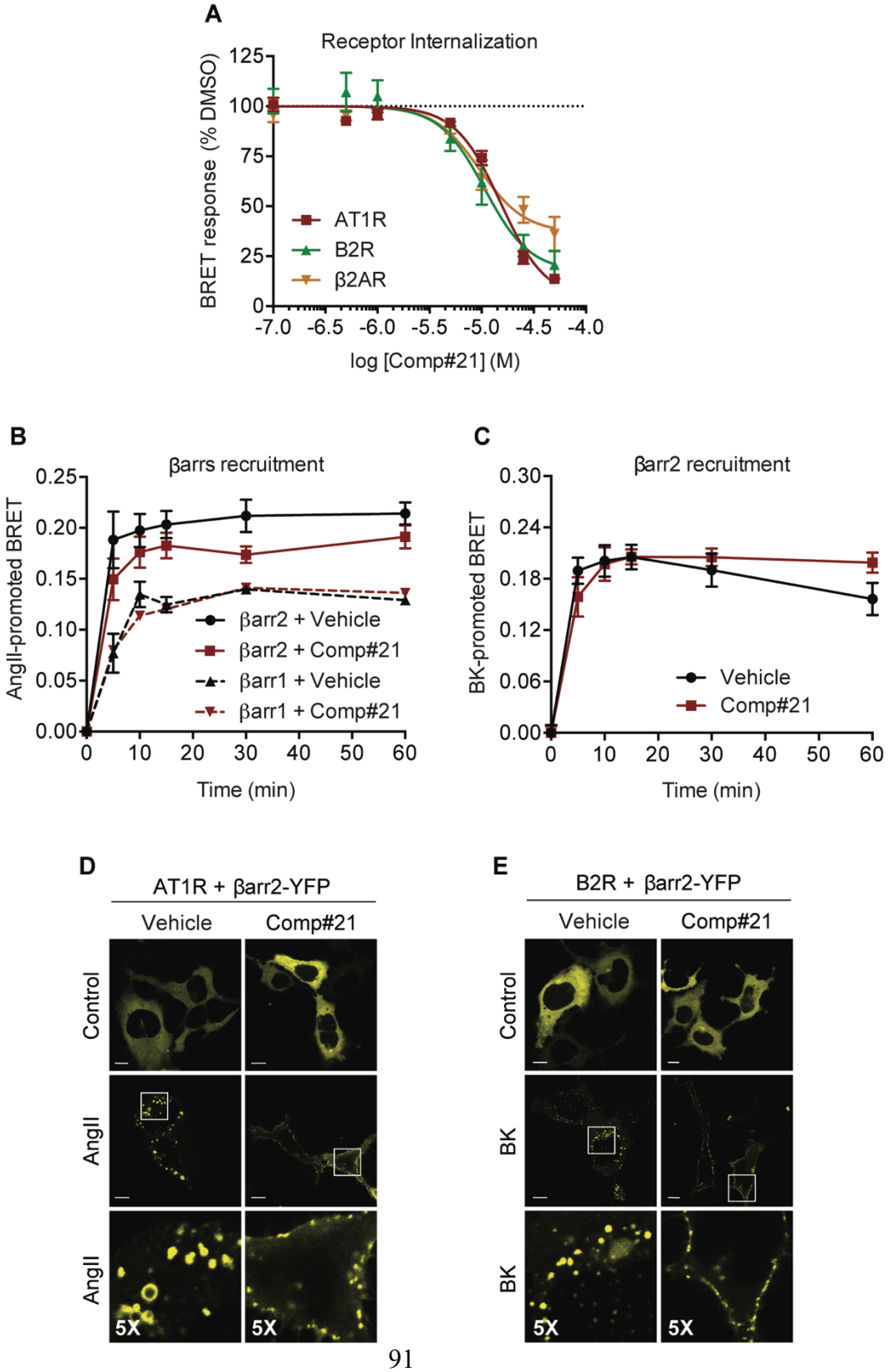
A
Receptor Internalization
BRET response (% DMSO)
125
100
75
50
25
0
AT1R
B2R
β2AR
-7.0 -6.5 -6.0 -5.5 -5.0 -4.5 -4.0
log [Comp#21] (M)
B
βarrs recruitment
AngII-promoted BRET
0.25
0.20
0.15
0.10
0.05
0.00
βarr2 + Vehicle
βarr2 + Comp#21
βarr1 + Vehicle
βarr1 + Comp#21
0 10 20 30 40 50 60
Time (min)
C
βarr2 recruitment
BK-promoted BRET
0.30
0.24
0.18
0.12
0.06
0.00
Vehicle
Comp#21
0 10 20 30 40 50 60
Time (min)
D
AT1R + βarr2-YFP
Vehicle
Comp#21
Control
AngII
AngII
5X
5X
E
B2R + βarr2-YFP
Vehicle
Comp#21
Control
BK
BK
5X
5X

**Figure 5.1. Comp#21 inhibits receptor trafficking. (A)** BRET recording of AT1R, B2R and $\beta_2$AR internalization into endosomes. Cells were transfected with AT1R-RlucII, B2R-RlucII or $\beta_2$AR-RlucII and rGFP-FYVE, serum starved, pretreated with vehicle (DMSO) or Comp#21 (at indicated concentrations) for 30 min and stimulated or not with 100 nM Angiotensin II or Bradykinin, or 10 μM Isoproterenol for 30 min. BRET responses were quantified as percent ligand-promoted BRET compared to vehicle (DMSO, dotted line). Data represent means ± SEM of four independent experiments. **(B)** BRET recording of the recruitment of β-arrestin1 and β-arrestin2 to AT1R. Cells were tranfected with AT1R-YFP and β-arrestin2-RlucII or β-arrestin1-RlucII, serum starved, pretreated with vehicle (DMSO) or Comp#21 (50 μM) for 30 min and stimulated or not with 100 nM AngII at indicated times. BRET responses were quantified as AngII-promoted BRET. Data represent means ± SEM of three independent experiments. **(C)** BRET recording of the recruitment of β-arrestin2 to B2R. Cells were transfected with B2R-YFP and β-arrestin2-RlucII, starved, pretreated with vehicle (DMSO) or Comp#21 (50 μM) for 30 min and stimulated or not with 100 nM Bradykinin at indicated times. BRET responses were quantified as BK-promoted BRET. Data represent means ± SEM of three independent experiments. **(D, E)** Confocal microscopy images of YFP-tagged β-arrestin2 internalization. Flag-AT1R or HA-B2R transfected HEK293 cells were starved, pretreated with vehicle (DMSO) or Comp#21 (50 μM) for 15 min and stimulated or not (control) with 100 nM AngII or BK for 15 min. Insets are zoomed in 5X. Scale bar, 10 μm.

5.2.2. Comp#21 targets Arf6 to inhibit GPCR internalization

Comp#21 inhibited the trafficking of receptor and β-arrestin2 into endosomes but did not affect the recruitment of β-arrestin2 to the PM. Therefore, it was hypothesized that Comp#21's target must be a process in between β-arrestin recruitment and β-arrestin/receptor internalization, such as the formation of clathrin-coated pits (CCPs). Since β-arrestin recruits the adaptor protein 2 (AP-2) to the PM to form the CCP, HEK293 cells were transfected with AT1R and BRET sensors that monitor the binding of β-arrestins and the β2-adaptin subunit of AP-2 (Hamdan et al., 2007). Cells were then treated with either vehicle, Comp#21 or the β-arrestin/AP-2 inhibitor Barbadin (Beautrait et al., 2017) for 30 min and stimulated or not with AngII at indicated times. Compared to vehicle, Comp#21 inhibited around 20% of β-arrestin2 binding to β2-adaptin, whereas Barbadin inhibited more than 50% of this interaction 2 min after AT1R stimulation (Figure 5.2A).

As another protein necessary for the formation of the CCPs and potential target of Comp#21, the small GTPase Arf6 was next tested using GST-pull down assay with the GST-GGA3-PBD effector protein, which pulls down the GTP-bound form of Arf6 (Takatsu, Yoshino, Toda, & Nakayama, 2002). HA-Arf6 and AT1R expressing cells were pretreated with Comp#21 or vehicle and receptor was stimulated or not with AngII. Quantification of the pull down assay in Figure 5.2B shows that after AT1R stimulation, GGA3-PBD pulled down around 70% less Arf6-GTP in Comp#21 treated cells as compared to vehicle. Complementary to this biochemical GST pulldown assay, the Arf BRET sensor was used to assess Comp#21's effects on Arf activation using a kinetics experiment. Cells expressing the Arf sensor and AT1R were treated with either vehicle or Comp#21 for 30 min and stimulated or not with AngII at indicated times. Compared to

DMSO, Comp#21 decreased the amount of Arf activation by 40-60% after 2 min AT1R stimulation (Figure 5.2C), further validating Arf6 as Comp#21's target.

Another member of the Arf family, Arf1, can also bind to GGA3-PBD, therefore, Comp#21's effects on this small G protein was next assessed using GST pull down assay. The HA-Arf1 western blots and quantification in Figure 5.3 show that GGA3-PBD still pulls down active Arf1 in the presence of Comp#21, similar to vehicle, suggesting that Comp#21 is selective to Arf6 GTPase.

To validate that Arf6 is required for receptor internalization, another set of BRET trafficking sensors (AT1R-RlucII and rGFP-CAAX) was used to assess the removal of AT1R from the PM in cells expressing AT1R and either mock (pcDNA3.1), wild type Arf6 or the dominant negative Arf6-T27N. AT1R internalized faster in the cells overexpressing wild type Arf6 than mock cells, and slower in the Arf6-T27N expressing cells (Figure 5.4A). If this AT1R trafficking is similarly assessed in cells pretreated with vehicle or Comp#21, Comp#21 behaves similarly to Arf6-T27N in slowing down the removal of AT1R from the plasma membrane compared to vehicle (Figure 5.4B). These data support the previous observation that Arf6 is involved in receptor internalization and suggests that Comp#21 targets this small G protein to inhibit receptor internalization.

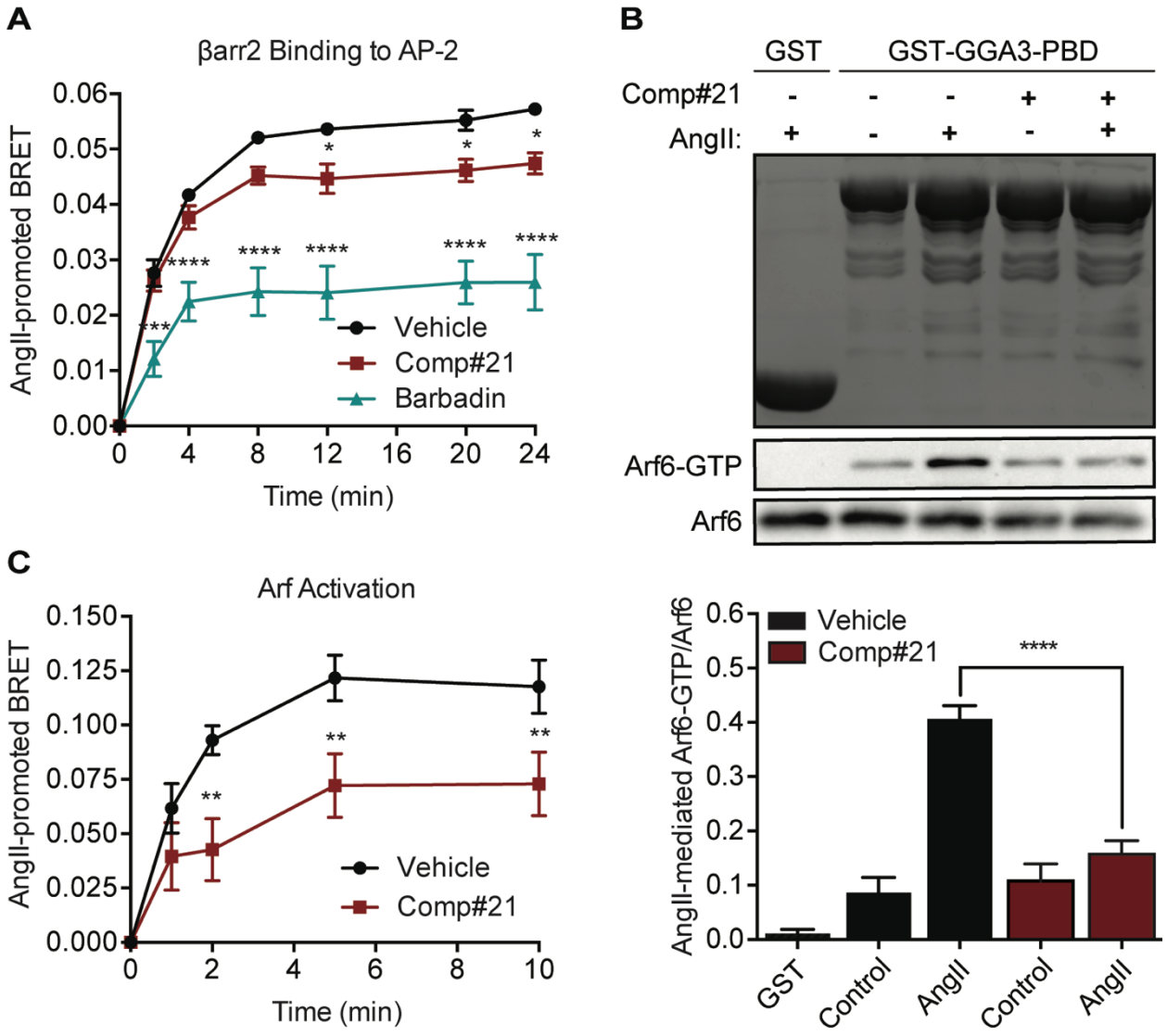
A
βarr2 Binding to AP-2
AngII-promoted BRET
Time (min)
Vehicle
Comp#21
Barbadin
B
GST
GST-GGA3-PBD
Comp#21
AngII:
Arf6-GTP
Arf6
C
Arf Activation
AngII-promoted BRET
Time (min)
Vehicle
Comp#21
AngII-mediated Arf6-GTP/Arf6
GST
Control
AngII
Control
AngII

**Figure 5.2. Comp#21 inhibits Arf6 activation. (A)** BRET recording of the binding of β-arrestin2 to AP-2 in clathrin-coated pits. Cells were transfected with β-arrestin2-RlucII and β2-adaptin-EYFP, serum starved, pretreated with vehicle (DMSO), Comp#21 (50 μM) or Barbadin (β-arrestin/AP-2 inhibitor, 100 μM) for 30 min and stimulated or not with 100 nM AngII at indicated times. BRET responses were quantified as AngII-promoted BRET. Data represent means ± SEM of three independent experiments, *p < 0.05, ****p < 0.0001, two-way ANOVA corrected with Dunnett's test. **(B)** GST pulldown of Arf6-GTP using GST and GST-GGA3-PBD coupled to glutathione beads. Cells transfected with HA-Arf6 and Flag-AT1R were serum starved, pretreated with vehicle (DMSO) or Comp#21 (50 μM) and stimulated or not (control) with 1 μM AngII for 5 min. Coomassie of GST and GST-GGA3-PBD proteins, representative western blots and the quantification of HA-Arf6 are shown. Arf6 activation was quantified as the amount of HA-Arf6-GTP divided by the total amount of HA-Arf6. Data are means ± SEM from three independent experiments, ****p <0.0001, one-way ANOVA with Bonferroni correction. (**C**) BRET assessment of the kinetics of AT1R-mediated Arf activation. HEK293 cells expressing GGA3-PBD-RlucII and rGFP-CAAX along with Flag-AT1R were serum starved, pretreated with vehicle (DMSO) or Comp#21 (50 μM) for 30 min and stimulated or not with 100 nM AngII at indicated times. Data were quantified as AngII-promoted BRET and represent means ± SEM of three independent experiments, **p < 0.01, unpaired Student's *t*-test.

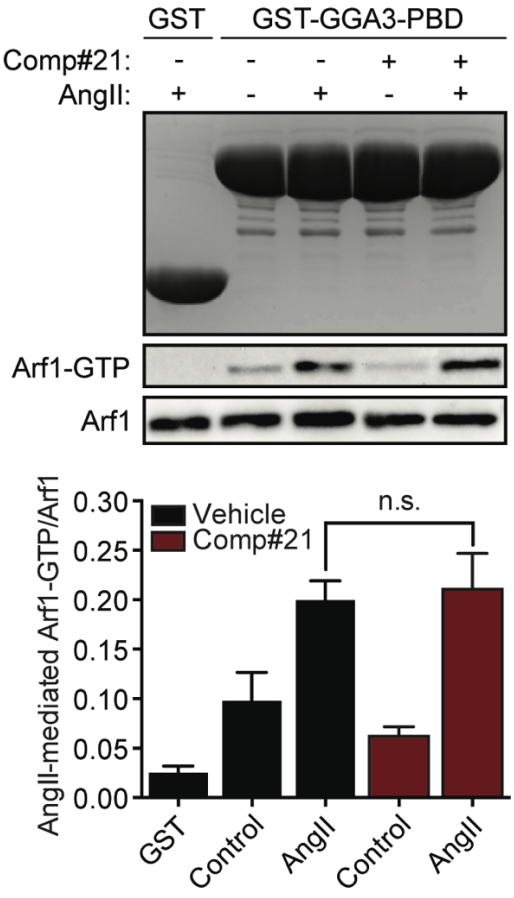


**Figure 5.3. Comp#21's effects on Arf1 activation.** GST pulldown of Arf1-GTP using GST and GST-GGA3-PBD coupled to glutathione beads. Cells transfected with HA-Arf1 and Flag-AT1R were serum starved, pretreated with vehicle (DMSO) or Comp#21 (50 μM) and stimulated or not (control) with 1 μM AngII for 5 min. Coomassie of GST and GST-GGA3-PBD proteins, representative western blots and the quantification of HA-Arf1 are shown. Arf1 activation was quantified as the amount of HA-Arf1-GTP divided by the total amount of HA-Arf1. Data are means ± SEM from three independent experiments.

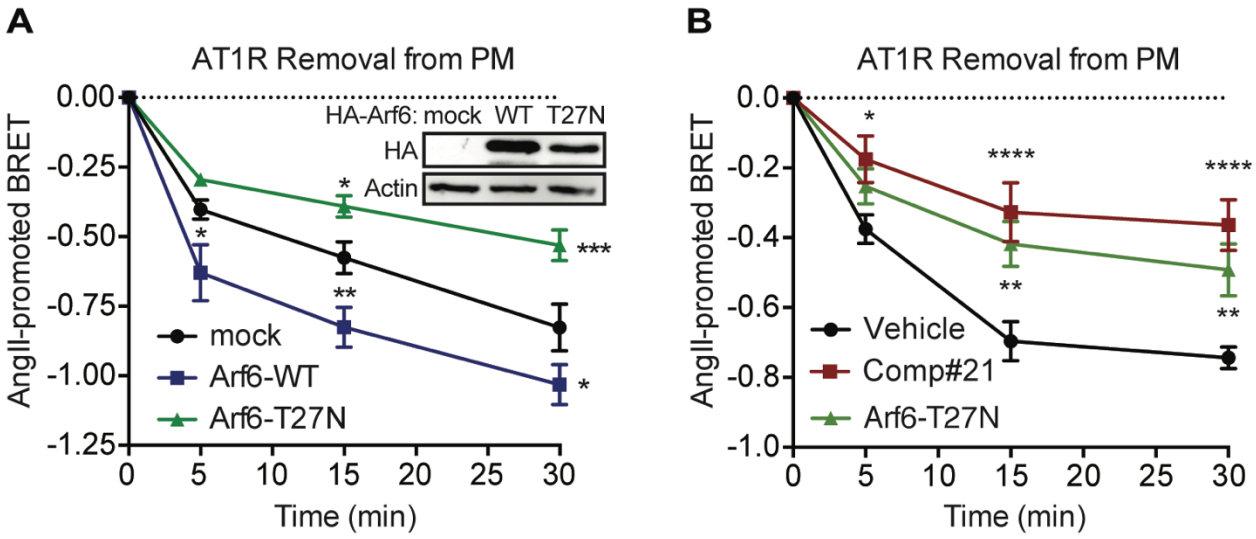


**Figure 5.4. Arf6-T27N and Comp#21 effects on AT1R internalization. (A)** BRET recordings of AT1R internalization represented as the removal of AT1R-RlucII from the PM (rGFP-CAAX). Cells were transfected with mock, HA-Arf6-WT or HA-Arf6-T27N and stimulated or not with 100 nM AngII at indicated times. Data were quantified as AngII-promoted BRET and represent means ± SEM of three independent experiments, *p < 0.05, **p < 0.01, ***p < 0.005, two-way ANOVA corrected with Dunnett's test. Shown above are representative blots of HA-tagged proteins and β-actin as a loading control. **(B)** BRET recordings of AT1R removal from the PM. Cells transfected with Arf6-T27N and cells transfected with vector were pretreated with either vehicle (DMSO), or Comp#21 (50 μM) for 30 min, then all cells were stimulated or not with 100 nM AngII at indicated times. Data were quantified as AngII-promoted BRET and represent means ± SEM of three independent experiments, *p < 0.05, **p < 0.01, ****p < 0.0001, two-way ANOVA corrected with Dunnett's test.

5.2.3. Comp#21 inhibits receptor signaling

Since AT1R has been reported to mediate MAPK activation by β-arrestins from endosomes after receptor endocytosis (Wei et al., 2003), it was hypothesized that if receptor internalization is inhibited by Comp#21, ERK1/2 signaling would also be impeeded. ERK1/2 activation was thus assessed by western blot and results show that Comp#21 not only inhibited AngII-mediated phosphorylation of ERK1/2 but also blocked the agonist-mediated response of B2R, β2AR and EGFR (Figure 5.5A). To determine if Comp#21's inhibition of ERK1/2 is through a G protein-dependent mechanism, Comp#21's effects on AT1R-mediated $G\alpha_q$, $G\alpha_{i3}$, and $G\alpha_{12/13}$ were determined using corresponding BRET sensors. To measure $G\alpha_q$ and $G\alpha_{i3}$ activation, the dissociation of their Gα and Gβγ subunits upon receptor stimulation results in a BRET response (Namkung, Radresa, et al., 2016; Quoyer et al., 2013). $G\alpha_{12/13}$ activation was assessed through its downstream effector Rho using the Rho BRET sensor (Namkung et al., 2018). Compared to vehicle, the activation of all three G proteins mediated by AT1R was not affected by Comp#21, whereas the $G_{q/11/14}$ inhibitor UBO-QIC (Schrage et al., 2015) completed blunted the $G\alpha_q$ BRET response (Figure 5.5B). Then, the activity of Comp#21 on kinases upstream in the MAPK cascade, such as PKC, MEK1 and BRAF, were evaluated. Here, PKC activation was measured using a unimolecular BRET sensor that changes conformation upon the phosphorylation of two threonine residues in PKC when PKC is activated, producing a BRET signal (Namkung et al., 2018). Compared to vehicle, Comp#21 did not affect the AT1R-mediated PKC activation (Figure 5.5B). To test Comp#21's effects on the kinase activity of MEK1/2 and BRAF, the phosphorylation levels of ERK1/2 were monitored in cells overexpressing wild type (WT) or constitutively active forms

of MEK1 (Flag-MEK1-DD) or BRAF (Flag-BRAF-V600E) and treated or not with Comp#21. In vehicle and Comp#21 conditions, both MEK1-DD (Figure 5.5C) and BRAF-V600E (Figure 5.5D) expression increased phosphorylated ERK1/2 levels by ~4-fold compared to both mock and MEK1-WT or BRAF-WT expressing cells, whereas the MEK1/2 inhibitor PD184352 (Sebolt-Leopold et al., 1999) completely blocked the MEK1-DD-mediated ERK1/2 activation. These data imply that $G\alpha_q$, $G\alpha_{i3}$, $G\alpha_{12/13}$ proteins, and PKC, MEK, and Raf kinases are not Comp#21's targets for inhibiting ERK1/2 phosphorylation.

As a RTK, EGFR activates ERK1/2 by a different mechanism than GPCRs, which does not involve Arf6 nor receptor endocytosis. To provide insight into the mechanisms by which Comp#21 inhibits these two types of receptors, the potency of Comp#21 on AT1R- and EGFR-mediated ERK1/2 phosporylation was next compared. Cells were pretreated with various concentrations of vehicle or compound and stimulated or not with ligand. Figure 5.6A shows there is a similar dose-dependent inhibition of Comp#21 on AngII- and EGF-mediated ERK1/2 phosporylation, with $IC_{50}$s of 5 μM and 4 μM, respectively. This suggests Comp#21 may inhibit GPCR and RTK signaling by a common target. To determine if Comp#21 specifically affects ERK1/2 signaling, the activation of Akt was tested using western blot (Figure 5.6B) and the PI3K/Akt BRET sensor described in Chapter 4.2.4 (Figure 5.6C). Both assays show that Comp#21 inhibits EGFR-mediated Akt with a similar potency with which it inhibits ERK1/2 activation (~5 μM), suggesting Comp#21 targets a protein that is involved in both ERK1/2 and Akt cascades.

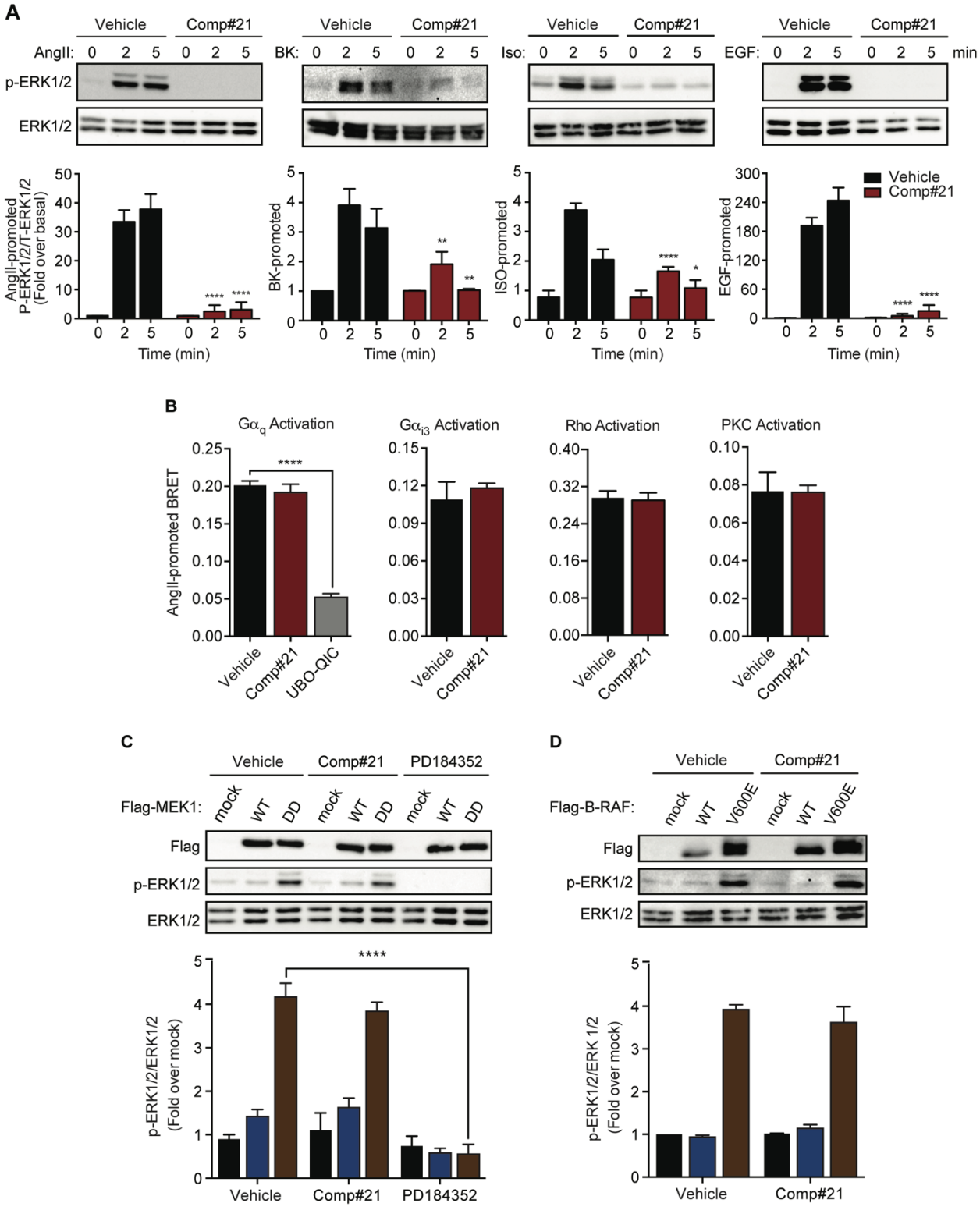
A
Vehicle
Comp#21
AngII: 0 2 5 0 2 5
BK: 0 2 5 0 2 5
Iso: 0 2 5 0 2 5
EGF: 0 2 5 0 2 5 min
p-ERK1/2
ERK1/2
AngII-promoted P-ERK1/2/T-ERK1/2 (Fold over basal)
BK-promoted
ISO-promoted
EGF-promoted
Time (min)
B
Gαq Activation
Gαi3 Activation
Rho Activation
PKC Activation
AngII-promoted BRET
Vehicle
Comp#21
UBO-QIC
C
PD184352
Flag-MEK1:
mock
WT
DD
Flag
p-ERK1/2
ERK1/2
p-ERK1/2/ERK1/2 (Fold over mock)
D
Flag-B-RAF:
V600E
p-ERK1/2/ERK 1/2 (Fold over mock)

**Figure 5.5. Comp#21 inhibits ERK1/2 activation. (A)** Kinetics of ERK1/2 phosphorylation mediated by AT1R, B2R, $\beta_2$AR and EGFR. Cells were transfected with Flag-AT1R, HA-B2R or HA-$\beta_2$AR, serum starved, pretreated with vehicle (DMSO) or Comp#21 (50 μM) for 30 min and stimulated with either AngII, BK, ISO or EGF, respectively, for the indicated times. Shown are representative western blots of phosphorylated ERK1/2 and total ERK1/2, quantified as p-ERK1/2 over ERK1/2 and normalized as fold over basal (0 min). Data represent means ± SEM of three independent experiments compared to DMSO, *p < 0.05, **p < 0.01, ****p < 0.0001, unpaired Student's *t*-test. **(B)** AT1R-mediated $G\alpha_q$, $G\alpha_{i3}$, $G\alpha_{12/13}$ (Rho) and PKC activation. HEK293 cells were transfected with AT1R and corresponding BRET sensors: polycistronic $G\alpha_q$ sensor; $G\alpha_{i3}$-RlucII, Flag-$G\beta_1$ and GFP10-$G\gamma_1$; PKN-RBD-RlucII and rGFP-CAAX or PKC sensor. Cells were serum starved, pretreated with vehicle (DMSO), Comp#21 (50 μM) or UBO-QIC (1 μM) for 30 min, and stimulated or not with 100 nM AngII for 2 min ($G\alpha_q$, $G\alpha_{i3}$ and Rho) or 5 min (PKC). BRET responses were quantified as AngII-promoted BRET and represent means ± SEM of three independent experiments. **(C, D)** MEK1- and BRAF-induced ERK1/2 phosphorylation. Cells were transfected with mock (pcDNA3.1), Flag-MEK1-WT, Flag-MEK1-DD, Flag-BRAF-WT or Flag-BRAF-V600E, serum starved, treated with vehicle (DMSO), Comp#21 (50 μM) or PD184352 (MEK1/2 inhibitor, 10 μM) for 30 min. Cells were washed and lysed. Shown are representative western blots of Flag, phosphorylated ERK1/2 and total ERK1/2, quantified as p-ERK1/2 over ERK1/2 and normalized as fold over mock. Data represent means ± SEM of three independent experiments, ****p < 0.0001, two-way ANOVA with Bonferroni correction.

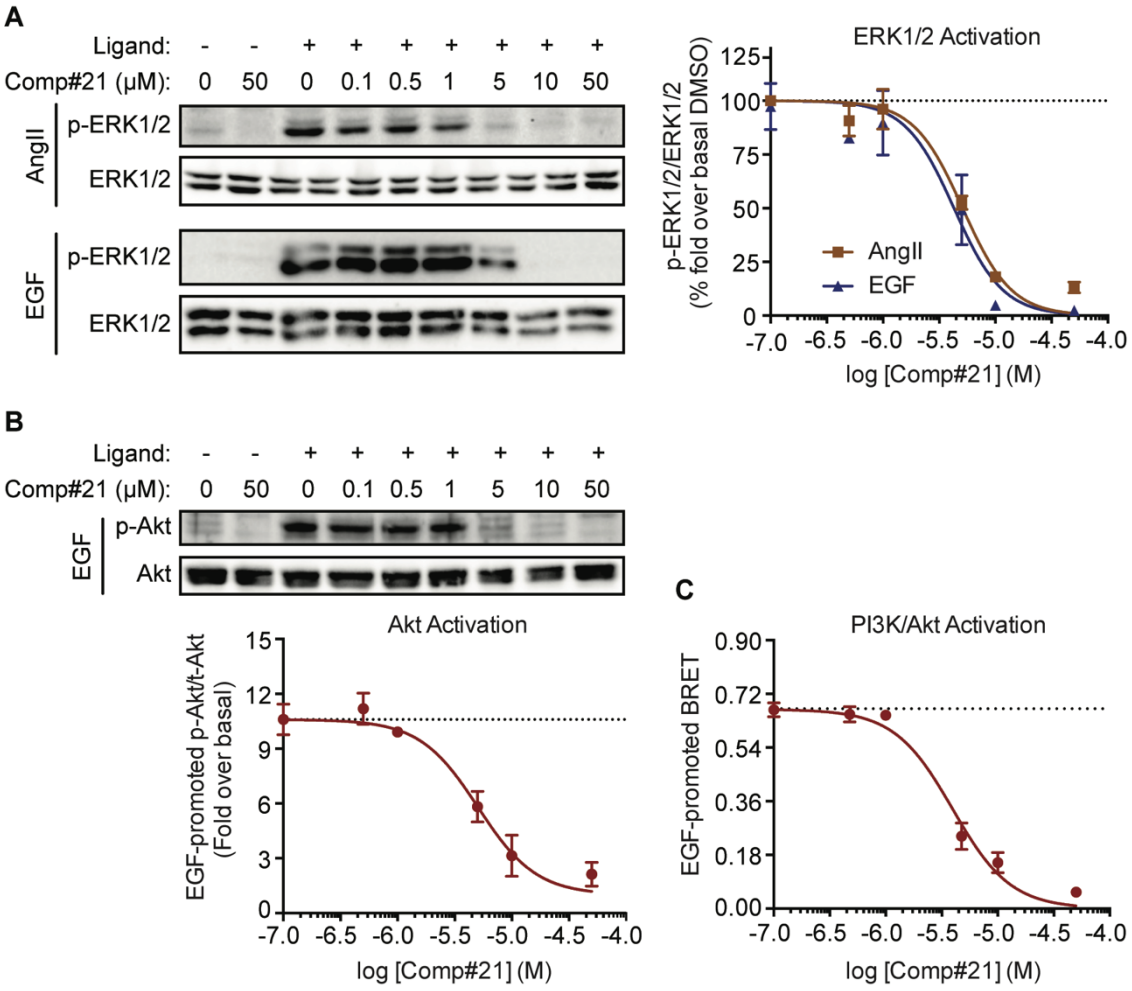
A
Ligand: - - + + + + + + +
Comp#21 (μM): 0 50 0 0.1 0.5 1 5 10 50
AngII
p-ERK1/2
ERK1/2
EGF
p-ERK1/2
ERK1/2
ERK1/2 Activation
p-ERK1/2/ERK1/2 (% fold over basal DMSO)
125
100
75
50
25
0
AngII
EGF
-7.0 -6.5 -6.0 -5.5 -5.0 -4.5 -4.0
log [Comp#21] (M)
B
Ligand: - - + + + + + + +
Comp#21 (μM): 0 50 0 0.1 0.5 1 5 10 50
EGF
p-Akt
Akt
Akt Activation
EGF-promoted p-Akt/t-Akt (Fold over basal)
15
12
9
6
3
0
-7.0 -6.5 -6.0 -5.5 -5.0 -4.5 -4.0
log [Comp#21] (M)
C
PI3K/Akt Activation
EGF-promoted BRET
0.90
0.72
0.54
0.36
0.18
0.00
-7.0 -6.5 -6.0 -5.5 -5.0 -4.5 -4.0
log [Comp#21] (M)

**Figure 5.6. Comp#21 inhibits Akt activation. (A)** AT1R- and EGFR-mediated ERK1/2 activation. Cells were transfected with Flag-AT1R, serum starved, pretreated with vehicle (DMSO) or Comp#21 (at indicated concentrations) and stimulated or not with either 100 nM AngII or 100 ng/ml EGF for 5 min. Shown are representative western blots of phosphorylated and total ERK1/2, quantified as p-ERK1/2 over ERK1/2 and normalized as fold over basal, percent compared to vehicle (DMSO, dotted line). Data represent means ± SEM of three independent experiments. **(B)** EGFR-mediated Akt activation. Cells were serum starved, pretreated with vehicle (DMSO) or Comp#21 (at indicated concentrations) and stimulated or not with 100 ng/ml EGF for 5 min. Shown are representative western blots of phosphorylated and total Akt, quantified as p-Akt over Akt and normalized as fold over basal, compared to vehicle (DMSO, dotted line). Data represent means ± SEM of three independent experiments. **(C)** Recording of PI3K/Akt BRET sensor activation by EGFR. Cells were serum starved, pretreated with vehicle (DMSO) or Comp#21 (at indicated concentrations) and stimulated or not with 100 ng/ml EGF for 5 min. BRET responses were quantified as EGF-promoted BRET, compared to vehicle (DMSO, dotted line). Data represent means ± SEM of three independent experiments.

5.2.4. Comp#21 targets Ras to inhibit ERK1/2 and Akt activation

Since the small GTPase Ras is upstream of both the MAPK and PI3K pathways, and is activated by both AT1R and EGFR, it was postulated that Comp#21 also targets this small G protein to regulate receptor signaling. Ras activation was first measured using GST-pull down assay with the GST-Raf1-RBD effector protein, which pulls down the GTP-bound form of Ras. Quantification of the pull down assay in Figure 5.7A and B shows that after both AT1R and EGFR stimulation, Raf1-RBD pulled down around 60% less Ras-GTP in cells treated with Comp#21 compared to vehicle treated cells. Complementary to this biochemical assay, the Ras BRET sensor was then used to assess Comp#21's effects on Ras activation. As shown in a kinetics experiment, Comp#21 decreased the amount of Ras activation by 50-70% after 2 min AT1R stimulation, compared to vehicle (Figure 5.7C). The direct activity of Comp#21 on Ras was next assessed using a GEF exchange assay, which monitors the kinetics uptake of fluorescent mant-GTP into a GTPase upon activation by a GEF (John et al., 1990). Here, purified H-Ras was activated using either its GEF SOS1 (purified) or EDTA to chemically mimic the role of SOS1 in chelating $Mg^{2+}$ from the active site of the GTPase and promoting nucleotide release (B. Zhang, Zhang, Wang, & Zheng, 2000). Rasarfin decreases in a dose-dependent manner the uptake of fluorescent mant-GTP into H-Ras after activation by either SOS1 (Figure 5.7D) or EDTA (Figure 5.7E), further validating Ras as Comp#21's second target.

To rule out the possibility that Comp#21 is a pan GTPase inhibitor, its effects on other small G proteins like Rho and Rac were also determined. First, Rho activation was measured using GST-pull down assay with the GST-Rhotekin-RBD effector protein, which pulls down the GTP-bound form of Rho. After AT1R stimulation, Rhotekin-RBD was able to pull down RhoA-GTP in

cells treated with Comp#21 similar to vehicle treated cells (Figure 5.8A). Then, using the panel of GTPase BRET sensors described in Chapter 4, the AT1R-mediated activation of Arf, Ras, Rho and Rac/Cdc42 sensors was measured in the absence or presence of Comp#21. The dose-response curves in Figure 5.8B show that Comp#21 is specific to Arf and Ras as it did not affect the activation of Rho nor Rac/Cdc42. Comp#21 is also more potent on Ras than Arf, with $IC_{50}$s of 0.7 μM and 7 μM, respectively. Nonetheless, Comp#21 is a specific **Ras** and **Arf in**hibitor, therefore, it was renamed Rasarfin.

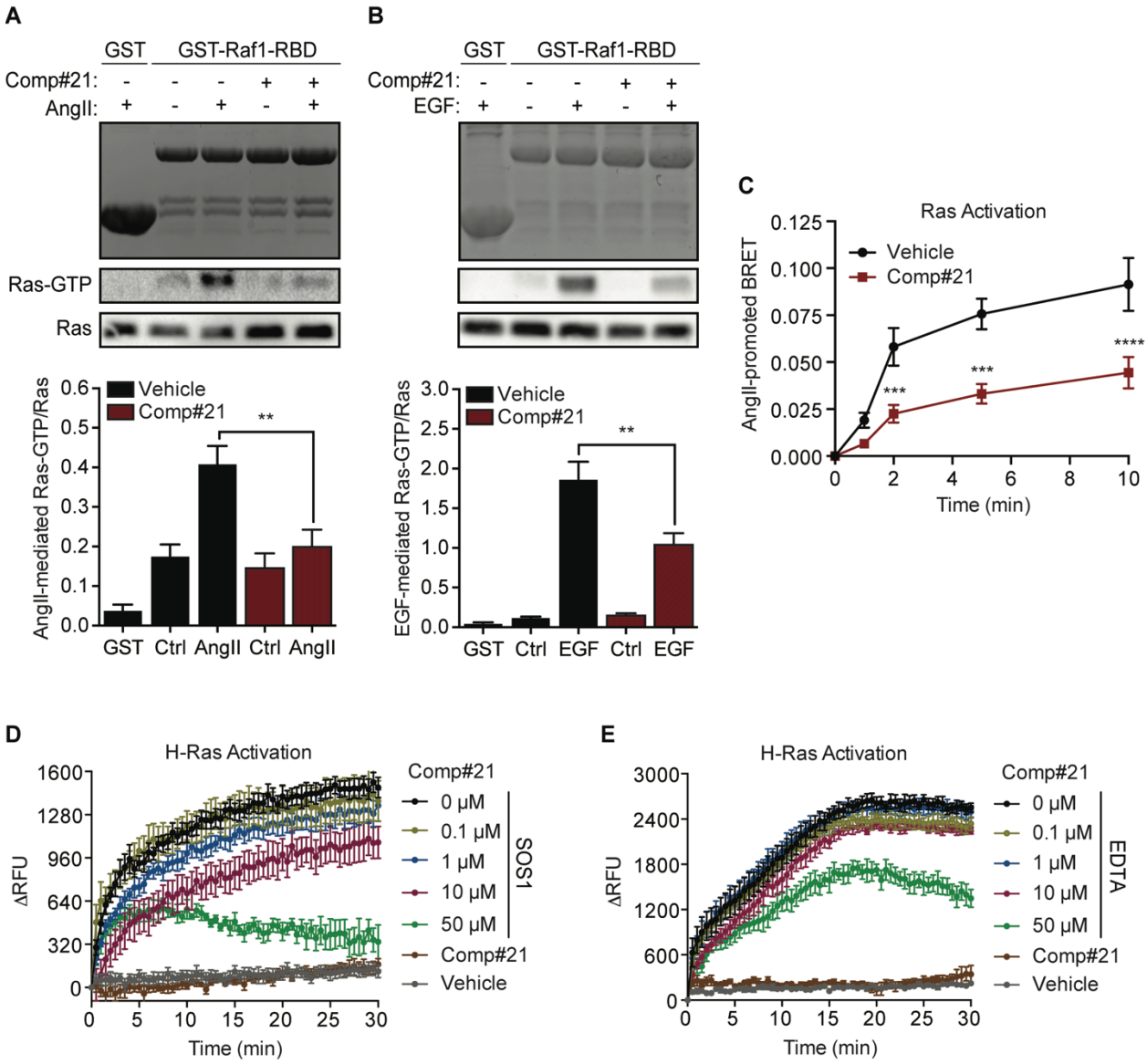
A
GST
GST-Raf1-RBD
Comp#21:
AngII:
Ras-GTP
Ras
Vehicle
Comp#21
AngII-mediated Ras-GTP/Ras
GST Ctrl AngII Ctrl AngII
B
GST
GST-Raf1-RBD
Comp#21:
EGF:
Vehicle
Comp#21
EGF-mediated Ras-GTP/Ras
GST Ctrl EGF Ctrl EGF
C
Ras Activation
Vehicle
Comp#21
AngII-promoted BRET
Time (min)
D
H-Ras Activation
Comp#21
0 μM
0.1 μM
1 μM
10 μM
50 μM
Comp#21
Vehicle
SOS1
ΔRFU
Time (min)
E
H-Ras Activation
Comp#21
0 μM
0.1 μM
1 μM
10 μM
50 μM
Comp#21
Vehicle
EDTA
ΔRFU
Time (min)

**Figure 5.7. Comp#21 inhibits Ras activation. (A, B)** GST pulldown of Ras-GTP using GST and GST-Raf1BD coupled to glutathione beads. Cells transfected with Flag-AT1R were serum starved, pretreated with vehicle (DMSO) or Comp#21 (50 μM) and stimulated or not (control) with 1 μM AngII or 100 ng/ml EGF for 5 min. Coomassie of GST and GST-Raf1-RBD proteins, representative western blots and the quantification of Ras are shown. Ras activation was quantified as the amount of Ras-GTP divided by the total amount of Ras. Data are means ± SEM from three independent experiments, *p < 0.05, **p < 0.001, one-way ANOVA with Bonferroni correction. **(C)** BRET assessment of the kinetics of AT1R-mediated Ras activation. HEK293 cells expressing Raf1-RBD-RlucII and rGFP-CAAX along with Flag-AT1R were serum starved, pretreated with vehicle (DMSO) or Comp#21 (50 μM) for 30 min and stimulated or not with 100 nM AngII at indicated times. Data were quantified as AngII-promoted BRET and represent means ± SEM of three independent experiments, ***p <0.005, ****p < 0.0001, unpaired Student's *t*-test. **(D, E)** In vitro kinetics measurement of fluorescence of mant-GTP exchange into purified H-Ras upon activation by **(D)** purified SOS1 or **(E)** 40mM EDTA and in the presence of vehicle (DMSO) or Comp#21 (at indicated concentrations). The relative fluorescence unit (RFU) was measured every 30 sec for 30 min and quantified as the delta RFU (RFU post-addition measurement minus five averaged RFU pre-addition measurements, per condition). Data represent means ± SEM of three independent experiments.

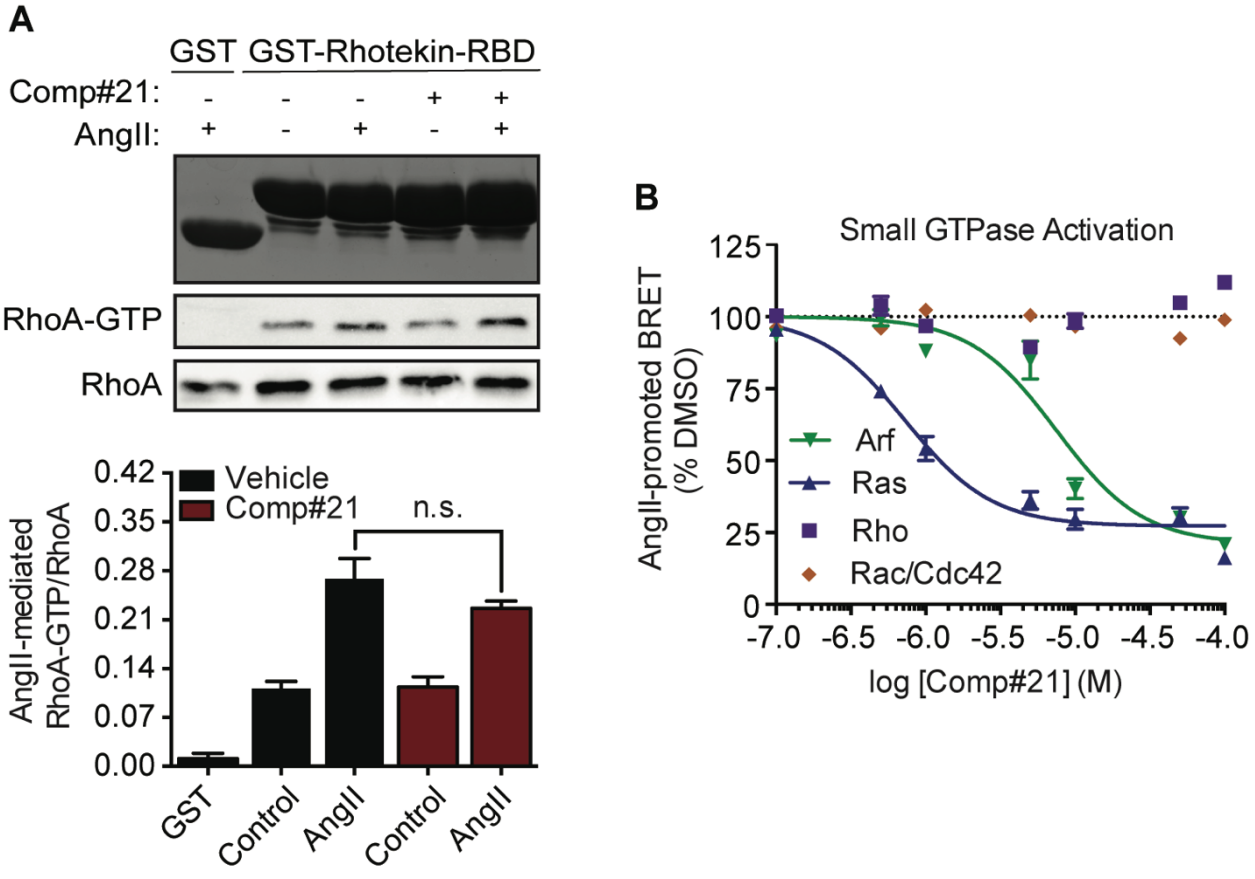
A
GST
GST-Rhotekin-RBD
Comp#21:
AngII:
RhoA-GTP
RhoA
AngII-mediated RhoA-GTP/RhoA
Vehicle
Comp#21
n.s.
GST
Control
AngII
Control
AngII
B
Small GTPase Activation
AngII-promoted BRET (% DMSO)
Arf
Ras
Rho
Rac/Cdc42
log [Comp#21] (M)

**Figure 5.8. Comp#21's effects on the activation of different GTPases. (A)** GST pulldown of Rho-GTP using GST and GST-Rhotekin-RBD coupled to glutathione beads. Cells transfected with Flag-AT1R were serum starved, pretreated with vehicle (DMSO) or Comp#21 (50 μM) and stimulated or not (control) with 1 μM AngII for 5 min. Coomassie of GST and GST-Rhotekin-RBD proteins, representative western blots and the quantification of RhoA are shown. RhoA activation was quantified as the amount of RhoA-GTP divided by the total amount of RhoA. Data are means ± SEM from three independent experiments. **(B)** BRET recording of the activation of Arf, Ras, Rho and Rac/Cdc42 sensors by AT1R. HEK293 cells expressing GGA3-PBD-RlucII, Raf1-RBD-RlucII, PKN-RlucII or PAK-CRIB-RlucII, respectively, and rGFP-CAAX along with Flag-AT1R were serum starved, pretreated with vehicle (DMSO) or Comp#21 (at indicated concentrations) for 30 min and stimulated or not with 100 nM AngII for 10 min (Arf6), 5 min (Ras) or 2 min (Rho and Rac/Cdc42). BRET responses were quantified as AngII-promoted BRET, percent compared to vehicle (DMSO, dotted line) and represent means ± SEM of three to four independent experiments.

5.2.5. Rasarfin targets Ras to inhibit signaling and Arf6 to block receptor internalization

Since Rasarfin inhibits both receptor internalization and signaling, the contribution of Ras and Arf6 in both pathways was assessed next. To determine if Ras is involved in receptor internalization, the removal of AT1R from the PM was assessed as previously performed in Figure 5.4. Cells expressing AT1R, trafficking sensors and either mock, wild type K-Ras or the dominant negative K-Ras-S17N were stimulated with AngII. Kinetic experiments show no difference between wild type and S17N K-Ras in affecting AT1R internalization (Figure 5.9A), consistent with Arf6 being Comp#21's target for inhibiting receptor internalization, whereas Ras is not involved. To determine the roles of Ras and Arf6 in MAPK activation, HEK293 cells were transfected with AT1R and either the wild type or dominant negative form of each GTPase, and their AngII-mediated ERK1/2 phosphorylation was assessed by western blot. Cells overexpressing Arf6-T27N displayed a similar (or better) kinetics of AngII-mediated ERK1/2 activation as cells expressing Arf6-WT (Figure 5.9B), whereas the overexpression of K-Ras-WT increased the phosphorylation of ERK1/2 over time more than mock (data not shown) and this increase was inhibited by overexpressing K-Ras-S17N, with a similar profile to mock conditions (Figure 5.9C). This confirms Ras' involvement in the MAPK cascade, whereas Arf6 does not seem to play a role. These data also suggest Ras and Arf6 are not involved in the same pathways to modulate receptor internalization and signaling to MAPK. Therefore, it can be concluded that Rasarfin's effects on ERK1/2 activation are Arf6-independent and its effects on AT1R internalization are Ras-independent.

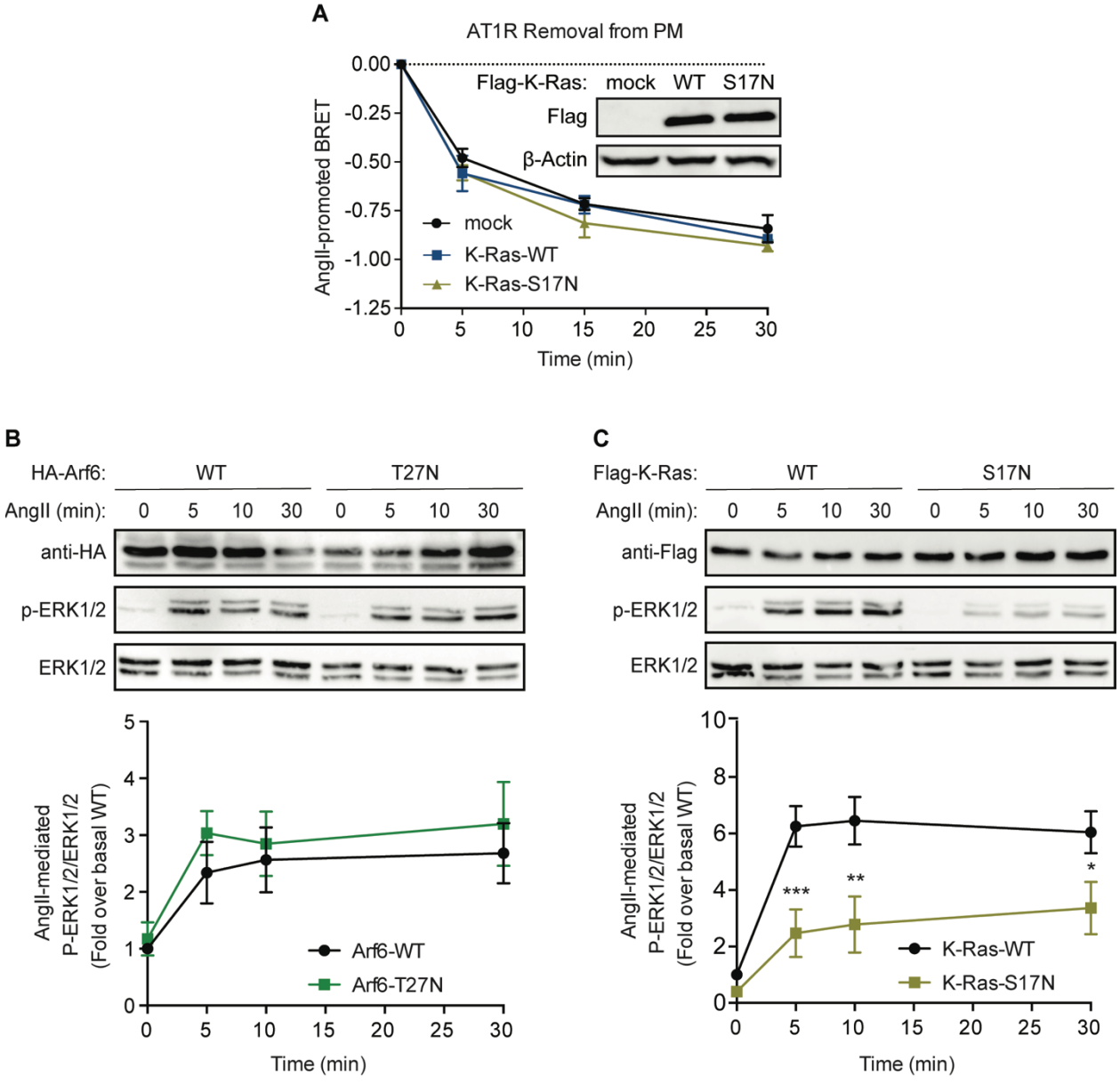
A
AT1R Removal from PM
AngII-promoted BRET
0.00
-0.25
-0.50
-0.75
-1.00
-1.25
Flag-K-Ras: mock WT S17N
Flag
β-Actin
mock
K-Ras-WT
K-Ras-S17N
0 5 10 15 20 25 30
Time (min)
B
HA-Arf6: WT T27N
AngII (min): 0 5 10 30 0 5 10 30
anti-HA
p-ERK1/2
ERK1/2
AngII-mediated P-ERK1/2/ERK1/2 (Fold over basal WT)
0 1 2 3 4 5
Arf6-WT
Arf6-T27N
0 5 10 15 20 25 30
Time (min)
C
Flag-K-Ras: WT S17N
AngII (min): 0 5 10 30 0 5 10 30
anti-Flag
p-ERK1/2
ERK1/2
AngII-mediated P-ERK1/2/ERK1/2 (Fold over basal WT)
0 2 4 6 8 10
***
**
*
K-Ras-WT
K-Ras-S17N
0 5 10 15 20 25 30
Time (min)

**Figure 5.9. The effects of Ras and Arf6 on receptor internalization and MAPK activation.** **(A)** BRET assessment of the kinetics of AT1R removal from the plasma membrane. Cells were transfected with AT1R-RlucII, rGFP-CAAX and either mock (pcDNA3.1), Flag-K-Ras-WT or Flag-K-Ras-S17N and stimulated or not with AngII at indicated times. BRET responses were quantified as AngII-promoted BRET and represent means ± SEM of three independent experiments. Shown above are representative western blots of Flag-tagged proteins and β-actin as a loading control. **(B, C)** Kinetics of AT1R-mediated ERK1/2 activation with K-Ras and Arf6 defective mutants. Cells were transfected with Flag-AT1R and HA-Arf6-WT, HA-Arf6-T27N, Flag-K-Ras-WT or Flag-K-Ras-S17N, serum starved and stimulated or not with 1 μM AngII at indicated times. Shown are representative western blots of HA, Flag, phosphorylated and total ERK1/2 protein, quantified as p-ERK over ERK and normalized as fold over basal. Data represent mean ± SEM of three independent experiments, *$p < 0.05$, **$p < 0.01$, ***$p < 0.005$, unpaired Student's *t*-test.

5.2.6. Computational studies reveal that Rasarfin binds Ras at the interface between Ras and SOS

The increased potency of Rasarfin on Ras than Arf6 prompted us to determine the binding site of Rasarfin on Ras and validate Ras as Rasarfin's target. Rasarfin in its proposed binding site was examined using molecular dynamics simulations and applying flexible docking of the molecule into the SOS1-bound X-ray structure of H-Ras (PDB: 1BKD) (see Chapter 3.11). A 100 ns simulation showed that the compound is stably bound in the effector binding interface between switch I and switch II of Ras (Figure 5.10A). Interactions between Rasarfin and Ras were then computed to determine which pharmacophores on Rasarfin bind to which residues on Ras. At the top end of the molecule, the benzofuran forms aromatic and hydrophobic interactions with the Thr74, Leu56, and Tyr40 residues of Ras (Figure 5.10B). There is a hydrogen bond (green arrow) that is formed between the amide on Rasarfin and the carbonyl oxygen of the backbone of Ile55. Furthermore, residues Thr74, Leu56, Tyr40, Ile55, Thr20, Ile21, Tyr32, Ala59 on Ras collectively form a strong hydrophobic pocket around the Chloro-atom on the phenyl ring in the center of Rasarfin, which stabilizes the aromatic ring and the compound. Lastly, the isopropyl moiety at the bottom end of the molecule is mainly oriented toward switch II and interacts with residues Ala59, Ile21 and Tyr32 on Ras (Figure 5.10B).

When docking Rasarfin into Ras with SOS bound, Rasarfin seems to be superimposed onto SOS inside the SOS-Ras complex. Rasarfin (in purple) establishes similar interactions with Ras (in grey) as SOS (in yellow) (Figure 5.10C). The alkyl chain of the Lys939 residue on SOS shares a H-bond with Asp57 in Ras and reaches into the binding groove, showing a similarly elongated conformation like Rasarfin. Furthermore, the furan of the benzofuran of Rasarfin is overlaying well with the His911 on SOS, which allows pi-pi stacking of the two aromatic rings. Residue

His911 on SOS reaches into the binding interface and interacts with Asp54 on Ras via a H-bond. Here, it is suggested that the benzofuran moiety of Rasarfin occupies the space of His911. Similarly, the hydrophobic residue Leu938 on SOS, which allows van der Waals interactions with the Ala59 on Ras, is located in close vicinity to the isopropyl moiety on Rasarfin, which also forms van der Waals interaction with the Ala59 on Ras (Figure 5.10C).

To gain insight into the indubitable importance of the Cl-substitution on the aromatic ring, an analog of Rasarfin with only the Cl- removed, **21.4**, was similarly docked into the calculated binding site of the SOS1-bound X-ray structure of H-Ras (PDB: 1BKD). Interactions between the pharmacophores in **21.4** and residues in Ras were then computed. **21.4**'s phenyl ring of the benzofuran interacts with Leu56 and Tyr40. The center phenyl ring without the chlorine forms weak hydrophobic interactions with Leu56, Thr20, Tyr32 and Tyr40 residues on Ras. Finally, hydrophobic interactions of the isopropyl moiety and Tyr32 can be observed (Figure 5.10D). Due to its missing chloro-substituent, **21.4**'s most favorable conformation contains less favorable van der Waals interactions with the Ras pocket compared to Rasarfin. In fact, when docking the two compounds simultaneously, we see that Rasarfin (in green) remains tightly bound to Ras for the entire 100ns simulation, while main interactions are disrupted with **21.4** (in red) and it detaches from the binding groove of Ras fairly quickly (Supplementary Video).

Rasarfin's binding mode was then validated by mutating select residues in Ras at the Ras-SOS interface that make important contacts with Rasarfin, such as Tyr32 and Tyr40, which are both located on switch I. To assess the inhibitory action of Rasarfin over different Ras subtypes, these two tyrosine residues were mutated to an alanine in K-Ras (single Y32A, Y40A and double Y32A/Y40A mutants) within the same Rasarfin binding site found in H-Ras ($Lys^{5}$-$Thr^{74}$). This

domain and residues are perfectly conserved among the Ras family members (Lukman, Grant, Gorfe, Grant, & McCammon, 2010; Wennerberg, Rossman, & Der, 2005). These were then overexpressed in cells along with AT1R and the Ras BRET sensor to assess Comp#21's effects on their activation. In the vehicle conditions, cells expressing K-Ras-Y32A or K-Ras-Y40A activated Ras sensor similarly to K-Ras-WT, whereas the double mutation (K-Ras-Y32A/Y40A) decreased by 45% the AngII-mediated Ras activation (compare black bars in Figure 5.11A). This is consistent with the decreased protein expression level of K-Ras-Y32A/Y40A seen in the Flag blot below. In fact, the pattern of decreased BRET response and protein expression level of the three K-Ras mutants is comparable to their ability to activate ERK1/2. Compared to cells expressing K-Ras-WT, cells expressing K-Ras-Y40A or K-Ras-Y32A/Y40A show a decreased phosphorylation of ERK1/2 (Figure 5.11B). Despite the important reduction in AT1R-mediated activation of K-Ras-Y32A/Y40A double mutant observed as compared to the other mutants and WT-K-Ras, only WT-K-Ras was significantly inhibited by Rasarfin (Figure 5.11A). Next, Rasarfin's effects on K-Ras-Y32A were then validated *in vitro* using purified wild type K-Ras and K-Ras-Y32A. As previously performed, each Ras was activated using purified SOS1 in the presence of vehicle (DMSO) or Rasarfin. Compared to vehicle, there is a decreased uptake of fluorescent mant-GTP into K-Ras-WT but not K-Ras-Y32A in the presence of Rasarfin with SOS1 (Figure 5.11C), confirming that Tyr32 is an important Ras residue for Rasarfin binding.

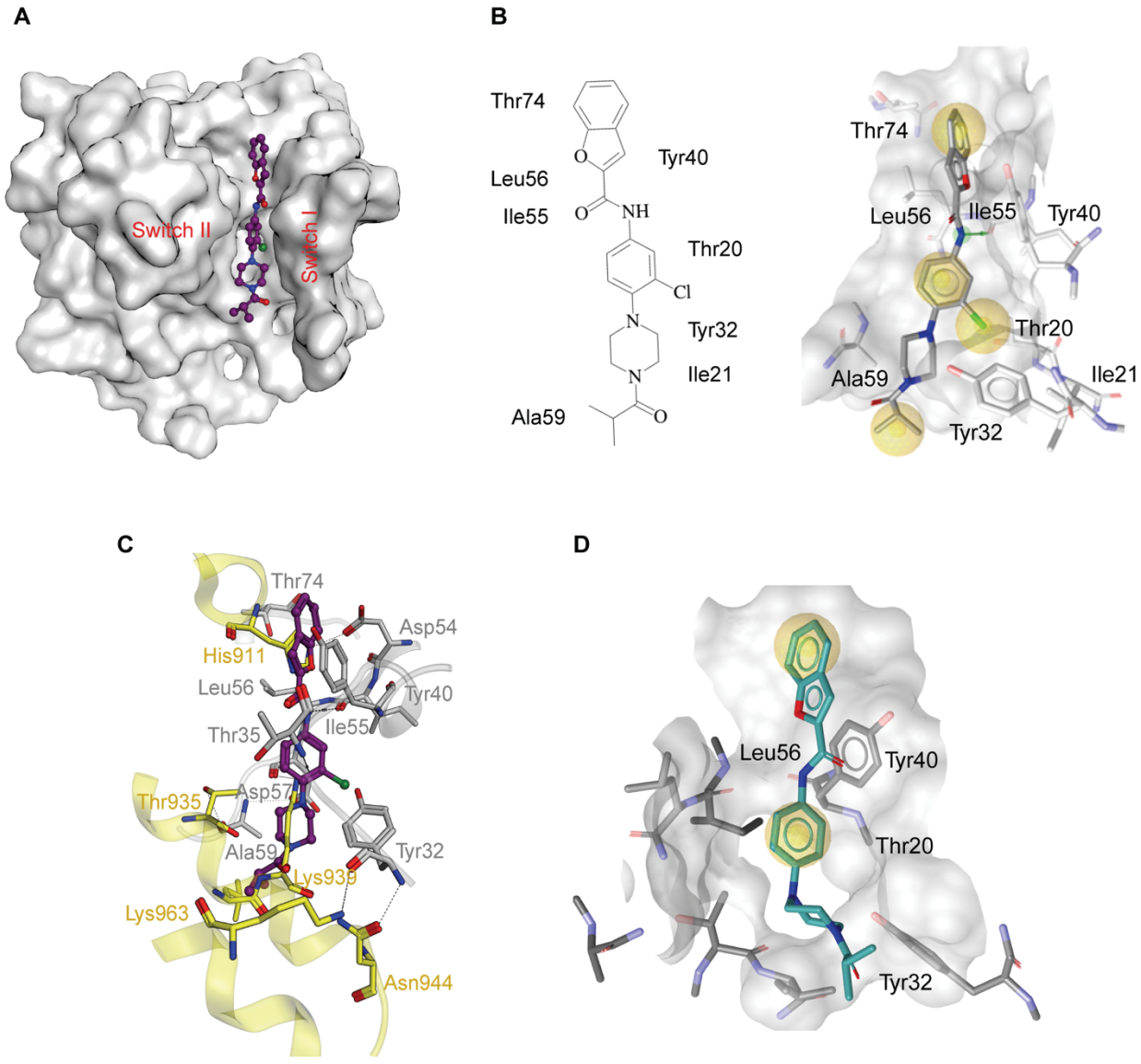
A
Switch II
Switch I
B
Thr74
Tyr40
Leu56
Ile55
Thr20
Cl
Tyr32
Ile21
Ala59
O
NH
N
Thr74
Leu56
Ile55
Tyr40
Thr20
Ile21
Ala59
Tyr32
C
Thr74
Asp54
His911
Leu56
Tyr40
Thr35
Ile55
Thr935
Asp57
Ala59
Tyr32
Lys939
Lys963
Asn944
D
Leu56
Tyr40
Thr20
Tyr32

**Figure 5.10. Computational studies reveal important interactions between Rasarfin and Ras.** **(A)** Ball and stick representation of Rasarfin (purple) bound to the groove between switch I and switch II on Ras (protein surface in grey). Snapshot of the bound compound after 100ns MD simulation. **(B)** 2D structure of Rasarfin with Ras residues labeled where they form interactions with Rasarfin. Stick representation of Rasarfin (in grey) embedded in the binding pocket of Ras (in grey). The same Ras residues interacting with Rasarfin are labeled. Yellow spheres correspond to hydrophobic interactions and green arrow shows H-bond donor on Rasarfin. **(C)** Rasarfin superimposed onto the Ras-SOS interface. Rasarfin is displayed in purple, using ball and stick representation. SOS residues are depicted in yellow and residues of Ras in grey. Interactions are shown as dashed lines. **(D)** Stick representation of **21.4** (aqua) embedded in the binding pocket of Ras (in grey). Yellow spheres correspond to hydrophobic interactions.

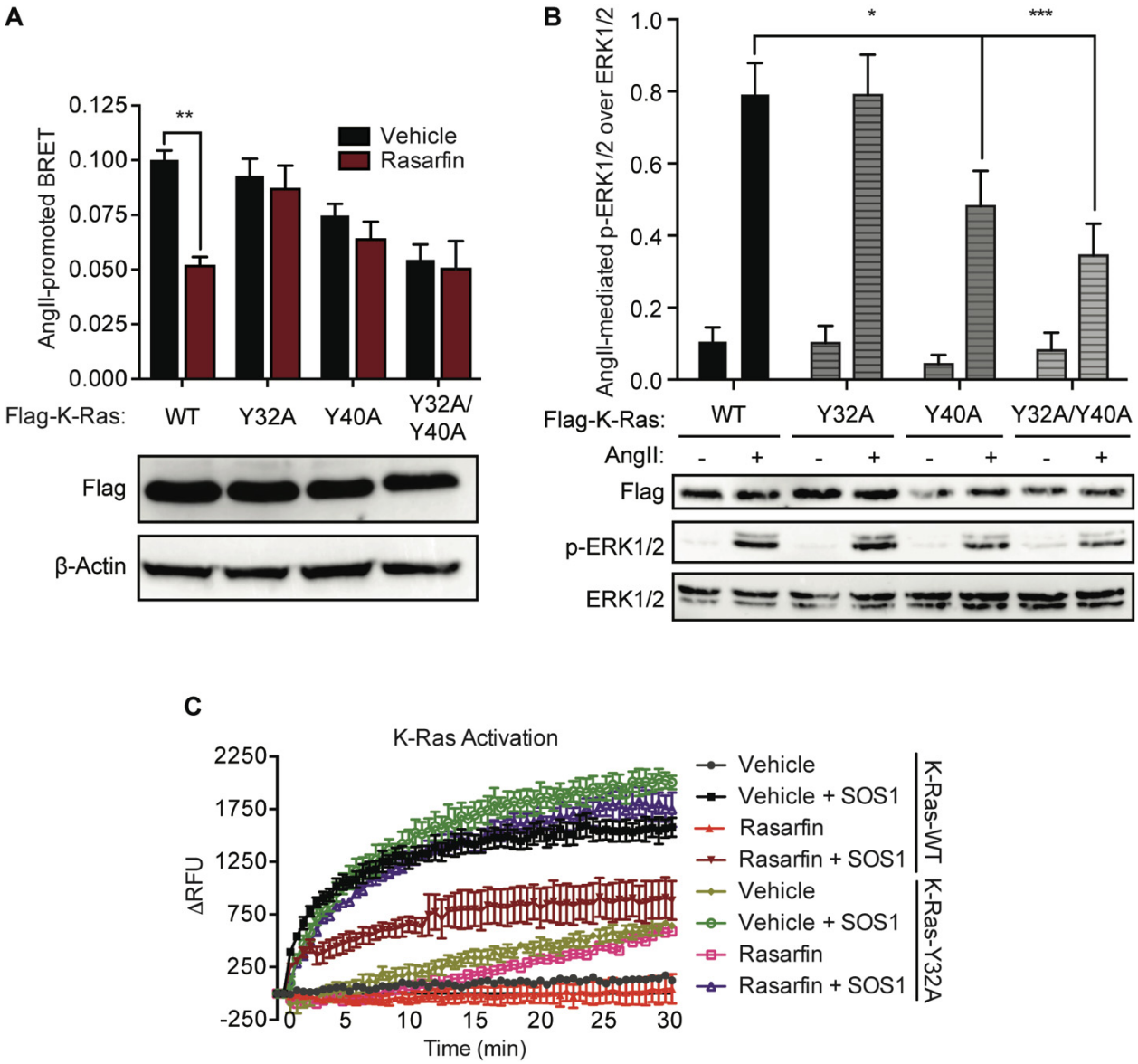
A
AngII-promoted BRET
0.125
0.100
0.075
0.050
0.025
0.000
**
Vehicle
Rasarfin
Flag-K-Ras:
WT
Y32A
Y40A
Y32A/
Y40A
Flag
β-Actin
B
AngII-mediated p-ERK1/2 over ERK1/2
1.0
0.8
0.6
0.4
0.2
0.0
*
***
Flag-K-Ras:
WT
Y32A
Y40A
Y32A/Y40A
AngII:
- + - + - + - +
Flag
p-ERK1/2
ERK1/2
C
K-Ras Activation
ΔRFU
2250
1750
1250
750
250
-250
0
5
10
15
20
25
30
Time (min)
Vehicle
Vehicle + SOS1
Rasarfin
Rasarfin + SOS1
Vehicle
Vehicle + SOS1
Rasarfin
Rasarfin + SOS1
K-Ras-WT
K-Ras-Y32A

**Figure 5.11. Validation of the binding mode of Rasarfin on Ras. (A)** BRET recordings of Ras sensor activation by AT1R with K-Ras mutants. HEK293 cells were transfected with Flag-AT1R, Raf1-RBD-RlucII, rGFP-CAAX and either Flag-K-Ras-WT, Flag-K-Ras-Y32A, Flag-K-Ras-Y40A or Flag-K-Ras-Y32A/Y40A, serum starved, pretreated with vehicle (DMSO) or Rasarfin (50 μM) for 30 min and stimulated or not with 100 nM AngII for 5 min. BRET responses were quantified as AngII-promoted BRET and represent means ± SEM of four independent experiments, **p < 0.001, two-way ANOVA with Bonferroni correction. Shown below are representative western blots of Flag-tagged proteins and β-actin. **(B)** AT1R-mediated ERK1/2 activation with K-Ras mutants. Cells were transfected with Flag-AT1R and either Flag-K-Ras-WT, Flag-K-Ras-Y32A, Flag-K-Ras-Y40A or Flag-K-Ras-Y32A/Y40A, serum starved and stimulated or not with 1 μM AngII for 5 min. Shown are representative western blots of Flag, phosphorylated and total ERK1/2 protein, quantified above as p-ERK over ERK. Data represent means ± SEM of seven independent experiments, *p < 0.05, ***p <0.005, two-way ANOVA with Dunnett's test. **(C)** In vitro kinetics measurement of fluorescence of mant-GTP binding to purified K-Ras-WT and K-Ras-Y32A upon activation by purified SOS1 and in the presence of vehicle (DMSO) or Rasarfin (50 μM). The relative fluorescence unit (RFU) was measured every 30 sec for 30 min and quantified as the delta RFU. Data represent means ± SEM of three independent experiments.

## 5.3. Summary

In this chapter, the mechanism of action of small molecule Comp#21 was characterized and named Rasarfin since it was shown to selectively inhibit small G proteins Ras and Arf6 but not heterotrimeric or other small G proteins. Rasarfin blocks agonist-promoted endocytosis of AT1R, B2R and β2AR and inhibits the activation of ERK1/2 by these receptors, including EGFR, as well as the activation of Akt. Furthermore, molecular dynamics simulations reveal important contact points between Rasarfin and Ras at the interface between Ras and its GEF SOS1, as well as the role the chlorine group on the phenyl ring of Rasarfin plays in stabilizing these interactions.

# CHAPTER 6. RESULTS

## IDENTIFICATION OF FUNCTIONALLY SELECTIVE ANALOGS OF RASARFIN

## 6.1. Preface to Chapter 6

Structure activity relationship (SAR) studies were performed on Rasarfin to determine which chemical groups are important for Rasarfin's function in order to optimize its potency and/or selectivity for Ras and Arf6. Here, I designed, performed and analyzed all experiments.

## 6.2. Results

### 6.2.1. SAR studies identify Rasarfin analogs that inhibit endocytosis and/or MAPK

Rasarfin's chemical groups (circled in red) were modified to generate eight different analogs (Figure 6.1A). The activity of these compounds was first tested on AT1R internalization, using the same BRET sensor as previously used for the HTS, and compared to the effect of Rasarfin. Results show that after 30 min of AT1R stimulation, Rasarfin blocked ~50% of receptor internalization compared to vehicle (DMSO), while **21.7** and **21.8** blocked ~30% and ~20%, respectively, and **21.1** to **21.6** had no significant effect (Figure 6.1B). The activity of **21.1** to **21.8** was then tested on the AT1R-mediated MAPK activation as done previously (Figure 5.5A). After 5 min receptor stimulation with AngII, ERK1/2 phosphorylation was inhibited by 85% and 70% with Rasarfin and **21.8**, respectively, while **21.2** and **21.7** inhibited ~20% each and **21.1**, **21.3**, **21.4**, **21.5** and **21.6** had no effect compared to vehicle (Figure 6.1C).

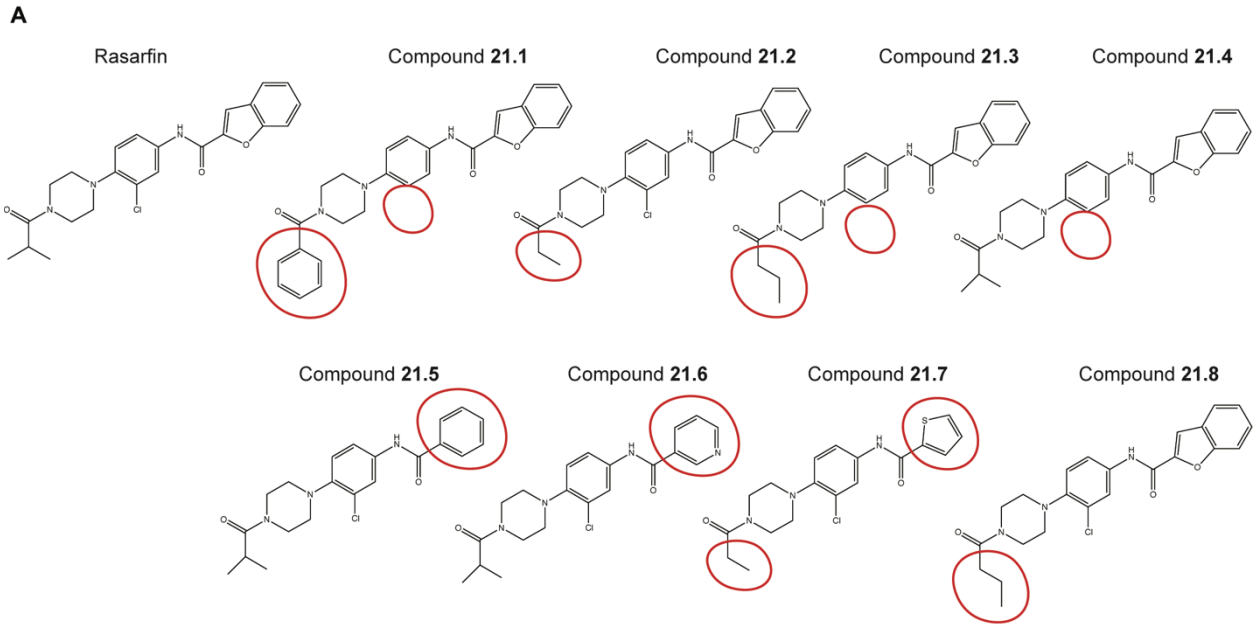
A
Rasarfin
Compound 21.1
Compound 21.2
Compound 21.3
Compound 21.4
Compound 21.5
Compound 21.6
Compound 21.7
Compound 21.8

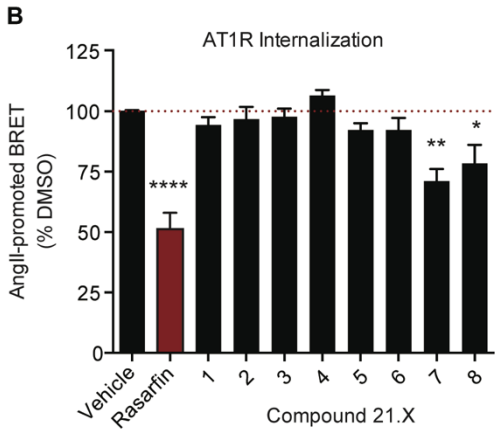
B
AT1R Internalization
AngII-promoted BRET (% DMSO)
125
100
75
50
25
0
****
**
*
Vehicle
Rasarfin
1
2
3
4
5
6
7
8
Compound 21.X

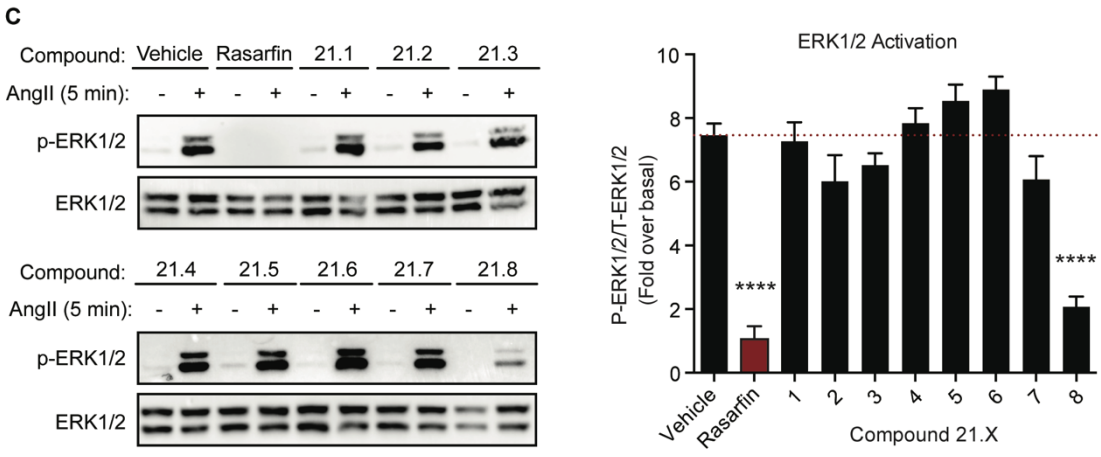
C
Compound: Vehicle Rasarfin 21.1 21.2 21.3
AngII (5 min): - + - + - + - + - +
p-ERK1/2
ERK1/2
Compound: 21.4 21.5 21.6 21.7 21.8
AngII (5 min): - + - + - + - + - +
p-ERK1/2
ERK1/2
ERK1/2 Activation
P-ERK1/2/T-ERK1/2 (Fold over basal)
10
8
6
4
2
0
****
****
Vehicle
Rasarfin
1
2
3
4
5
6
7
8
Compound 21.X

**Figure 6.1. SAR studies identify Rasarfin analogs that inhibit endocytosis and/or MAPK.** **(A)** Structures of Compounds **21.1**-**21.8**, analogs of Rasarfin. Modified chemical groups are circled in red. **(B)** BRET recording of AT1R internalization into endosomes. Cells were transfected with AT1R-RlucII and rGFP-FYVE, serum starved, pretreated with vehicle (DMSO), 50 μM Rasarfin or **21.1**-**21.8** for 30 min and stimulated or not with 100 nM AngII for 30 min. BRET responses were quantified as AngII-promoted BRET, percent compared to vehicle (DMSO, red dotted line). Data represent means ± SEM of four independent experiments, *p < 0.05, **p < 0.001, ****p < 0.0001, one-way ANOVA with Dunnett's test. **(C)** AT1R-mediated ERK1/2 activation. Cells were transfected with Flag-AT1R, serum starved, pretreated with vehicle (DMSO), 50 μM Rasarfin or **21.1**-**21.8** for 30 min then stimulated or not with 1 μM AngII for 5 min. Shown are representative western blots of phosphorylated and total ERK1/2 protein, quantified as p-ERK1/2 over ERK1/2 and normalized as fold over basal. Red dotted line: vehicle (DMSO). Data represent means ± SEM of five independent experiments, ****p < 0.0001, one-way ANOVA with Dunnett's test.

6.2.2. Functional selectivity of Compounds **21.4, 21.7** and **21.8**

Since Compounds **21.7** and **21.8** showed some selectivity towards receptor internalization and/or MAPK activation, they were studied further. Their direct effects on Ras were next determined *in vitro* using **21.4** as a negative control. As previously performed, purified H-Ras was activated using EDTA or purified SOS1 in the presence of vehicle (DMSO), Rasarfin, **21.4**, **21.7** or **21.8**. Compared to vehicle, there is a decreased uptake of fluorescent mant-GTP into H-Ras in the presence of Rasarfin and **21.8** with both EDTA (Figure 6.2A) and SOS1 (Figure 6.2B), whereas **21.4** and **21.7** had no effect in either case. These data are consistent with the MAPK data (Figure 6.1C), suggesting that **21.8** inhibits ERK1/2 phosphorylation through Ras. Therefore, its effect on Ras activation was assessed next using the Ras BRET sensor. Consistent with their similar structures, Rasarfin and **21.8** inhibited Ras by 47% and 45%, respectively, whereas **21.4** and **21.7** did not have an effect on Ras activation (Figure 6.2C). Yet, when the Arf BRET sensor was used to compare the effect of the three analogs on Arf activation, only Rasarfin and **21.8** had a significant inhibitory effect (Figure 6.2D).

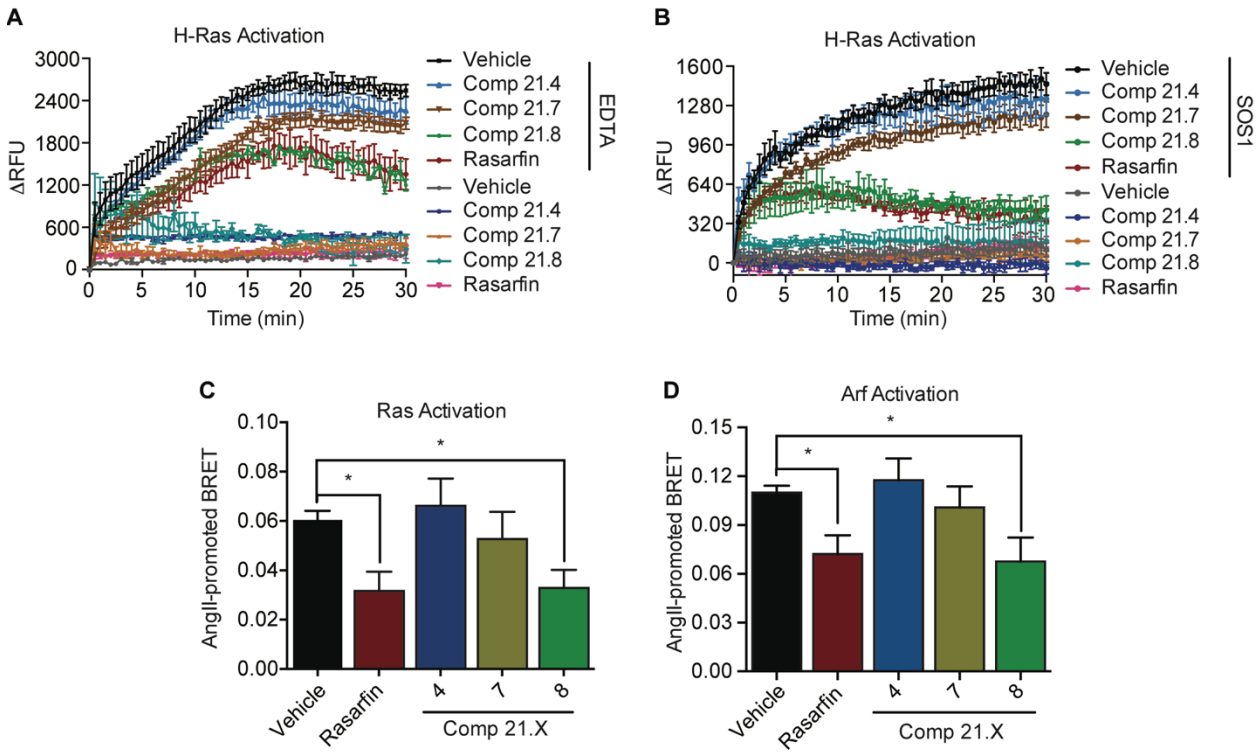


**Figure 6.2. Functional selectivity of Compounds 21.4, 21.7 and 21.8. (A, B**) In vitro kinetics of mant-GTP uptake into H-Ras. Purified H-Ras was activated using **(A)** 40mM EDTA or **(B)** purified SOS1 in the presence of vehicle (DMSO), 50 µM Rasarfin, **21.4**, **21.7** or **21.8**. The relative fluorescence unit (RFU) was measured every 30 sec for 30 min and quantified as the delta RFU. Data represent means ± SEM of three independent experiments. **(C)** BRET assessment of AT1R-mediated Ras activation. HEK293 cells expressing Raf1-RBD-RlucII and rGFP-CAAX along with Flag-AT1R were serum starved, pretreated with vehicle (DMSO) or 50 µM Rasarfin, **21.4**, **21.7** or **21.8** for 30 min and stimulated or not with 100 nM AngII for 5 min. **(D)** BRET assessment of AT1R-mediated Arf activation. HEK293 cells expressing GGA3-PBD-RlucII and rGFP-CAAX along with Flag-AT1R were serum starved, pretreated with vehicle (DMSO) or 50 µM Rasarfin,

**21.4**, **21.7** or **21.8** for 30 min and stimulated or not with 100 nM AngII for 10 min. Data were quantified as AngII-promoted BRET and represent means ± SEM of five independent experiments, *p <0.05, unpaired Student's *t*-test.

## 6.3. Summary

In this chapter, SAR studies were performed to generate eight analogs of Rasarfin. Screening the compounds on AT1R internalization and ERK1/2 signaling revealed **21.7**'s partial selectivity towards receptor internalization and **21.8**'s similar selectivity towards MAPK and Ras activation as Rasarfin.

# CHAPTER 7. GENERAL DISCUSSION

7.1. Development of new BRET sensors

The study of signaling events by receptors and pharmacological agents to develop new therapeutics requires sensitive and reliable assays. In the past, small G protein activity has been monitored using effector binding domains. As the largest GTPase family identified, Ras was the first protein for which probes were developed as a basis for further studies on these proteins. In 1997, the minimal Ras-binding domain (RBD) of Raf1 (amino acids 51-131) was found to serve as an activation-specific probe for Ras since it can strongly and specifically bind Ras-GTP versus Ras-GDP (de Rooij & Bos, 1997) and has since been used for both biochemical and live-cell imaging studies of Ras activation (Rubio, 2005). For example, to directly visualize the compartmentalization of Ras and Raf proteins, (Jiang & Sorkin, 2002) fused CFP/YFP at the amino and carboxyl terminus, respectively, and used live-cell fluorescence imaging microscopy combined with the fluorescence resonance energy transfer (FRET) technique to study the involvement of these proteins in the activation of Ras. CFP-Ras was found to bind GTP and was converted to GDP by a GAP, whereas SOS GEF promoted association of CFP-Ras with GTP. Moreover, the Ras binding domain of c-Raf-1 (RBD) tagged with YFP (RBD-YFP) specifically bound to GTP-loaded CFP-Ras, which allowed energy transfer from CFP-Ras to RBD-YFP (Jiang & Sorkin, 2002). Here, FRET microscopy is used to visually monitor the interaction of Ras and Raf, localizing within the same compartment, which results in an increase in fluorescence. In this thesis, we have taken a similar approach to develop a BRET sensor to quantitatively measure Ras activity by tagging the Ras binding domain of Raf1 with RlucII (Raf1-RBD-RlucII) and monitoring its recruitment to the plasma membrane tagged with rGFP (rGFP-CAAX) upon the activation of Ras by receptors, resulting in a BRET response.

Moreover, biochemical approaches used to study small GTPase activation, such as the GST pulldown (Vikis & Guan, 2004) have only limited temporal resolution, have no spatial resolution, are difficult to quantify, and are not always amenable for high-throughput monitoring of responses in living cells. Therefore, BRET-based sensors, which are more quantitative, have been developed to study Ras activation using an intramolecular Ras-RBD construct that changes conformation upon AngII and EGF stimulation of Ras (Balla et al., 2011) or by tagging and monitoring the interaction between different mutant Ras and effector proteins (Bery et al., 2018; Bery & Rabbitts, 2019). In our case, the sensors monitor Raf trafficking to the PM, which will only occur when Ras is activated. Therefore, an increase in BRET response is an indirect measure of Raf-RBD binding to Ras-GTP. Compared to the two previously described BRET sensors, we also restricted our study to Ras interaction with wild type Raf-RBD. However, since Ras itself is not fluorescently tagged, we have the flexibility to overexpress any defective Ras protein of interest and monitor its interaction with Raf. The caveat is that the sensor also records the response from the endogenous Ras still present in the system and possibly competes for Raf binding. However, the increase and decrease in BRET responses recorded from overexpressing constitutively active and dominant negative GTPase forms, respectively, confirmed that the sensors can record defective GTPase activity accordingly. Cells transfected with K-Ras-G12V and K-Ras-S17N, and $SOS^{cat}$-CAAX showed no further effector recruitment after AT1R stimulation because the GTPases' constitutive activity inherently recruited the effectors to the PM, independently of receptor stimulation.

These approaches used to study Ras have been applied to study the activation of other GTPases, such as Arfs, where a fragment of a downstream effector protein is fused to fluorescent reporter proteins that constitute a FRET donor/acceptor pair. To localize Arf activation inside live

cells, the FRET pair is based on the interaction between GTP-bound Arfs and GGA-family protein GGA and Tom1 (GAT) domains. Efficient energy transfer is achieved when an activated nucleotide-bound Arf binds to the GAT domains of downstream effector GGA3, which is regulated by a GAP and a GEF (Beemiller, Hoppe, & Swanson, 2006; B. Hall et al., 2008). However, this FRET energy transfer efficiency is still too low for accurate quantification. Therefore, we took a similar approach to develop the first BRET sensor to measure Arf activity with greater sensitivity. We tagged the protein binding domain of GGA3 with RlucII (GGA3-PBD-RlucII) and monitored its recruitment to the plasma membrane tagged with rGFP (rGFP-CAAX) upon the activation of Arf by receptors, resulting in a BRET response. Since the PBD region of GGA3 has a high affinity for both Arf1-GTP and Arf6-GTP, we could not exclude the fact that the sensor may record both Arf1 and Arf6 activation, which would complicate the interpretation of the BRET sensor activation data with Rasarfin. However, the GST pulldown assays for Arf1 and Arf6 activation show that Rasarfin inhibits Arf6 only. One way to circumvent this limitation is to overexpress the GTPase of interest to specifically study its activation.

As for measuring Rac activity, others have similarly tagged a fragment of p21 activated kinase (PAK) effector, which binds specifically to activated and tagged Rac1, generating a FRET response (Hanna, Miskolci, Cox, & Hodgson, 2014; Hodgson, Shen, & Hahn, 2010). Moreover, to measure Cdc42 activation, cysteine labeling was used to incorporate the environment sensitive fluorophore 4-N,N-dimethylamino-1,8-naphthalimide (4-DMN) into the GTPase binding domain of the WASP protein. This construct binds only the active, GTP-bound conformation of Cdc42 to produce a fluorescence signal (Goguen, Loving, & Imperiali, 2011). In this thesis, we show the development of the first BRET sensor to measure Rac/Cdc42 activity by using a similar approach

to the Rac FRET sensor. We tagged the CRIB domain of PAK with RlucII (PAK-CRIB-RlucII) and monitored its recruitment to the plasma membrane tagged with rGFP (rGFP-CAAX) upon the activation of Rac by receptors, resulting in a BRET response. Similar to the PBD domain of GGA3, the CRIB region of PAK has a high affinity for both Rac-GTP and Cdc42-GTP, so we could not either exclude that this sensor may record both Rac and Cdc42 activation. Similar to the Arf sensor, the overexpression of GTPase of interest could resolve this issue. When validating the Rac/Cdc42 BRET sensor, we used defective forms of Rac1 only. Although the exercise was not done with overexpressing Cdc42 defective proteins, we assumed the results would be similar to Rac1 defective proteins given that Rac and Cdc42 interact similarly with PAK-PBD, therefore, we named it Rac/Cdc42 sensor.

Unlike BRET sensors, FRET approaches have been mainly used for live-cell imaging and therefore, not suited for target kinetics and pharmacological experiments for drug discovery. On the other hand, these new GTPase BRET sensors can differentiate the activation profiles of the GTPases and receptors in terms of kinetics and potency. Our data showed that AngII is a better activator of Arf than EGF, whereas EGFR is a more potent activator of Ras than AT1R, and that Rac/Cdc42 has the fastest kinetics and is similarly activated by both receptors. In HEK293 cells, AT1R-mediated protein trafficking to endosomes or ER and Golgi mainly involves Arfs proteins, whereas EGFR has not been shown to be heavily involved in the activation of Arf-mediated pathways. Therefore, the AT1R-mediated activation of Arfs is more easily detected by the BRET sensors than the BRET responses of Arf activation mediated by EGFR. The opposite is true for Ras activation, where we see a greater BRET response for EGFR-mediated activation of the Ras sensor compared to AT1R, consistent with EGFR being the main activator of Ras and Ras

pathways and AT1R having a less prominent role in directly activating Ras because AT1R can mediate Ras pathways by other means such as G proteins and β-arrestin. On the other hand, most research on Rac/Cdc42 activation has shown to be mainly activated by EGFR. Therefore, the similar activation profile recorded by AT1R and EGFR by the Rac/Cdc42 BRET sensors could provide insight into a more prominent role for AT1R in activating Rac and Cdc42 proteins.

Akt signaling has also been previously measured using FRET-based kinase activity reporters. One design is based on a kinase-dependent molecular switch flanked by a pair of fluorescent proteins, which consists of a substrate domain and a phosphoamino acid binding domain. Phosphorylation of the substrate causes an intramolecular reorganization due to binding of the phospho-substrate to the binding domain, which leads to a change in the distance or orientation between the FRET pair, resulting in a change in FRET recording (Gao & Zhang, 2008). This intramolecular change in protein conformation upon kinase phosphorylation approach is what we recently used to design BRET sensors for measuring PKC activity (Namkung et al., 2018). Another group has engineered a fluorescent fusion protein to assess Akt activity at the single cell level. A clover FP was fused to FoxO1 transcription factor, a well-characterized Akt substrate that contains three Akt phosphorylation sites. The FoxO1-clover reporter protein rapidly translocates from the nucleus to the cytoplasm in response to Akt stimulation (Gross & Rotwein, 2015). To investigate the spatiotemporal regulation of Akt, others have developed FRET probes composed of a PH domain of Akt, tagged with YFP, and catalytic domains of Akt, tagged with CFP. FRET level is low in the cytosolic inactive state and high in the membrane-recruited active state, as the FRET level increases when the probe is phosphorylated and activated on the plasma membrane (Yoshizaki, Mochizuki, Gotoh, & Matsuda, 2007). In general, these Akt FRET sensors monitor

the phosphorylation state of the Akt probe as a measure of kinase activity. In this thesis, we took a similar approach to develop the first BRET sensor to measure PI3K/Akt activity. We tagged the PH domain of Akt with RlucII (Akt (PH)-RlucII) and monitored its recruitment to $PIP_3$ at the plasma membrane tagged with rGFP (rGFP-CAAX) upon the activation of PI3K by receptors, resulting in a BRET response. Here, the sensor is an indirect measure of kinase activity since the PH domain of Akt will only bind to $PIP_3$ when PI3K phosphorylates plasma membrane-bound $PIP_2$. We validate that the $PIP_3$-PH interaction occurs at the PM since an increase in BRET response will only occur when the PM-bound $PIP_3$ and the rGFP probe (anchored at the PM through its CAAX motif) are in close proximity. Moreover, when we stimulate the PI3K/Akt BRET sensor using EGF, the rapid kinetics curve observed is similar to the signaling kinetics of other membrane proteins and consistent with EGFR being a potent activator of Akt. As further validation, the treatment with the PI3K inhibitor, Wortmannin, resulted in a decreased BRET response. Finally, the Akt sensor could reproduce the same $IC_{50}$ of Rasarfin on Akt signaling (4 μM) as determine by the western blot experiments testing Rasarfin's effects on Akt phosphorylation (5 μM). Moreover, the inhibitory effects measured by Rasarfin using classical biochemical assays, such as western blot for Akt activation and the GST pulldowns for Ras, Arf6 and Rho activation, are comparable to those recorded using the PI3K/Akt, Ras, Arf and Rho BRET sensors, respectively, showing the versatility and convenience of using BRET sensors to sensitively measure and study protein kinesis. In addition, the dose-response curves generated using the BRET sensors to assess Rasarfin's potency on AngII-mediated activation of the four GTPases (Arf, Ras, Rho and Rac/Cdc42; Figure 5.8B) demonstrate the ease with which one can use these BRET sensors to compare the pharmacological properties of drugs, ligands and receptors

on the signaling of these small G proteins. In fact, working in 96-well plates, these BRET sensors are also amenable to high-throughput formats, making them useful for drug discovery platforms to improve the screening, identification, optimization and development of new therapeutics targeting these proteins.

### 7.2. Rasarfin targets Arf6 to block receptor internalization

BRET-based biosensors have been successfully used to discover and characterize small molecule inhibitors. With the similar goal of distinguishing the respective contributions of β-arrestin recruitment to the receptor and β-arrestin-promoted endocytosis in propagating receptor signaling, we previously used a computational approach to identify compounds that specifically inhibit the interaction of β-arrestin and AP-2 (Beautrait et al., 2017). In this thesis, our approach was to first identify modulators of AT1R trafficking using BRET sensors that monitor AT1R internalization (Namkung, Le Gouill, et al., 2016). This high-throughput screen phenotypically identified potentiators and inhibitors of AT1R and B2R endocytosis with no a priori target, thereby providing us with a selection of compounds that may act on various proteins involved in receptor trafficking, besides β-arrestins, and which could provide insights into other mechanisms of action or targets involved in regulating receptor internalization. Indeed, from these inhibitors of receptor endocytosis, we identified more specifically a compound, Rasarfin, that targets Arf6 GTPase, which is involved in clathrin- and non-clathrin-mediated endocytosis of multiple GPCRs (Houndolo et al., 2005). We validated the important role of Arf6 in receptor endocytosis by demonstrating that the dominant negative form of Arf6 blocks AT1R endocytosis. As an Arf6 inhibitor, Rasarfin blocks clathrin-mediated endocytosis of three prototypical GPCRs (AT1R, B2R

and β2AR) without interfering with the translocation of β-arrestin to the receptor, nor β-arrestin interaction with AP-2. As such, Rasarfin can be added to the list of existing pharmacological endocytic inhibitors such as dynasore (Macia et al., 2006), dynoles (T. A. Hill et al., 2009) and dyngos (McCluskey et al., 2013), which inhibit all dynamin-dependent endocytic pathways, and pitstop1/2 (von Kleist et al., 2011), which inhibit both clathrin-dependent and -independent endocytosis (Dutta, Williamson, Cole, & Donaldson, 2012). However, we cannot conclude that Rasarfin only inhibits Arf6- and/or clathrin-mediated endocytosis since we did not assess Rasarfin's effects on receptors that internalize via non-Arf6-, non-clathrin mediated pathways, such as the vasoactive intestinal peptide receptor (VIPR), a GPCR whose caveolae-dependent internalization is not dependent on Arf6, and the transferrin receptor, a non-GPCR whose constitutive endocytosis is not affected by Arf6 depletion (Houndolo et al., 2005). In addition, Rasarfin's inhibitory effects on EGFR-mediated ERK1/2 signaling may raise the question about Rasarfin's effects on EGFR internalization, which we have not shown either. However, we believed EGFR internalization in HEK293 cells would not be affected since its mechanisms of clathrin-mediated receptor endocytosis include autophosphorylation, receptor dimerization, the recruitment of adaptor protein Grb2 and E3 ubiquitin ligase (Dutta et al., 2012; Jiang, Huang, Marusyk, & Sorkin, 2003; Q. Wang, Villeneuve, & Wang, 2005; Z. Wang & Moran, 1996), and does not require Arf6 like GPCRs.

Furthermore, we propose a direct inhibitory mechanism for Rasarfin binding to Ras, its main target, but did not provide one for Rasarfin binding to Arf6, its secondary target. Therefore, we cannot exclude the possibility that Rasarfin may bind Arf6 in a similar binding pocket as Ras, such as the guanine nucleotide binding site, which has five regions with the highest degree of

sequence conservation among GTPases: two regions constitute most of the phosphate and $Mg^{2+}$ binding site and are located in the first half of the G domain, two regions are involved in guanosine binding and are located in the C-terminal half of the GTPase, and another region is responsible for GTP hydrolysis (Valencia, Chardin, Wittinghofer, & Sander, 1991; Vetter & Wittinghofer, 2001). Moreover, we cannot rule out the other possibility that Rasarfin may target Arf GEFs, like the Arf inhibitors brefeldin A (BFA) and secinH3. Brefeldin A, which prevents the binding of cytosolic coat proteins onto membranes by inhibiting the GTP-dependent interaction of Arf with the Golgi membrane, was the first Arf inhibitor discovered. BFA inhibits high-molecular weight, BFA-sensitive GEFs such as GBF1, BIG1 and BIG2. Therefore, both class I and class II Arfs can accommodate BFA in their interface with such GEFs (Donaldson, Finazzi, & Klausner, 1992). However, class III Arf6 is insensitive to BFA since it interacts with high-molecular weight, BFA-resistant GEFs, such as cytohesins-1, -2, and -3, EFA6 and BRAGs (Casanova, 2007).

Therefore, the next approach targeting the Sec7 domain of these GEFs, which is conserved among Arf GEFs, led to the development of the Sec7 inhibitor H3 (secinH3). It binds and inhibits the GEF activity of cytohesins, such as cytohesin-2 (ARNO), consequently inhibiting both Arf1 and Arf6 activity (Hafner et al., 2006). Unlike Rasarfin, these inhibitors target multiple Arfs by inhibiting Arf-GEFs rather than Arf6 directly, so their non-specific activity may render them less potent and have different effects on Arf-dependent processes. However, more recently, compound NAV2729, a direct inhibitor of Arf6, was discovered and shown to prevent GNAQ/GEP100 GEF complex from binding and activating Arf6, resulting in reduced uveal melanoma cell proliferation in a mouse model. Unlike Rasarfin, it does not, inhibit the activity of H-Ras. A structural homology model of the Arf6/ARNO complex predicts NAV-2729 binds Arf6 in its GEF-binding site, which

does not overlap with the nucleotide-binding pocket (Yoo et al., 2016). Therefore, we cannot either exclude the third possibility that Rasarfin may directly bind Arf6 at its GEF ARNO interface. However, Rasarfin's lack of inhibition on Arf1 would suggest otherwise and rather reinforces the notion that there are flexible regions in protein-protein complexes which can provide druggable sites for selectively targeting different proteins and signaling pathways.

Although structures of Arf6 with its GEFs are currently unavailable, *in silico* screening approaches have been used to discover inhibitors of Arf1, more specifically, targeting a flexible pocket near the Arf1-ARNO interface. Compound LM11 targets the Arf1-GDP/cytohesin-2 Sec7 domain complex, interacting more specifically with K38 in the switch I region of Arf1. Interestingly, LM11 does not distinguish between BFA-insensitive and sensitive Arf-GEFs, yet it does not inhibit the activation of Arf6 (Viaud et al., 2007). Even though they bind the same GEFs, of the five human Arf genes, Arf1 and Arf6 are the most dissimilar in sequence, being only 66% identical at the amino acid level (Figure 7.1) (Peters et al., 1995). The few sequence differences lead to important conformational differences between Arf1 and Arf6 switch regions (Macia, Chabre, & Franco, 2001; Ménétrey, Macia, Pasqualato, Franco, & Cherfils, 2000), which may explain Rasarfin's selectivity on these small G proteins.

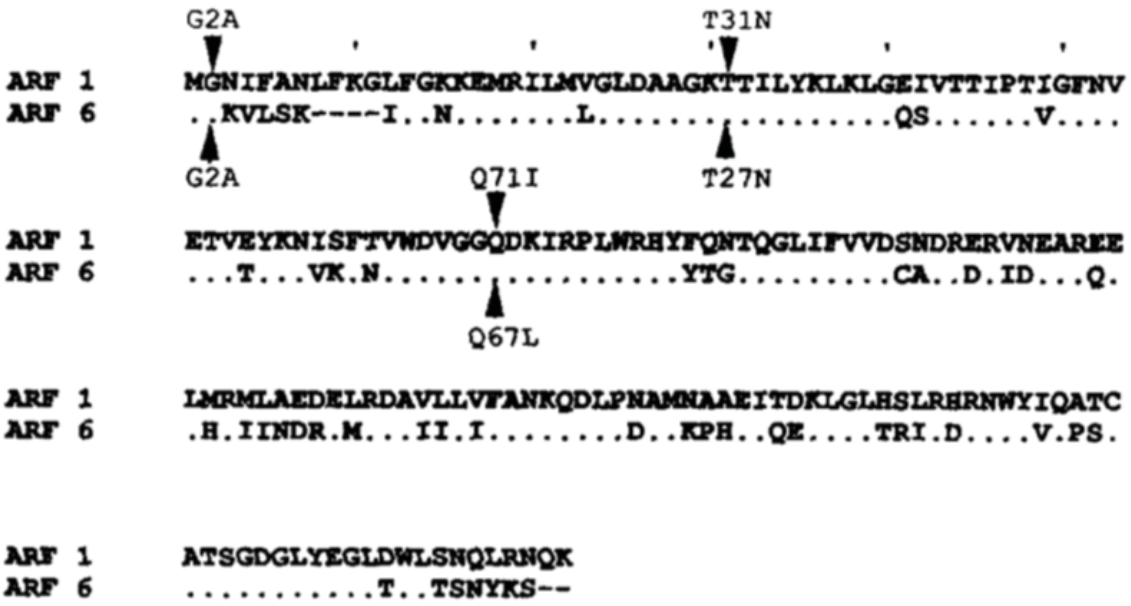


**Figure 7.1. Amino acid sequence comparison of human Arf1 and Arf6.** The full sequence of Arf1 is shown along with the aligned differences found in Arf6. Figure and text adapted with permission from Rockefeller University Press (Peters et al., 1995).

7.3. Rasarfin targets Ras to inhibit receptor signaling

When Rasarfin was identified as an endocytic inhibitor, we thought it was a promising tool to help dissect the role of β-arrestin-mediated receptor internalization in GPCR signaling. Indeed, Rasarfin was found to inhibit the activation of ERK1/2 elicited by AT1R, B2R and β2AR stimulation. However, its additional inhibitory effects on EGFR-mediated ERK1/2 and Akt activation demonstrated that Rasarfin was not β-arrestin/GPCR specific nor MAPK specific but

involved a common target that was not Arf6 nor involved in receptor endocytosis. We validated Ras as a second target by showing that Rasarfin does not affect important signaling effectors of the MAPK cascade, such as the PKC, MEK and BRAF kinases. Although we cannot rule out the possibility that Rasarfin interacts with other targets in cells, we found that it did not affect the activation of other monomeric G proteins, such as Rho, Rac/Cdc42 and Arf1, nor the heterotrimeric $G\alpha_q$ and $G\alpha_{i3}$ proteins, supporting a selective mode of action.

Here, the identification of a Ras inhibitor was serendipitous since other Ras inhibitors have been previously identified using NMR-based fragment screens of compounds against the crystal structure of GDP-bound K-Ras (Hillig et al., 2019; Sun et al., 2012), *in silico* virtual screening (Evelyn et al., 2014; Shima et al., 2013) and BRET-based Ras biosensors in an *in vitro* high-throughput screening of compounds (Bery et al., 2018).

The current approaches for the development of Ras inhibitors in cancer therapy are using direct inhibitors of Ras or Ras GEFs and GAPs, blocking Ras prenylation for membrane association or targeting Ras effectors and Ras downstream or upstream signalling (Downward, 2003; Papke & Der, 2017). Attachment of Ras proteins to the plasma membrane is required for effective Ras signaling and is initiated by the enzyme farnesyl protein transferase, which prenylates the protein. Therefore, the first developed anti-cancer drugs targeting Ras were farnesyl transferase inhibitors (FTIs). The incorporation of geranylgeranyl rather than farnesyl into Ras alters its subcellular localization or protein-protein interaction, causing changes in Ras signaling and reduces its ability to mediate tumour cell survival, growth, proliferation, migration and metastasis. FTIs have some antitumor activity in the clinic, but fail over time as they seem to act through targets other than Ras (Berndt, Hamilton, & Sebti, 2011; Whyte et al., 1997). Compared

to Rasarfin, the non-specific mechanism of action of this class of FTIs makes them not suitable candidates as Ras inhibitors. The same goes for Ras inhibitors that have been developed to act on EGFR and ERBB2 upstream activators of Ras. Antibodies directed against ERBB2 have been licensed for the treatment of breast cancer, whereas small-molecule inhibitors of EGFR tyrosine kinase activity show potential against lung cancer in clinical trials. They inhibit receptor autophosphorylation and transphosphorylation so that Ras may not be activated in oncogenic cells (Downward, 2003). However, these compounds are only effective in patients who have oncogenic RTK signaling. Patients with tumors expressing an oncogenic form of Ras do not benefit from such compounds because oncogenic Ras acts downstream to circumvent the need for an oncogenic RTK to induce cell proliferation and survival (Castellano & Downward, 2011). Therefore, Rasarfin, being a direct inhibitor of Ras, would be a better option than EGFR inhibitors to inhibit Ras since it should remain effective even in the presence of oncogenic RTK.

The continued search for better Ras inhibitors led to the development of kinase inhibitors that block either Raf or MEK in the MAPK pathway downstream of Ras. B-Raf mutations, such as the V600E, have been identified in a significant percentage of tumours, making Raf a great target for inhibiting Ras signaling. However, Raf inhibitors are only effective in patients with B-Raf-V600E-mutated tumours since non-V600E-mutant B-Raf forms require dimerization for their catalytic activity and thus may be resistant. Unlike B-Raf, activating mutations in MEK are found at very low percentages in human tumours. Nonetheless, as MEK lies downstream of Ras and Raf, mediating the transmission of growth factor signaling from activated Raf to ERK, it has become an attractive drug target for Ras- and Raf-mutant tumours. On the other hand, there has been limited progress in the development of ERK1- and ERK2-selective inhibitors. This is partly due

to the assumption that, as ERK is the only known downstream target of MEK, no additive benefit would result from an ERK inhibitor compared to a MEK inhibitor. Therefore, combinatorial treatment involving Raf inhibitors with MEK or ERK inhibitors is a validated option to further improve the efficacy of these drugs in the treatment of oncogenic Ras signaling (Samatar & Poulikakos, 2014). However, Rasarfin targeting Ras directly may be a more potent anti-cancer therapy than those targeting downstream Ras effectors since we would avoid the need for multiple treatments, as well as reduce the risk of off-target effects.

Other Ras-related therapies include inhibitors of Akt/PKB or PI3K kinase activity, which are activated by oncogenic Ras mutations and by a loss in PTEN tumour-suppressor gene in cancers. The interaction of Ras with the catalytic p110α isoform of PI3K is required for normal growth factor signaling and for Ras-driven tumor formation in mice with mutations in the PI3KCA gene encoding p110α (Gupta et al., 2007). Therefore, Rasarfin inhibiting the PI3K/Akt pathway provides another Ras downstream target for cell survival.

Even with this grand selection of anti-cancer drugs currently available, Ras remains an active area of research due to its continued undruggable properties. Our identification of Rasarfin provides an additional tool for the study and treatment of oncogenic Ras-mediated pathways.

### 7.4. Rasarfin's structural features for binding Ras

Developing small molecules that disrupt Ras signaling to its effectors is challenging since the proteins lack well-defined hydrophobic pockets. Protein-protein interactions typically involve flat and rather large binding sites, which often leads to small molecules displaying low affinity or specificity (Cox, Fesik, Kimmelman, Luo, & Der, 2014). However, targeting "hot spots" on the

contact surfaces of proteins can lead to inhibitors showing drug-like potencies. These small molecules seem to bind deeper on the contact surface of the protein than their natural protein partner does (Arkin & Wells, 2004; Trinh, Upadhyaya, Qian, & Pei, 2016; Wells & McClendon, 2007). Even though these interfaces are large areas, mutational studies have shown that in most cases, small subsets of residues involved in protein binding contribute the most to the binding free energy (Clackson & Wells, 1995; Moreira, Fernandes, & Ramos, 2007; Thanos, DeLano, & Wells, 2006). Indeed, the docking analyses used in the studies identifying Barbadin (Beautrait et al., 2017) and Rasarfin, here, support the targeting of such protein-protein interaction hot spots.

The computational studies map Rasarfin's site of action to the Ras SOS1-binding site and the structure activity relationship studies define the chemical moieties in Rasarfin essential for its inhibitory activity. The benzofuran forms aromatic and hydrophobic interactions with the Thr74, Leu56, and Tyr40 residues of Ras. The amide forms a hydrogen bond with the carbonyl oxygen of the backbone of Ile55. The isopropyl moiety interacts with residues Ala59, Ile21 and Tyr32. Eight residues on Ras (Thr74, Leu56, Tyr40, Ile55, Thr20, Ile21, Tyr32, Ala59) collectively form a strong hydrophobic pocket around the Chloro-atom, stabilizing the aromatic ring and the compound. This chlorine is indispensable for Rasarfin binding, as shown with molecular dynamics simulation with the halogen-free analog, **21.4**. The well-filled pocket on the Ras-SOS interface tightly embraces the chloro-substitution of Rasarfin and forms energetically favorable van der Waals interactions, keeping the molecule in a sterically restricted position. This contrasts with **21.4**, which did not face such steric hinderance because the aromatic ring was able to turn and even fully rotate in the absence of this bulky Cl-atom, leading to significant displacement of the compound from the proposed binding groove after a relatively short simulation time. Furthermore,

due to its missing chloro-substituent, **21.4** forms similar but fewer interactions with Ras compared to Rasarfin (Figure 5.10D). **21.4**'s phenyl ring of the benzofuran interacts with Leu56 and Tyr40 but the interaction with Thr74 is lost. There is also a weaker, even insignificant, hydrogen bond that is formed between the amide on **21.4** and the carbonyl oxygen of the backbone of Ile55. Compared to Rasarfin, the center phenyl ring of **21.4** forms weak hydrophobic interactions with four versus eight residues on Ras (i.e. Leu56, Thr20, Tyr32 and Tyr40). Lastly, the hydrophobic interactions of the isopropyl moiety with Tyr32 is maintained, but its interaction with Ala59 is lost. These differences in interactions observed between **21.4** and Ras compared to Rasarfin and Ras suggest that these are important hot spots for Rasarfin binding to Ras.

We further validated this binding modality by mutating some of the described residues in the small G protein believed to make important contacts with Rasarfin, such as Tyr32 and Tyr40. Residue Tyr32 interacts with the isopropyl moiety and is located on switch I, in direct vicinity of the phenyl ring possessing the Chloro substitution on Rasarfin. The MD simulations suggest Tyr32 plays a crucial role in stabilizing the compound by preventing the Chloro-substitution from turning outwards and displacing the inhibitor from the binding site. Due to the steric restriction introduced by the bulky halogen, Rasarfin is forced into an elongated shape in which it binds strongly to the binding pocket. Residue Tyr40 is similarly located on switch I and establishes hydrophobic interactions with the benzofuran and chlorine of Rasarfin. Tyr32 and Tyr40 are also two of the few residues which also maintain important interactions between Compound 4 and Ras. Therefore, it was predicted that replacing them with an alanine would lead to weakened compound-protein interactions. Furthermore, these residues are located far from the orthosteric binding site of Ras, so mutations of these residues were believed to be the least likely to compromise protein function.

Using the Ras BRET sensor, we show that K-Ras-Y32A and K-Ras-Y40A can no longer bind Rasarfin and its inhibitory effects are lost because the aromatic ring can now move and turns the Chloro-substituent outwards, allowing Rasarfin to leave the binding pocket of Ras. This data confirmed that these are important residues for Rasarfin binding to Ras.

Additionally, the docking simulations performed in this study suggest that Rasarfin binds Ras between switch I and switch II, in the SOS-binding site. SOS1 acts on Ras by inserting a helix into a conformationally opened allosteric binding site on Ras, enabling the GDP to escape from the binding site. As SOS1 binds transiently, it leaves the binding site as soon as a GTP molecule enters the nucleotide binding site. One group was successful in designing cell-permeable synthetic α-helix mimics based on the structure of SOS that interfere with Ras-SOS interaction and downregulate Ras signaling (Patgiri, Yadav, Arora, & Bar-Sagi, 2011). Docking of Rasarfin in the SOS-bound crystal structure of Ras showed that Rasarfin occupies a large part of the hydrophobic binding groove, in which helix H of SOS1 would be embedded. Moreover, when bound to Rasarfin, Ras seems to be in a Ras-SOS-bound-like conformation to accommodate the compound in the aforementioned groove. Rasarfin extends to the orthosteric binding site of the nucleotide and is hypothesized to also occupy the space where $Mg^{2+}$ usually binds Ras in the GTP-bound form. Analogous to SOS interaction with Ras, the binding of Rasarfin to Ras leads to conformational changes in Ras, which disrupts the carefully established water network in and around the nucleotide binding site, preventing the binding of $Mg^{2+}$ or GTP. As such, one would predict Rasarfin could be an anti-cancer drug candidate because it also targets the Ras GTP-binding site, which is conserved among defective Ras proteins, and would therefore be less resistant to the Ras mutations found in many cancers.

More recently, there have been a wave of Ras-SOS inhibitors identified that bind to the GEF catalytic site (Cdc25 domain), inhibiting SOS-mediated nucleotide exchange on Ras and preventing Ras activation (Abbott et al., 2018; Hillig et al., 2019; Hodges et al., 2018). In the case of the 4,6-dichloro-2-methyl-3-aminoethyl-indole (DCAI) compound, it inhibits SOS nucleotide release from Ras in an SOS-dependent manner only. When EDTA is used to chemically mimic the role of SOS1 to chelate $Mg^{2+}$ from the active site of the GTPase and promote nucleotide release, DCAI had no effect on the rate of EDTA-stimulated nucleotide release from K-Ras (Maurer et al., 2012). We show that Rasarfin does not directly act on SOS1 to inhibit Ras activation because Rasarfin inhibited both the SOS1- and EDTA-mediated mant-GTP binding to Ras. However, we observe a greater decrease in fluorescence when SOS1 is added compared to EDTA (Figure 5.7D and E), suggesting the potential need to engage the SOS-Ras interaction for the full and efficacious binding of Rasarfin. Interestingly, from the three small molecule binding sites ("sites" A, B and C) at the interface of the Ras-SOS complex that have been discovered by (Winter et al., 2015), the benzofuran part of Rasarfin binds the "site B" on Ras, which is a portion of the binding groove (i.e. interactions with His911 on SOS and Thr74 on Ras). Whereas, the fragment-like molecules reported by (Maurer et al., 2012) bind to a region between switch II and helix 4 of Ras-GDP to inhibit SOS-mediated nucleotide exchange activity. Rasarfin is distinct from these other Ras inhibitors as it covers almost the full length of the SOS-Ras interface on Ras. Such binding modality of a drug on Ras could lead to the development of a new class of Ras inhibitors.

Furthermore, aligning the sequences of H-Ras and Arf6, using NCBI's Basic Local Alignment Search Tool (BLAST) (Altschul, Gish, Miller, Myers, & Lipman, 1990), shows that residues are not well conserved among these two small G proteins, including those for Rasarfin

binding on Ras (Figure 7.2), suggesting that they share a common conformational tertiary structure, which may be responsible for Rasarfin binding to both small G proteins rather than a primary sequence homology. Despite this sequence dissimilarity, Rasarfin is selective for Ras and Arf6 as it did not inhibit other small G proteins like Rho or Rac/Cdc42, which are closely related small G proteins and, in some cases, regulated by common GEFs (Schmidt & Hall, 2002; Snyder et al., 2002). These findings are consistent with observations from their respective structures with GEFs, suggesting that important residues in the hydrophobic groove between the switch domains of these small G proteins (*e.g.* Trp58 in RhoA, Trp56 in Rac, and Phe56 in Cdc42) induce a conformation that would interfere with Rasarfin binding if it was binding in this similar region as Ras (Snyder et al., 2002).

```
H-RAS       ----------MTEYKLVVVGAGGVGKSALTIQLIQNHFVDEYDPTIEDSYRKQVVIDGET   50
ARF6        MGKVLSKIFGNKEMWILMLGLDAAGKTTILYKLKLGQSVTTI-PTVG--FNV-ETVTYKN   56
                         *      *    **      *     *    **

H-RAS       CLLDILDTAGLEEYSAMRDQYMRTGEGFLCVFAINNTKSFEDIHQYREQIKRVKDSDDVP   110
ARF6        VKFNVWDVGGQDKIRPLWRHYYTGTQGLIFVVDCADRDRIDEARQELHRIINDREMRDAI   116
                  *  *          *     *   *             *    *       *

H-RAS       MVLVGNKCDLAARTVESRQAQDLARSYGIPYIE-------TS-AKTRQGVEDAFYTLVRE   162
ARF6        ILIFANKQDLPDAMKP----HEIQEKLGLTRIRDRNWYVQPSCATSGDGLYEGLTWLTSN   172
                 ** **                 *   *         * *            *

H-RAS       IRQH        166
ARF6        YKS-        175
```

**Figure 7.2. Amino acid sequence comparison of human H-Ras and Arf6.** The sequence alignment of H-Ras and Arf6 using NCBI's BLAST. Conserved residues are indicated by an asterisk and the amino acids identified in Rasarfin binding to H-Ras are in red.

Computational studies provide valuable information for predicting the binding of compounds to their targets when a structure is available. However, NMR remains a robust method to screen, characterize and optimize lead compounds because of its highly sensitive ability to identify binding sites, affinities, and ligand poses at the level of individual amino acids regardless of target protein function (Hajduk et al., 1999; Peng, Lepre, Fejzo, Abdul-Manan, & Moore, 2001; Rovnyak, Hoch, Stern, & Wagner, 2004; Ziarek, Peterson, Lytle, & Volkman, 2011). In fact, NMR mapping of the ligand-binding sites on Ras revealed five areas with a high propensity for ligand binding and the potential to modulate Ras activity (Maurer & Wang, 2013). These areas can be compared to those identified for Rasarfin-Ras binding using MD simulation. Using NMR to identify the ligand-binding pocket and demonstrating that Rasarfin definitely binds to Ras would complement such findings. Improving the affinity for binding would also provide the foundation for further optimization, aiming for sub-micromolar cellular activity.

### 7.5. Implications of Rasarfin in cancer

As mentioned throughout this work, Ras inhibitors have been developed primarily for the treatment of cancers. Ras proteins control signaling pathways that are key regulators of normal cell growth and malignant transformation. They are aberrant in most human tumours due to activating mutations in the Ras genes themselves or to alterations in upstream or downstream signaling components. Therefore, numerous rational therapies that target Ras pathways have been developed to inhibit tumour growth, survival and spread. Indeed, several of these new therapeutic agents are showing promise in the clinic and many more are being developed (Downward, 2003). Data assessing Rasarfin's effects on Ras activation in MDA-MB-231 cells, the only breast cancer

cell line which carries the K-Ras mutation G13D (Kozma et al., 1987) and has increased Ras and Arf6 activity (Eckert et al., 2004; Hashimoto et al., 2004; Morishige et al., 2008), using GST pulldown show that Rasarfin blocks the activity of both Ras and Arf6 in these cells (Giubilaro, personal communication). Other data show that Rasarfin blocks MDA-MB-231 cell proliferation in a dose-dependent manner (Giubilaro, personal communication). Here, we suggest Rasarfin blocks oncogenic Ras signaling by acting through the Ras-Raf-MEK-ERK pathway and can be added to the growing list of anti-proliferative agents currently available. This conclusion was validated using **21.8**, which we showed is also a Ras inhibitor and blocks MDA-MB-231 cell proliferation. Results with **21.4**, the Rasarfin analog that we identified as a non-Ras inhibitor and does not affect MDA-MB-231 cell proliferation (Giubilaro, personal communication), further confirm Ras' involvement in cell proliferation and survival. Although we previously suggested that SOS needed to be engaged for Rasarfin to bind Ras, its inhibitory effects here on oncogenic Ras open the possibility that Rasarfin may simply require Ras to be in an active conformation for it to bind, since constitutively active Ras do not require SOS to be activated like wild type Ras. However, computational studies with Rasarfin and K-Ras-G13D crystal structure would need to be performed to validate that Rasafin inhibits this defective Ras protein. This is exactly how small molecules that irreversibly bind to the oncogenic mutant, K-Ras-G12C, have been developed. Contrary to Rasarfin, these compounds rely on the mutant cysteine for binding and therefore do not affect the wild type Ras protein. Binding of these inhibitors to K-Ras-G12C disrupts both switch I and switch II, favouring the GDP-bound Ras state and impairing binding to Raf (Mortier et al., 2020; Ostrem, Peters, Sos, Wells, & Shokat, 2013). In addition, *in silico* screening of Rasarfin's interaction with several oncogenic Ras structures with mutations such as G12C, G12D,

G12V and G13D would determine its specificity and use as an anti-cancer drug candidate for pancreatic, lung, colorectal, cervical and breast cancers.

There is increasing evidence showing that the GEFs and GAPs controlling the GDP-GTP cycling of the Ras superfamily can also contribute to cancer by either promoting or suppressing tumour progression and growth. GEFs and GAPs are deregulated in cancer by somatic mutation, changes in gene expression and through post-translational mechanisms owing to aberrant signaling caused by alterations in upstream oncogene or tumour suppressor function. Efforts to develop inhibitors of GTPase GEFs and GAPs have been and are currently being employed (Vigil, Cherfils, Rossman, & Der, 2010). Therefore, Rasarfin binding Ras in its SOS-binding site to inhibit Ras GEF activity exemplifies its potential as an anti-cancer candidate.

Because Ras coordinately activates both the PI3K and MAPK signaling pathways, it has also been very attractive to use a combination of MAPK pathway (either Raf, MEK or ERK) and PI3K inhibitors in the treatment of Ras-driven cancers (Asati et al., 2016; Garcia-Echeverria, 2009). Indeed, the activation of the PI3K pathway, either by PI3KCA mutations or PTEN loss, has been shown to be a major resistance mechanism that impairs the efficiency of MEK inhibitors in K-Ras mutated cancers (Engelman et al., 2008; Kinkade et al., 2008). Therefore, Rasarfin targeting these two main Ras pathways further emphasizes its promising role in cancer treatment. Encouragingly, co-inhibition of both pathways has been successful in reducing tumor growth in xenograft cancer models and in genetically engineered mouse models (Castellano & Downward, 2011). Other groups have also recently reported on the discovery of Ras-SOS inhibitors that, similarly to Rasarfin, inhibit both ERK and Akt phosphorylation to control cancer cell proliferation

and survival, but interact in a different hydrophobic pocket near the Ras switch domains (Bery et al., 2018; Burns et al., 2018; Burns et al., 2014; Evelyn et al., 2014).

In cancer cells, the mechanism of Arf6 activation and signaling are different from those in HEK293 cells. In response to EGF stimulation, Arf6 is activated by an Arf GEF (GEP100, EFA6 or ARNO) and then recruits its downstream effector, Rac1, which regulates cytoskeleton remodeling and extracellular matrix degradation, ultimately accelerating breast cancer cell invasion and metastasis. In addition, Arf6 can also promote tumor cell proliferation and survival by activating PLD-mTOR and p38 pathways, simultaneously. Several molecules inhibiting the activation of Arf6, such as secinH3, or its upstream/downstream factors can block the process of invasion, migration and proliferation of tumor cells expressing high levels of Arf6, such as breast, pancreatic and lung cancer, *in vivo* and *in vitro* (Hashimoto et al., 2004; R. Li et al., 2017; Morishige et al., 2008). In contrast, AT1R-mediated HEK293 cell migration involves Arf6 activation by ARNO, which are both scaffolded by the C-terminal tail of β-arrestin (Charles, Namkung, Cotton, Laporte, & Claing, 2016). Since Arf6 and its effectors are other promising drug targets for tumor chemotherapy, Rasarfin's effects on HEK293 and cancer cell migration could be studied further. That being said, Rasarfin may have different effects on Arf6-mediated pathways depending on the cell type and GEF that activates it. In this study, Rasarfin's effects were limited to Arf6- and clathrin-mediated receptor endocytosis. Nonetheless, having a dual GTPase inhibitor, such as Rasarfin, is advantageous since targeting both Ras and Arf6, which are involved in breast cancer invasive activities, for example, may result in a better therapeutic outcome.

7.7. Optimization of Rasarfin into functionally selective analogs

The dominant negative form of Ras having no effect on AT1R internalization and the dominant negative form of Arf6 having no effect on MAPK activation confirms the dual role of Rasarfin in independently inhibiting both Ras and Arf6. In fact, Rasarfin having two targets is consistent with the difference in potencies found for Rasarfin inhibiting Ras and Arf6 activation (0.7 μM and 7 μM, respectively), which are consistent with the potencies calculated for MAPK activation and AT1R internalization (4 μM and 10 μM, respectively). That being said, Rasarfin may serve as a lead scaffold for the generation of more potent Ras and Arf6 inhibitors. In this thesis, performing SAR on Rasarfin provides insights for the development of analogs selective for Ras and Arf6. Complementary to the molecular docking of **21.4** onto Ras, which showed that the chlorine substituent on the phenyl ring of Rasarfin is indispensible for Rasarfin binding Ras, BRET and western blot experiments showed that **21.4** has no effect on receptor internalization nor MAPK activation, suggesting that the chlorine should be maintained for future compound optimization steps. Indeed, **21.7** and **21.8**, which retain the chlorine, show inhibitory effects compared to **21.1**, **21.3** and **21.4**, which lack the chlorine. However, possessing the chlorine does not guarantee activity on Ras and Arf6 since **21.2**, **21.5** and **21.6**, which retain the chlorine, have no effect on receptor internalization nor MAPK activation (Figure 6.1). These compounds may have other structural features which impede their functional activity. Unlike **21.4**, **21.7**, and **21.8**, we have not explored their effects on Ras and Arf6 activation to conclude. Furthermore, we have not either established the role of the chlorine subsitutent in the interaction of Rasarfin with Arf6, which may explain its functional selectivity towards Ras.

Moreover, **21.7,** which has the benzofuran replaced by a thiophene and isopropyl by an ethyl, showed some selectivity towards receptor internalization and reduced efficacy on the MAPK pathway, and **21.8**, which only has the isopropyl replaced by an n-propyl, was just as potent as Rasarfin in inhibiting MAPK and reduced efficacy on receptor internalization, suggesting a different binding mode on Ras and/or Arf6 than Rasarfin. Indeed, identifying the structural determinants responsible for their biological activity should provide insights for the development of more Ras-or Arf6-selective Rasarfin analogs. Similar to Rasarfin, **21.8** inhibited EDTA-mediated mant-GTP binding to Ras, so it is probably not binding SOS1 but may also need to engage the SOS-Ras interaction for a full and efficacious binding to Ras. Also, **21.8** inhibited Ras to a similar extent as Rasarfin, suggesting it is also targeting more selectively this small G protein. However, further studies would need to be performed to determine if Compound 8 directly binds and inhibits Ras with the same mode of action as Rasarfin. Moreover, determining the potencies of **21.7** and **21.8** on Ras/MAPK and Arf6/AT1R internalization and comparing them to that of Rasarfin would also help explain these differences in activity.

Interestingly, **21.7**, the only analog that shows some inhibitory effects on AT1R internalization, has low activity on Arf6, suggesting it affects receptor internalization with a different mechanism of action than Rasarfin. Exploring its chemical properties further and comparing it to Rasarfin may lead to the development of more selective endocytic inhibitors. Potential endocytic targets could include the small G proteins of the Rab family, in particular, Rab5, which is localized to early endosomes and the plasma membrane, regulating early steps of the endocytic process. Mediating endosome fusion of clathrin-coated vesicles from the plasma membrane to early endosomes makes it an ideal target for receptor internalization to explore next.

On the other hand, to expand the search for inhibitors of receptor trafficking, Rab4 and Rab11 would be other choices. Rab4, which is also present on early endosomes, mediates endocytic recycling directly from the early endosomes to the plasma membrane, whereas Rab11, which is localized to recycling endosomes, mediates endocytic trafficking from the recycling endosome and to the plasma membrane (Stenmark, 2009; Zerial & McBride, 2001). As such, this also opens the possibility of Rasarfin inhibiting other small G proteins, such as the Rabs described, or other effectors involved in regulating receptor trafficking, which were not explored in this thesis. Identifying the target of these compounds could provide further insights into the regulation of receptor internalization and trafficking.

## CONTRIBUTION TO ORIGINAL RESEARCH

This thesis furthers our knowledge of the molecular and cellular mechanisms regulating G protein-coupled receptor internalization and signaling. We describe the identification and characterization of a new endocytic inhibitor, Comp#21, which was initially discovered to help dissect β-arrestin's signaling function from its endocytic function. It turns out this small molecule, named Rasarfin, has a dual role of inhibiting small G proteins Ras and Arf6, which are involved in receptor signaling to ERK1/2 and receptor internalization via CCPs, respectively.

In Chapter 4, we developed a suite of BRET-based sensors for studying the activation of small GTPases Ras, Arf and Rac/Cdc42, and kinase PI3K. This method enables us to perform kinetics experiments and generate response curves to pharmacologically characterize drugs, ligands and receptors acting on these small G proteins. Developing means to efficiently study protein activation in live cells, in real time and in high-throughput screening formats is useful for both drug and basic research discovery programs.

In Chapter 5, we identified and characterized Rasarfin as a dual inhibitor of both small G proteins Ras and Arf6. Furthermore, our computational studies reveal that Rasarfin is the first small molecule to bind a large part of the Ras-SOS binding interface, opening new means to block this small G protein. The discovery of a Ras inhibitor is of great interest in the field of cancer research, where oncogenic Ras plays a major role in tumor development and progression. However, Rasarfin can also be useful to study Arf6-mediated receptor internalization and signaling pathways. As a new pharmacological tool, Rasarfin can help to further study the role of these GTPases in the internalization versus signaling of receptors in normal and cancer cells.

In Chapter 6, we performed SAR studies to identify structural determinants responsible for Rasarfin's inhibitory effects and its functional selectivity. Hence, Rasarfin may serve as a lead scaffold to develop the next generation of more potent and selective inhibitors of Ras and Arf6.

## REFERENCES


Abbott, J. R., Hodges, T. R., Daniels, R. N., Patel, P. A., Kennedy, J. P., Howes, J. E., . . . Fesik, S. W. (2018). Discovery of Aminopiperidine Indoles That Activate the Guanine Nucleotide Exchange Factor SOS1 and Modulate RAS Signaling. *J Med Chem, 61*(14), 6002-6017. doi:10.1021/acs.jmedchem.8b00360

Ahn, S., Maudsley, S., Luttrell, L. M., Lefkowitz, R. J., & Daaka, Y. (1999). Src-mediated tyrosine phosphorylation of dynamin is required for beta2-adrenergic receptor internalization and mitogen-activated protein kinase signaling. *J Biol Chem, 274*(3), 1185-1188. doi:10.1074/jbc.274.3.1185

Ahn, S., Nelson, C. D., Garrison, T. R., Miller, W. E., & Lefkowitz, R. J. (2003). Desensitization, internalization, and signaling functions of beta-arrestins demonstrated by RNA interference. *Proc Natl Acad Sci U S A, 100*(4), 1740-1744. doi:10.1073/pnas.262789099

Ahn, S., Shenoy, S. K., Wei, H., & Lefkowitz, R. J. (2004). Differential kinetic and spatial patterns of beta-arrestin and G protein-mediated ERK activation by the angiotensin II receptor. *J Biol Chem, 279*(34), 35518-35525. doi:10.1074/jbc.M405878200

Altschul, S. F., Gish, W., Miller, W., Myers, E. W., & Lipman, D. J. (1990). Basic local alignment search tool. *J Mol Biol, 215*(3), 403-410. doi:10.1016/s0022-2836(05)80360-2

Anborgh, P. H., Seachrist, J. L., Dale, L. B., & Ferguson, S. S. (2000). Receptor/beta-arrestin complex formation and the differential trafficking and resensitization of beta2-adrenergic and angiotensin II type 1A receptors. *Mol Endocrinol, 14*(12), 2040-2053. doi:10.1210/mend.14.12.0565

Anderson, J. M., & Cormier, M. J. (1973). Lumisomes, the cellular site of bioluminescence in coelenterates. *J Biol Chem, 248*(8), 2937-2943.

Angers, S., Salahpour, A., Joly, E., Hilairet, S., Chelsky, D., Dennis, M., & Bouvier, M. (2000). Detection of beta 2-adrenergic receptor dimerization in living cells using bioluminescence resonance energy transfer (BRET). *Proc Natl Acad Sci U S A, 97*(7), 3684-3689. doi:10.1073/pnas.060590697

Arcaro, A., & Wymann, M. P. (1993). Wortmannin is a potent phosphatidylinositol 3-kinase inhibitor: the role of phosphatidylinositol 3,4,5-trisphosphate in neutrophil responses. *Biochem J, 296 ( Pt 2)*, 297-301. doi:10.1042/bj2960297

Arkin, M. R., & Wells, J. A. (2004). Small-molecule inhibitors of protein-protein interactions: progressing towards the dream. *Nat Rev Drug Discov, 3*(4), 301-317. doi:10.1038/nrd1343

Asati, V., Mahapatra, D. K., & Bharti, S. K. (2016). PI3K/Akt/mTOR and Ras/Raf/MEK/ERK signaling pathways inhibitors as anticancer agents: Structural and pharmacological perspectives. *Eur J Med Chem, 109*, 314-341. doi:10.1016/j.ejmech.2016.01.012

Attramadal, H., Arriza, J. L., Aoki, C., Dawson, T. M., Codina, J., Kwatra, M. M., . . . Lefkowitz, R. J. (1992). Beta-arrestin2, a novel member of the arrestin/beta-arrestin gene family. *J Biol Chem, 267*(25), 17882-17890.

Baker, A., Saltik, M., Lehrmann, H., Killisch, I., Mautner, V., Lamm, G., . . . Cotten, M. (1997). Polyethylenimine (PEI) is a simple, inexpensive and effective reagent for condensing and linking plasmid DNA to adenovirus for gene delivery. *Gene Ther, 4*(8), 773-782. doi:10.1038/sj.gt.3300471

Balla, A., Erdelyi, L. S., Soltesz-Katona, E., Balla, T., Varnai, P., & Hunyady, L. (2011). Demonstration of angiotensin II-induced Ras activation in the trans-Golgi network and endoplasmic reticulum using bioluminescence resonance energy transfer-based biosensors. *J Biol Chem, 286*(7), 5319-5327. doi:10.1074/jbc.M110.176933

Bannert, N., Craig, S., Farzan, M., Sogah, D., Santo, N. V., Choe, H., & Sodroski, J. (2001). Sialylated O-glycans and sulfated tyrosines in the NH2-terminal domain of CC chemokine receptor 5 contribute to high affinity binding of chemokines. *J Exp Med, 194*(11), 1661-1673. doi:10.1084/jem.194.11.1661

Beaulieu, J. M., Sotnikova, T. D., Marion, S., Lefkowitz, R. J., Gainetdinov, R. R., & Caron, M. G. (2005). An Akt/beta-arrestin 2/PP2A signaling complex mediates dopaminergic neurotransmission and behavior. *Cell, 122*(2), 261-273. doi:10.1016/j.cell.2005.05.012

Beautrait, A., Paradis, J. S., Zimmerman, B., Giubilaro, J., Nikolajev, L., Armando, S., . . . Bouvier, M. (2017). A new inhibitor of the beta-arrestin/AP2 endocytic complex reveals interplay between GPCR internalization and signalling. *Nat Commun, 8*, 15054. doi:10.1038/ncomms15054

Beemiller, P., Hoppe, A. D., & Swanson, J. A. (2006). A phosphatidylinositol-3-kinase-dependent signal transition regulates ARF1 and ARF6 during Fcgamma receptor-mediated phagocytosis. *PLoS Biol, 4*(6), e162. doi:10.1371/journal.pbio.0040162

Benovic, J. L., Strasser, R. H., Caron, M. G., & Lefkowitz, R. J. (1986). Beta-adrenergic receptor kinase: identification of a novel protein kinase that phosphorylates the agonist-occupied form of the receptor. *Proc Natl Acad Sci U S A, 83*(9), 2797-2801. doi:10.1073/pnas.83.9.2797

Berndt, N., Hamilton, A. D., & Sebti, S. M. (2011). Targeting protein prenylation for cancer therapy. *Nat Rev Cancer, 11*(11), 775-791. doi:10.1038/nrc3151

Berridge, M. J. (1993). Inositol trisphosphate and calcium signalling. *Nature, 361*(6410), 315-325. doi:10.1038/361315a0

Berridge, M. J., & Irvine, R. F. (1984). Inositol trisphosphate, a novel second messenger in cellular signal transduction. *Nature, 312*(5992), 315-321. doi:10.1038/312315a0

Bery, N., Cruz-Migoni, A., Bataille, C. J., Quevedo, C. E., Tulmin, H., Miller, A., . . . Rabbitts, T. H. (2018). BRET-based RAS biosensors that show a novel small molecule is an inhibitor of RAS-effector protein-protein interactions. *Elife, 7*. doi:10.7554/eLife.37122

Bery, N., & Rabbitts, T. H. (2019). Bioluminescence Resonance Energy Transfer 2 (BRET2)-Based RAS Biosensors to Characterize RAS Inhibitors. *Curr Protoc Cell Biol, 83*(1), e83. doi:10.1002/cpcb.83

Birnbaumer, L., Codina, J., Yatani, A., Mattera, R., Graf, R., Olate, J., . . . et al. (1989). Molecular basis of regulation of ionic channels by G proteins. *Recent Prog Horm Res, 45*, 121-206; discussion 206-128. doi:10.1016/b978-0-12-571145-6.50008-x

Bishop, A. L., & Hall, A. (2000). Rho GTPases and their effector proteins. *Biochem J, 348 Pt 2*, 241-255.

Boriack-Sjodin, P. A., Margarit, S. M., Bar-Sagi, D., & Kuriyan, J. (1998). The structural basis of the activation of Ras by Sos. *Nature, 394*(6691), 337-343. doi:10.1038/28548

Bos, J. L. (1989). ras oncogenes in human cancer: a review. *Cancer Res, 49*(17), 4682-4689.

Bourne, H. R., Sanders, D. A., & McCormick, F. (1991). The GTPase superfamily: conserved structure and molecular mechanism. *Nature, 349*(6305), 117-127. doi:10.1038/349117a0

Bridges, T. M., & Lindsley, C. W. (2008). G-protein-coupled receptors: from classical modes of modulation to allosteric mechanisms. *ACS Chem Biol, 3*(9), 530-541. doi:10.1021/cb800116f

Burns, M. C., Howes, J. E., Sun, Q., Little, A. J., Camper, D. V., Abbott, J. R., . . . Fesik, S. W. (2018). High-throughput screening identifies small molecules that bind to the RAS:SOS:RAS complex and perturb RAS signaling. *Anal Biochem, 548*, 44-52. doi:10.1016/j.ab.2018.01.025

Burns, M. C., Sun, Q., Daniels, R. N., Camper, D., Kennedy, J. P., Phan, J., . . . Fesik, S. W. (2014). Approach for targeting Ras with small molecules that activate SOS-mediated nucleotide exchange. *Proc Natl Acad Sci U S A, 111*(9), 3401-3406. doi:10.1073/pnas.1315798111

Casanova, J. E. (2007). Regulation of Arf activation: the Sec7 family of guanine nucleotide exchange factors. *Traffic, 8*(11), 1476-1485. doi:10.1111/j.1600-0854.2007.00634.x

Castellano, E., & Downward, J. (2011). RAS Interaction with PI3K: More Than Just Another Effector Pathway. *Genes Cancer, 2*(3), 261-274. doi:10.1177/1947601911408079

Chardin, P., Paris, S., Antonny, B., Robineau, S., Béraud-Dufour, S., Jackson, C. L., & Chabre, M. (1996). A human exchange factor for ARF contains Sec7- and pleckstrin-homology domains. *Nature, 384*(6608), 481-484. doi:10.1038/384481a0

Charles, R., Namkung, Y., Cotton, M., Laporte, S. A., & Claing, A. (2016). beta-Arrestin-mediated Angiotensin II Signaling Controls the Activation of ARF6 Protein and Endocytosis in Migration of Vascular Smooth Muscle Cells. *J Biol Chem, 291*(8), 3967-3981. doi:10.1074/jbc.M115.684357

Chikumi, H., Vazquez-Prado, J., Servitja, J. M., Miyazaki, H., & Gutkind, J. S. (2002). Potent activation of RhoA by Galpha q and Gq-coupled receptors. *J Biol Chem, 277*(30), 27130-27134. doi:10.1074/jbc.M204715200

Chiloeches, A., Paterson, H. F., Marais, R., Clerk, A., Marshall, C. J., & Sugden, P. H. (1999). Regulation of Ras.GTP loading and Ras-Raf association in neonatal rat ventricular myocytes by G protein-coupled receptor agonists and phorbol ester. Activation of the extracellular signal-regulated kinase cascade by phorbol ester is mediated by Ras. *J Biol Chem, 274*(28), 19762-19770. doi:10.1074/jbc.274.28.19762

Clackson, T., & Wells, J. A. (1995). A hot spot of binding energy in a hormone-receptor interface. *Science, 267*(5196), 383-386. doi:10.1126/science.7529940

Claing, A., Chen, W., Miller, W. E., Vitale, N., Moss, J., Premont, R. T., & Lefkowitz, R. J. (2001). beta-Arrestin-mediated ADP-ribosylation factor 6 activation and beta 2-adrenergic receptor endocytosis. *J Biol Chem, 276*(45), 42509-42513. doi:10.1074/jbc.M108399200

Claing, A., Laporte, S. A., Caron, M. G., & Lefkowitz, R. J. (2002). Endocytosis of G protein-coupled receptors: roles of G protein-coupled receptor kinases and beta-arrestin proteins. *Prog Neurobiol, 66*(2), 61-79.

Colicelli, J. (2004). Human RAS superfamily proteins and related GTPases. *Sci STKE, 2004*(250), Re13. doi:10.1126/stke.2502004re13

Cotton, M., Boulay, P. L., Houndolo, T., Vitale, N., Pitcher, J. A., & Claing, A. (2007). Endogenous ARF6 interacts with Rac1 upon angiotensin II stimulation to regulate

membrane ruffling and cell migration. *Mol Biol Cell, 18*(2), 501-511. doi:10.1091/mbc.e06-06-0567

Cox, A. D., Fesik, S. W., Kimmelman, A. C., Luo, J., & Der, C. J. (2014). Drugging the undruggable RAS: Mission possible? *Nat Rev Drug Discov, 13*(11), 828-851. doi:10.1038/nrd4389

D'Souza-Schorey, C., & Chavrier, P. (2006). ARF proteins: roles in membrane traffic and beyond. *Nat Rev Mol Cell Biol, 7*(5), 347-358. doi:10.1038/nrm1910

Daaka, Y., Luttrell, L. M., Ahn, S., Della Rocca, G. J., Ferguson, S. S., Caron, M. G., & Lefkowitz, R. J. (1998). Essential role for G protein-coupled receptor endocytosis in the activation of mitogen-activated protein kinase. *J Biol Chem, 273*(2), 685-688. doi:10.1074/jbc.273.2.685

de Gasparo, M., Catt, K. J., Inagami, T., Wright, J. W., & Unger, T. (2000). International union of pharmacology. XXIII. The angiotensin II receptors. *Pharmacol Rev, 52*(3), 415-472.

de Rooij, J., & Bos, J. L. (1997). Minimal Ras-binding domain of Raf1 can be used as an activation-specific probe for Ras. *Oncogene, 14*(5), 623-625. doi:10.1038/sj.onc.1201005

Delom, F., & Fessart, D. (2011). Role of Phosphorylation in the Control of Clathrin-Mediated Internalization of GPCR. *Int J Cell Biol, 2011*, 246954. doi:10.1155/2011/246954

DerMardirossian, C., & Bokoch, G. M. (2005). GDIs: central regulatory molecules in Rho GTPase activation. *Trends Cell Biol, 15*(7), 356-363. doi:10.1016/j.tcb.2005.05.001

Devost, D., Audet, N., Zhou, C., Kobayashi, H., Bonin, H., Lukashova, V., . . . Hébert, T. E. (2016). Cellular and subcellular context determine outputs from signaling biosensors. *Methods Cell Biol, 132*, 319-337. doi:10.1016/bs.mcb.2015.11.010

DeWire, S. M., Ahn, S., Lefkowitz, R. J., & Shenoy, S. K. (2007). Beta-arrestins and cell signaling. *Annu Rev Physiol, 69*, 483-510. doi:10.1146/annurev.physiol.69.022405.154749

Dise, R. S., Frey, M. R., Whitehead, R. H., & Polk, D. B. (2008). Epidermal growth factor stimulates Rac activation through Src and phosphatidylinositol 3-kinase to promote colonic epithelial cell migration. *Am J Physiol Gastrointest Liver Physiol, 294*(1), G276-285. doi:10.1152/ajpgi.00340.2007

Donaldson, J. G., Finazzi, D., & Klausner, R. D. (1992). Brefeldin A inhibits Golgi membrane-catalysed exchange of guanine nucleotide onto ARF protein. *Nature, 360*(6402), 350-352. doi:10.1038/360350a0

Donaldson, J. G., & Jackson, C. L. (2000). Regulators and effectors of the ARF GTPases. *Curr Opin Cell Biol, 12*(4), 475-482. doi:10.1016/s0955-0674(00)00119-8

Donaldson, J. G., & Jackson, C. L. (2011). ARF family G proteins and their regulators: roles in membrane transport, development and disease. *Nat Rev Mol Cell Biol, 12*(6), 362-375. doi:10.1038/nrm3117

Downward, J. (1996). Control of ras activation. *Cancer Surv, 27*, 87-100.

Downward, J. (1998). Ras signalling and apoptosis. *Curr Opin Genet Dev, 8*(1), 49-54. doi:10.1016/s0959-437x(98)80061-0

Downward, J. (2003). Targeting RAS signalling pathways in cancer therapy. *Nat Rev Cancer, 3*(1), 11-22. doi:10.1038/nrc969

Dutt, P., Nguyen, N., & Toksoz, D. (2004). Role of Lbc RhoGEF in Galpha12/13-induced signals to Rho GTPase. *Cell Signal, 16*(2), 201-209. doi:10.1016/s0898-6568(03)00132-3

Dutta, D., Williamson, C. D., Cole, N. B., & Donaldson, J. G. (2012). Pitstop 2 is a potent inhibitor of clathrin-independent endocytosis. *PLoS One, 7*(9), e45799. doi:10.1371/journal.pone.0045799

Ebrahimi, F. A., & Chess, A. (1998). Olfactory G proteins: simple and complex signal transduction. *Curr Biol, 8*(12), R431-433. doi:10.1016/s0960-9822(98)70271-4

Eckert, L. B., Repasky, G. A., Ulkü, A. S., McFall, A., Zhou, H., Sartor, C. I., & Der, C. J. (2004). Involvement of Ras activation in human breast cancer cell signaling, invasion, and anoikis. *Cancer Res, 64*(13), 4585-4592. doi:10.1158/0008-5472.Can-04-0396

Eichel, K., Jullie, D., & von Zastrow, M. (2016). beta-Arrestin drives MAP kinase signalling from clathrin-coated structures after GPCR dissociation. *Nat Cell Biol, 18*(3), 303-310. doi:10.1038/ncb3307

Engelman, J. A., Chen, L., Tan, X., Crosby, K., Guimaraes, A. R., Upadhyay, R., . . . Wong, K. K. (2008). Effective use of PI3K and MEK inhibitors to treat mutant Kras G12D and PIK3CA H1047R murine lung cancers. *Nat Med, 14*(12), 1351-1356. doi:10.1038/nm.1890

Evelyn, C. R., Duan, X., Biesiada, J., Seibel, W. L., Meller, J., & Zheng, Y. (2014). Rational design of small molecule inhibitors targeting the Ras GEF, SOS1. *Chem Biol, 21*(12), 1618-1628. doi:10.1016/j.chembiol.2014.09.018

Ferguson, S. S. (2001). Evolving concepts in G protein-coupled receptor endocytosis: the role in receptor desensitization and signaling. *Pharmacol Rev, 53*(1), 1-24.

Ferguson, S. S., Downey, W. E., 3rd, Colapietro, A. M., Barak, L. S., Menard, L., & Caron, M. G. (1996). Role of beta-arrestin in mediating agonist-promoted G protein-coupled receptor internalization. *Science, 271*(5247), 363-366. doi:10.1126/science.271.5247.363

Flower, D. R. (1999). Modelling G-protein-coupled receptors for drug design. *Biochim Biophys Acta, 1422*(3), 207-234. doi:10.1016/s0304-4157(99)00006-4

Foord, S. M., Bonner, T. I., Neubig, R. R., Rosser, E. M., Pin, J. P., Davenport, A. P., . . . Harmar, A. J. (2005). International Union of Pharmacology. XLVI. G protein-coupled receptor list. *Pharmacol Rev, 57*(2), 279-288. doi:10.1124/pr.57.2.5

Frank, S., Upender, S., Hansen, S. H., & Casanova, J. E. (1998). ARNO is a guanine nucleotide exchange factor for ADP-ribosylation factor 6. *J Biol Chem, 273*(1), 23-27. doi:10.1074/jbc.273.1.23

Fredriksson, R., Lagerstrom, M. C., Lundin, L. G., & Schioth, H. B. (2003). The G-protein-coupled receptors in the human genome form five main families. Phylogenetic analysis, paralogon groups, and fingerprints. *Mol Pharmacol, 63*(6), 1256-1272. doi:10.1124/mol.63.6.1256

Freedman, N. J., Liggett, S. B., Drachman, D. E., Pei, G., Caron, M. G., & Lefkowitz, R. J. (1995). Phosphorylation and desensitization of the human beta 1-adrenergic receptor. Involvement of G protein-coupled receptor kinases and cAMP-dependent protein kinase. *J Biol Chem, 270*(30), 17953-17961. doi:10.1074/jbc.270.30.17953

Fukuhara, S., Murga, C., Zohar, M., Igishi, T., & Gutkind, J. S. (1999). A novel PDZ domain containing guanine nucleotide exchange factor links heterotrimeric G proteins to Rho. *J Biol Chem, 274*(9), 5868-5879. doi:10.1074/jbc.274.9.5868

Gales, C., Rebois, R. V., Hogue, M., Trieu, P., Breit, A., Hebert, T. E., & Bouvier, M. (2005). Real-time monitoring of receptor and G-protein interactions in living cells. *Nat Methods, 2*(3), 177-184. doi:10.1038/nmeth743

Gao, X., & Zhang, J. (2008). Spatiotemporal analysis of differential Akt regulation in plasma membrane microdomains. *Mol Biol Cell, 19*(10), 4366-4373. doi:10.1091/mbc.E08-05-0449

Garcia-Echeverria, C. (2009). Protein and lipid kinase inhibitors as targeted anticancer agents of the Ras/Raf/MEK and PI3K/PKB pathways. *Purinergic Signal, 5*(1), 117-125. doi:10.1007/s11302-008-9111-5

Giguere, P., Rochdi, M. D., Laroche, G., Dupre, E., Whorton, M. R., Sunahara, R. K., . . . Parent, J. L. (2006). ARF6 activation by Galpha q signaling: Galpha q forms molecular complexes with ARNO and ARF6. *Cell Signal, 18*(11), 1988-1994. doi:10.1016/j.cellsig.2006.03.003

Gilman, A. G. (1987). G proteins: transducers of receptor-generated signals. *Annu Rev Biochem, 56*, 615-649. doi:10.1146/annurev.bi.56.070187.003151

Goguen, B. N., Loving, G. S., & Imperiali, B. (2011). Development of a fluorogenic sensor for activated Cdc42. *Bioorg Med Chem Lett, 21*(17), 5058-5061. doi:10.1016/j.bmcl.2011.04.051

Goldberg, J. (1998). Structural basis for activation of ARF GTPase: mechanisms of guanine nucleotide exchange and GTP-myristoyl switching. *Cell, 95*(2), 237-248. doi:10.1016/s0092-8674(00)81754-7

Gonzalez-Maeso, J., & Meana, J. J. (2006). Heterotrimeric g proteins: insights into the neurobiology of mood disorders. *Curr Neuropharmacol, 4*(2), 127-138. doi:10.2174/157015906776359586

Goodman, O. B., Jr., Krupnick, J. G., Santini, F., Gurevich, V. V., Penn, R. B., Gagnon, A. W., . . . Benovic, J. L. (1996). Beta-arrestin acts as a clathrin adaptor in endocytosis of the beta2-adrenergic receptor. *Nature, 383*(6599), 447-450. doi:10.1038/383447a0

Goupil, E., Fillion, D., Clement, S., Luo, X., Devost, D., Sleno, R., . . . Hebert, T. E. (2015). Angiotensin II type I and prostaglandin F2alpha receptors cooperatively modulate signaling in vascular smooth muscle cells. *J Biol Chem, 290*(5), 3137-3148. doi:10.1074/jbc.M114.631119

Gross, S. M., & Rotwein, P. (2015). Akt signaling dynamics in individual cells. *J Cell Sci, 128*(14), 2509-2519. doi:10.1242/jcs.168773

Gupta, S., Ramjaun, A. R., Haiko, P., Wang, Y., Warne, P. H., Nicke, B., . . . Downward, J. (2007). Binding of ras to phosphoinositide 3-kinase p110alpha is required for ras-driven tumorigenesis in mice. *Cell, 129*(5), 957-968. doi:10.1016/j.cell.2007.03.051

Gutkind, J. S. (2000). Regulation of mitogen-activated protein kinase signaling networks by G protein-coupled receptors. *Sci STKE, 2000*(40), re1. doi:10.1126/stke.2000.40.re1

Hafner, M., Schmitz, A., Grune, I., Srivatsan, S. G., Paul, B., Kolanus, W., . . . Famulok, M. (2006). Inhibition of cytohesins by SecinH3 leads to hepatic insulin resistance. *Nature, 444*(7121), 941-944. doi:10.1038/nature05415

Hajduk, P. J., Gerfin, T., Boehlen, J. M., Haberli, M., Marek, D., & Fesik, S. W. (1999). High-throughput nuclear magnetic resonance-based screening. *J Med Chem, 42*(13), 2315-2317. doi:10.1021/jm9901475

Hall, A. (1990). The cellular functions of small GTP-binding proteins. *Science, 249*(4969), 635-640. doi:10.1126/science.2116664

Hall, A. (1994). Small GTP-binding proteins and the regulation of the actin cytoskeleton. *Annu Rev Cell Biol, 10*, 31-54. doi:10.1146/annurev.cb.10.110194.000335

Hall, B., McLean, M. A., Davis, K., Casanova, J. E., Sligar, S. G., & Schwartz, M. A. (2008). A fluorescence resonance energy transfer activation sensor for Arf6. *Anal Biochem, 374*(2), 243-249. doi:10.1016/j.ab.2007.11.032

Hamdan, F. F., Percherancier, Y., Breton, B., & Bouvier, M. (2006). Monitoring protein-protein interactions in living cells by bioluminescence resonance energy transfer (BRET). *Curr Protoc Neurosci, Chapter 5*, Unit 5.23. doi:10.1002/0471142301.ns0523s34

Hamdan, F. F., Rochdi, M. D., Breton, B., Fessart, D., Michaud, D. E., Charest, P. G., . . . Bouvier, M. (2007). Unraveling G protein-coupled receptor endocytosis pathways using real-time monitoring of agonist-promoted interaction between beta-arrestins and AP-2. *J Biol Chem, 282*(40), 29089-29100. doi:10.1074/jbc.M700577200

Hamm, H. E., Deretic, D., Hofmann, K. P., Schleicher, A., & Kohl, B. (1987). Mechanism of action of monoclonal antibodies that block the light activation of the guanyl nucleotide-binding protein, transducin. *J Biol Chem, 262*(22), 10831-10838.

Hanna, S., Miskolci, V., Cox, D., & Hodgson, L. (2014). A new genetically encoded single-chain biosensor for Cdc42 based on FRET, useful for live-cell imaging. *PLoS One, 9*(5), e96469. doi:10.1371/journal.pone.0096469

Harden, T. K., Waldo, G. L., Hicks, S. N., & Sondek, J. (2011). Mechanism of activation and inactivation of Gq/phospholipase C-beta signaling nodes. *Chem Rev, 111*(10), 6120-6129. doi:10.1021/cr200209p

Hashimoto, S., Onodera, Y., Hashimoto, A., Tanaka, M., Hamaguchi, M., Yamada, A., & Sabe, H. (2004). Requirement for Arf6 in breast cancer invasive activities. *Proc Natl Acad Sci U S A, 101*(17), 6647-6652. doi:10.1073/pnas.0401753101

Hausdorff, W. P., Caron, M. G., & Lefkowitz, R. J. (1990). Turning off the signal: desensitization of beta-adrenergic receptor function. *Faseb j, 4*(11), 2881-2889.

Hausdorff, W. P., Lohse, M. J., Bouvier, M., Liggett, S. B., Caron, M. G., & Lefkowitz, R. J. (1990). Two kinases mediate agonist-dependent phosphorylation and desensitization of the beta 2-adrenergic receptor. *Symp Soc Exp Biol, 44*, 225-240.

Hawes, B. E., van Biesen, T., Koch, W. J., Luttrell, L. M., & Lefkowitz, R. J. (1995). Distinct pathways of Gi- and Gq-mediated mitogen-activated protein kinase activation. *J Biol Chem, 270*(29), 17148-17153. doi:10.1074/jbc.270.29.17148

Herrmann, C., Martin, G. A., & Wittinghofer, A. (1995). Quantitative analysis of the complex between p21ras and the Ras-binding domain of the human Raf-1 protein kinase. *J Biol Chem, 270*(7), 2901-2905. doi:10.1074/jbc.270.7.2901

Hescheler, J., Rosenthal, W., Trautwein, W., & Schultz, G. (1987). The GTP-binding protein, Go, regulates neuronal calcium channels. *Nature, 325*(6103), 445-447. doi:10.1038/325445a0

Hill, S. J. (2006). G-protein-coupled receptors: past, present and future. *Br J Pharmacol, 147 Suppl 1*, S27-37. doi:10.1038/sj.bjp.0706455

Hill, T. A., Gordon, C. P., McGeachie, A. B., Venn-Brown, B., Odell, L. R., Chau, N., . . . McCluskey, A. (2009). Inhibition of dynamin mediated endocytosis by the dynoles--synthesis and functional activity of a family of indoles. *J Med Chem, 52*(12), 3762-3773. doi:10.1021/jm900036m

Hillig, R. C., Sautier, B., Schroeder, J., Moosmayer, D., Hilpmann, A., Stegmann, C. M., . . . Bader, B. (2019). Discovery of potent SOS1 inhibitors that block RAS activation via disruption of the RAS-SOS1 interaction. *Proc Natl Acad Sci U S A, 116*(7), 2551-2560. doi:10.1073/pnas.1812963116

Hodges, T. R., Abbott, J. R., Little, A. J., Sarkar, D., Salovich, J. M., Howes, J. E., . . . Fesik, S. W. (2018). Discovery and Structure-Based Optimization of Benzimidazole-Derived Activators of SOS1-Mediated Nucleotide Exchange on RAS. *J Med Chem, 61*(19), 8875-8894. doi:10.1021/acs.jmedchem.8b01108

Hodgson, L., Shen, F., & Hahn, K. (2010). Biosensors for characterizing the dynamics of rho family GTPases in living cells. *Curr Protoc Cell Biol, Chapter 14*, Unit 14.11.11-26. doi:10.1002/0471143030.cb1411s46

Houndolo, T., Boulay, P. L., & Claing, A. (2005). G protein-coupled receptor endocytosis in ADP-ribosylation factor 6-depleted cells. *J Biol Chem, 280*(7), 5598-5604. doi:10.1074/jbc.M411456200

Jiang, X., Huang, F., Marusyk, A., & Sorkin, A. (2003). Grb2 regulates internalization of EGF receptors through clathrin-coated pits. *Mol Biol Cell, 14*(3), 858-870. doi:10.1091/mbc.e02-08-0532

Jiang, X., & Sorkin, A. (2002). Coordinated traffic of Grb2 and Ras during epidermal growth factor receptor endocytosis visualized in living cells. *Mol Biol Cell, 13*(5), 1522-1535. doi:10.1091/mbc.01-11-0552

John, J., Sohmen, R., Feuerstein, J., Linke, R., Wittinghofer, A., & Goody, R. S. (1990). Kinetics of interaction of nucleotides with nucleotide-free H-ras p21. *Biochemistry, 29*(25), 6058-6065. doi:10.1021/bi00477a025

Kedziora, K. M., Leyton-Puig, D., Argenzio, E., Boumeester, A. J., van Butselaar, B., Yin, T., . . . Moolenaar, W. H. (2016). Rapid Remodeling of Invadosomes by Gi-coupled Receptors: DISSECTING THE ROLE OF Rho GTPases. *J Biol Chem, 291*(9), 4323-4333. doi:10.1074/jbc.M115.695940

Kenakin, T. (1995). Agonist-receptor efficacy. I: Mechanisms of efficacy and receptor promiscuity. *Trends Pharmacol Sci, 16*(6), 188-192. doi:10.1016/s0165-6147(00)89020-3

Kenakin, T. (2003). Ligand-selective receptor conformations revisited: the promise and the problem. *Trends Pharmacol Sci, 24*(7), 346-354. doi:10.1016/s0165-6147(03)00167-6

Kenakin, T. (2019). Biased Receptor Signaling in Drug Discovery. *Pharmacol Rev, 71*(2), 267-315. doi:10.1124/pr.118.016790

Kendall, R. T., Strungs, E. G., Rachidi, S. M., Lee, M. H., El-Shewy, H. M., Luttrell, D. K., . . . Luttrell, L. M. (2011). The beta-arrestin pathway-selective type 1A angiotensin receptor (AT1A) agonist [Sar1,Ile4,Ile8]angiotensin II regulates a robust G protein-independent signaling network. *J Biol Chem, 286*(22), 19880-19891. doi:10.1074/jbc.M111.233080

Khan, S. M., Sleno, R., Gora, S., Zylbergold, P., Laverdure, J. P., Labbe, J. C., . . . Hebert, T. E. (2013). The expanding roles of Gbetagamma subunits in G protein-coupled receptor signaling and drug action. *Pharmacol Rev, 65*(2), 545-577. doi:10.1124/pr.111.005603

Khoury, E., Clement, S., & Laporte, S. A. (2014). Allosteric and biased g protein-coupled receptor signaling regulation: potentials for new therapeutics. *Front Endocrinol (Lausanne), 5*, 68. doi:10.3389/fendo.2014.00068

Khoury, E., Nikolajev, L., Simaan, M., Namkung, Y., & Laporte, S. A. (2014). Differential regulation of endosomal GPCR/beta-arrestin complexes and trafficking by MAPK. *J Biol Chem, 289*(34), 23302-23317. doi:10.1074/jbc.M114.568147

Kinkade, C. W., Castillo-Martin, M., Puzio-Kuter, A., Yan, J., Foster, T. H., Gao, H., . . . Abate-Shen, C. (2008). Targeting AKT/mTOR and ERK MAPK signaling inhibits hormone-refractory prostate cancer in a preclinical mouse model. *J Clin Invest, 118*(9), 3051-3064. doi:10.1172/jci34764

Kirchhausen, T. (2000). Clathrin. *Annu Rev Biochem, 69*, 699-727. doi:10.1146/annurev.biochem.69.1.699

Kobilka, B. K. (2007). G protein coupled receptor structure and activation. *Biochim Biophys Acta, 1768*(4), 794-807. doi:10.1016/j.bbamem.2006.10.021

Kohout, T. A., Lin, F. S., Perry, S. J., Conner, D. A., & Lefkowitz, R. J. (2001). beta-Arrestin 1 and 2 differentially regulate heptahelical receptor signaling and trafficking. *Proc Natl Acad Sci U S A, 98*(4), 1601-1606. doi:10.1073/pnas.041608198

Kozasa, T., Jiang, X., Hart, M. J., Sternweis, P. M., Singer, W. D., Gilman, A. G., . . . Sternweis, P. C. (1998). p115 RhoGEF, a GTPase activating protein for Galpha12 and Galpha13. *Science, 280*(5372), 2109-2111. doi:10.1126/science.280.5372.2109

Kozma, S. C., Bogaard, M. E., Buser, K., Saurer, S. M., Bos, J. L., Groner, B., & Hynes, N. E. (1987). The human c-Kirsten ras gene is activated by a novel mutation in codon 13 in the breast carcinoma cell line MDA-MB231. *Nucleic Acids Res, 15*(15), 5963-5971. doi:10.1093/nar/15.15.5963

Krueger, K. M., Daaka, Y., Pitcher, J. A., & Lefkowitz, R. J. (1997). The role of sequestration in G protein-coupled receptor resensitization. Regulation of beta2-adrenergic receptor dephosphorylation by vesicular acidification. *J Biol Chem, 272*(1), 5-8. doi:10.1074/jbc.272.1.5

Krupnick, J. G., & Benovic, J. L. (1998). The role of receptor kinases and arrestins in G protein-coupled receptor regulation. *Annu Rev Pharmacol Toxicol, 38*, 289-319. doi:10.1146/annurev.pharmtox.38.1.289

Kwon, M., & Firestein, B. L. (2013). DNA transfection: calcium phosphate method. *Methods Mol Biol, 1018*, 107-110. doi:10.1007/978-1-62703-444-9_10

Lagerstrom, M. C., & Schioth, H. B. (2008). Structural diversity of G protein-coupled receptors and significance for drug discovery. *Nat Rev Drug Discov, 7*(4), 339-357. doi:10.1038/nrd2518

Laporte, S. A., Oakley, R. H., Holt, J. A., Barak, L. S., & Caron, M. G. (2000). The interaction of beta-arrestin with the AP-2 adaptor is required for the clustering of beta 2-adrenergic receptor into clathrin-coated pits. *J Biol Chem, 275*(30), 23120-23126. doi:10.1074/jbc.M002581200

Laporte, S. A., Oakley, R. H., Zhang, J., Holt, J. A., Ferguson, S. S., Caron, M. G., & Barak, L. S. (1999). The beta2-adrenergic receptor/betaarrestin complex recruits the clathrin adaptor AP-2 during endocytosis. *Proc Natl Acad Sci U S A, 96*(7), 3712-3717. doi:10.1073/pnas.96.7.3712

Larhammar, D., Blomqvist, A. G., & Wahlestedt, C. (1993). The receptor revolution--multiplicity of G-protein-coupled receptors. *Drug Des Discov, 9*(3-4), 179-188.

Latek, D., Modzelewska, A., Trzaskowski, B., Palczewski, K., & Filipek, S. (2012). G protein-coupled receptors--recent advances. *Acta Biochim Pol, 59*(4), 515-529.

Li, H. Y., Cao, K., & Zheng, Y. (2003). Ran in the spindle checkpoint: a new function for a versatile GTPase. *Trends Cell Biol, 13*(11), 553-557. doi:10.1016/j.tcb.2003.09.003

Li, R., Peng, C., Zhang, X., Wu, Y., Pan, S., & Xiao, Y. (2017). Roles of Arf6 in cancer cell invasion, metastasis and proliferation. *Life Sci, 182*, 80-84. doi:10.1016/j.lfs.2017.06.008

Lohse, M. J., Benovic, J. L., Codina, J., Caron, M. G., & Lefkowitz, R. J. (1990). beta-Arrestin: a protein that regulates beta-adrenergic receptor function. *Science, 248*(4962), 1547-1550. doi:10.1126/science.2163110

Lukman, S., Grant, B. J., Gorfe, A. A., Grant, G. H., & McCammon, J. A. (2010). The distinct conformational dynamics of K-Ras and H-Ras A59G. *PLoS Comput Biol, 6*(9). doi:10.1371/journal.pcbi.1000922

Luttrell, L. M., Ferguson, S. S., Daaka, Y., Miller, W. E., Maudsley, S., Della Rocca, G. J., . . . Lefkowitz, R. J. (1999). Beta-arrestin-dependent formation of beta2 adrenergic receptor-Src protein kinase complexes. *Science, 283*(5402), 655-661. doi:10.1126/science.283.5402.655

Luttrell, L. M., & Lefkowitz, R. J. (2002). The role of beta-arrestins in the termination and transduction of G-protein-coupled receptor signals. *J Cell Sci, 115*(Pt 3), 455-465.

Luttrell, L. M., Roudabush, F. L., Choy, E. W., Miller, W. E., Field, M. E., Pierce, K. L., & Lefkowitz, R. J. (2001). Activation and targeting of extracellular signal-regulated kinases by beta-arrestin scaffolds. *Proc Natl Acad Sci U S A, 98*(5), 2449-2454. doi:10.1073/pnas.041604898

Luttrell, L. M., Wang, J., Plouffe, B., Smith, J. S., Yamani, L., Kaur, S., . . . Lefkowitz, R. J. (2018). Manifold roles of beta-arrestins in GPCR signaling elucidated with siRNA and CRISPR/Cas9. *Sci Signal, 11*(549). doi:10.1126/scisignal.aat7650

Lutz, S., Shankaranarayanan, A., Coco, C., Ridilla, M., Nance, M. R., Vettel, C., . . . Tesmer, J. J. (2007). Structure of Galphaq-p63RhoGEF-RhoA complex reveals a pathway for the activation of RhoA by GPCRs. *Science, 318*(5858), 1923-1927. doi:10.1126/science.1147554

Macia, E., Chabre, M., & Franco, M. (2001). Specificities for the small G proteins ARF1 and ARF6 of the guanine nucleotide exchange factors ARNO and EFA6. *J Biol Chem, 276*(27), 24925-24930. doi:10.1074/jbc.M103284200

Macia, E., Ehrlich, M., Massol, R., Boucrot, E., Brunner, C., & Kirchhausen, T. (2006). Dynasore, a cell-permeable inhibitor of dynamin. *Dev Cell, 10*(6), 839-850. doi:10.1016/j.devcel.2006.04.002

Mackay, D. J., & Hall, A. (1998). Rho GTPases. *J Biol Chem, 273*(33), 20685-20688. doi:10.1074/jbc.273.33.20685

Marinissen, M. J., & Gutkind, J. S. (2001). G-protein-coupled receptors and signaling networks: emerging paradigms. *Trends Pharmacol Sci, 22*(7), 368-376. doi:10.1016/s0165-6147(00)01678-3

Marte, B. M., & Downward, J. (1997). PKB/Akt: connecting phosphoinositide 3-kinase to cell survival and beyond. *Trends Biochem Sci, 22*(9), 355-358. doi:10.1016/s0968-0004(97)01097-9

Matsubara, H., Kanasaki, M., Murasawa, S., Tsukaguchi, Y., Nio, Y., & Inada, M. (1994). Differential gene expression and regulation of angiotensin II receptor subtypes in rat cardiac fibroblasts and cardiomyocytes in culture. *J Clin Invest, 93*(4), 1592-1601. doi:10.1172/jci117139

Maurer, T., Garrenton, L. S., Oh, A., Pitts, K., Anderson, D. J., Skelton, N. J., . . . Fang, G. (2012). Small-molecule ligands bind to a distinct pocket in Ras and inhibit SOS-mediated nucleotide exchange activity. *Proc Natl Acad Sci U S A, 109*(14), 5299-5304. doi:10.1073/pnas.1116510109

Maurer, T., & Wang, W. (2013). NMR study to identify a ligand-binding pocket in Ras. *Enzymes, 33 Pt A*, 15-39. doi:10.1016/b978-0-12-416749-0.00002-6

Maurice, P., Guillaume, J. L., Benleulmi-Chaachoua, A., Daulat, A. M., Kamal, M., & Jockers, R. (2011). GPCR-interacting proteins, major players of GPCR function. *Adv Pharmacol, 62*, 349-380. doi:10.1016/b978-0-12-385952-5.00001-4

McCluskey, A., Daniel, J. A., Hadzic, G., Chau, N., Clayton, E. L., Mariana, A., . . . Robinson, P. J. (2013). Building a better dynasore: the dyngo compounds potently inhibit dynamin and endocytosis. *Traffic, 14*(12), 1272-1289. doi:10.1111/tra.12119

McDonald, P., Chow, C., Miller, W., Laporte, S., Field, M., Lin, F., . . . Lefkowitz, R. (2000). beta-Arrestin 2: A receptor-regulated MAPK scaffold for the activation of JNK3. *Science, 290*(5496), 1574-1577. doi:10.1126/science.290.5496.1574

McDonald, P. H., Chow, C. W., Miller, W. E., Laporte, S. A., Field, M. E., Lin, F. T., . . . Lefkowitz, R. J. (2000). Beta-arrestin 2: a receptor-regulated MAPK scaffold for the activation of JNK3. *Science, 290*(5496), 1574-1577. doi:10.1126/science.290.5496.1574

McDonald, P. H., Cote, N. L., Lin, F. T., Premont, R. T., Pitcher, J. A., & Lefkowitz, R. J. (1999). Identification of NSF as a beta-arrestin1-binding protein. Implications for beta2-adrenergic receptor regulation. *J Biol Chem, 274*(16), 10677-10680. doi:10.1074/jbc.274.16.10677

Ménétrey, J., Macia, E., Pasqualato, S., Franco, M., & Cherfils, J. (2000). Structure of Arf6-GDP suggests a basis for guanine nucleotide exchange factors specificity. *Nat Struct Biol, 7*(6), 466-469. doi:10.1038/75863

Miller, W. E., Maudsley, S., Ahn, S., Khan, K. D., Luttrell, L. M., & Lefkowitz, R. J. (2000). beta-arrestin1 interacts with the catalytic domain of the tyrosine kinase c-SRC. Role of beta-arrestin1-dependent targeting of c-SRC in receptor endocytosis. *J Biol Chem, 275*(15), 11312-11319. doi:10.1074/jbc.275.15.11312

Molinari, P., Casella, I., & Costa, T. (2008). Functional complementation of high-efficiency resonance energy transfer: a new tool for the study of protein binding interactions in living cells. *Biochem J, 409*(1), 251-261. doi:10.1042/bj20070803

Moreira, I. S., Fernandes, P. A., & Ramos, M. J. (2007). Hot spots--a review of the protein-protein interface determinant amino-acid residues. *Proteins, 68*(4), 803-812. doi:10.1002/prot.21396

Morishige, M., Hashimoto, S., Ogawa, E., Toda, Y., Kotani, H., Hirose, M., . . . Sabe, H. (2008). GEP100 links epidermal growth factor receptor signalling to Arf6 activation to induce breast cancer invasion. *Nat Cell Biol, 10*(1), 85-92. doi:10.1038/ncb1672

Morrison, D. K. (2012). MAP kinase pathways. *Cold Spring Harb Perspect Biol, 4*(11). doi:10.1101/cshperspect.a011254

Mortier, J., Friberg, A., Badock, V., Moosmayer, D., Schroeder, J., Steigemann, P., . . . Christ, C. D. (2020). Computationally Empowered Workflow Identifies Novel Covalent Allosteric Binders for KRAS(G12C). *ChemMedChem*. doi:10.1002/cmdc.201900727

Mossessova, E., Gulbis, J. M., & Goldberg, J. (1998). Structure of the guanine nucleotide exchange factor Sec7 domain of human arno and analysis of the interaction with ARF GTPase. *Cell, 92*(3), 415-423. doi:10.1016/s0092-8674(00)80933-2

Murga, C., Laguinge, L., Wetzker, R., Cuadrado, A., & Gutkind, J. S. (1998). Activation of Akt/protein kinase B by G protein-coupled receptors. A role for alpha and beta gamma subunits of heterotrimeric G proteins acting through phosphatidylinositol-3-OH kinasegamma. *J Biol Chem, 273*(30), 19080-19085. doi:10.1074/jbc.273.30.19080

Namkung, Y., Le Gouill, C., Lukashova, V., Kobayashi, H., Hogue, M., Khoury, E., . . . Laporte, S. A. (2016). Monitoring G protein-coupled receptor and beta-arrestin trafficking in live cells using enhanced bystander BRET. *Nat Commun, 7*, 12178. doi:10.1038/ncomms12178

Namkung, Y., LeGouill, C., Kumar, S., Cao, Y., Teixeira, L. B., Lukasheva, V., . . . Laporte, S. A. (2018). Functional selectivity profiling of the angiotensin II type 1 receptor using pathway-wide BRET signaling sensors. *Sci Signal, 11*(559). doi:10.1126/scisignal.aat1631

Namkung, Y., Radresa, O., Armando, S., Devost, D., Beautrait, A., Le Gouill, C., & Laporte, S. A. (2016). Quantifying biased signaling in GPCRs using BRET-based biosensors. *Methods, 92*, 5-10. doi:10.1016/j.ymeth.2015.04.010

Nishizuka, Y. (1984). The role of protein kinase C in cell surface signal transduction and tumour promotion. *Nature, 308*(5961), 693-698. doi:10.1038/308693a0

Nishizuka, Y. (1988). The molecular heterogeneity of protein kinase C and its implications for cellular regulation. *Nature, 334*(6184), 661-665. doi:10.1038/334661a0

Oakley, R. H., Laporte, S. A., Holt, J. A., Barak, L. S., & Caron, M. G. (1999). Association of beta-arrestin with G protein-coupled receptors during clathrin-mediated endocytosis dictates the profile of receptor resensitization. *J Biol Chem, 274*(45), 32248-32257. doi:10.1074/jbc.274.45.32248

Oakley, R. H., Laporte, S. A., Holt, J. A., Caron, M. G., & Barak, L. S. (2000). Differential affinities of visual arrestin, beta arrestin1, and beta arrestin2 for G protein-coupled receptors delineate two major classes of receptors. *J Biol Chem, 275*(22), 17201-17210. doi:10.1074/jbc.M910348199

Ostrem, J. M., Peters, U., Sos, M. L., Wells, J. A., & Shokat, K. M. (2013). K-Ras(G12C) inhibitors allosterically control GTP affinity and effector interactions. *Nature, 503*(7477), 548-551. doi:10.1038/nature12796

Overington, J. P., Al-Lazikani, B., & Hopkins, A. L. (2006). How many drug targets are there? *Nat Rev Drug Discov, 5*(12), 993-996. doi:10.1038/nrd2199

Papke, B., & Der, C. J. (2017). Drugging RAS: Know the enemy. *Science, 355*(6330), 1158-1163. doi:10.1126/science.aam7622

Paradis, J. S., Ly, S., Blondel-Tepaz, E., Galan, J. A., Beautrait, A., Scott, M. G., . . . Bouvier, M. (2015). Receptor sequestration in response to beta-arrestin-2 phosphorylation by ERK1/2 governs steady-state levels of GPCR cell-surface expression. *Proc Natl Acad Sci U S A, 112*(37), E5160-5168. doi:10.1073/pnas.1508836112

Patgiri, A., Yadav, K. K., Arora, P. S., & Bar-Sagi, D. (2011). An orthosteric inhibitor of the Ras-Sos interaction. *Nat Chem Biol, 7*(9), 585-587. doi:10.1038/nchembio.612

Peach, M. J. (1977). Renin-angiotensin system: biochemistry and mechanisms of action. *Physiol Rev, 57*(2), 313-370. doi:10.1152/physrev.1977.57.2.313

Peng, J. W., Lepre, C. A., Fejzo, J., Abdul-Manan, N., & Moore, J. M. (2001). Nuclear magnetic resonance-based approaches for lead generation in drug discovery. *Methods Enzymol, 338*, 202-230. doi:10.1016/s0076-6879(02)38221-1

Peters, P. J., Hsu, V. W., Ooi, C. E., Finazzi, D., Teal, S. B., Oorschot, V., . . . Klausner, R. D. (1995). Overexpression of wild-type and mutant ARF1 and ARF6: distinct perturbations of nonoverlapping membrane compartments. *J Cell Biol, 128*(6), 1003-1017. doi:10.1083/jcb.128.6.1003

Peterson, Y. K., & Luttrell, L. M. (2017). The Diverse Roles of Arrestin Scaffolds in G Protein-Coupled Receptor Signaling. *Pharmacol Rev, 69*(3), 256-297. doi:10.1124/pr.116.013367

Pfleger, K. D., & Eidne, K. A. (2006). Illuminating insights into protein-protein interactions using bioluminescence resonance energy transfer (BRET). *Nat Methods, 3*(3), 165-174. doi:10.1038/nmeth841

Pierce, K. L., & Lefkowitz, R. J. (2001). Classical and new roles of beta-arrestins in the regulation of G-protein-coupled receptors. *Nat Rev Neurosci, 2*(10), 727-733. doi:10.1038/35094577

Pierce, K. L., Premont, R. T., & Lefkowitz, R. J. (2002). Seven-transmembrane receptors. *Nat Rev Mol Cell Biol, 3*(9), 639-650. doi:10.1038/nrm908

Pitcher, J. A., Freedman, N. J., & Lefkowitz, R. J. (1998). G protein-coupled receptor kinases. *Annu Rev Biochem, 67*, 653-692. doi:10.1146/annurev.biochem.67.1.653

Pitcher, J. A., Payne, E. S., Csortos, C., DePaoli-Roach, A. A., & Lefkowitz, R. J. (1995). The G-protein-coupled receptor phosphatase: a protein phosphatase type 2A with a distinct subcellular distribution and substrate specificity. *Proc Natl Acad Sci U S A, 92*(18), 8343-8347. doi:10.1073/pnas.92.18.8343

Poupart, M. E., Fessart, D., Cotton, M., Laporte, S. A., & Claing, A. (2007). ARF6 regulates angiotensin II type 1 receptor endocytosis by controlling the recruitment of AP-2 and clathrin. *Cell Signal, 19*(11), 2370-2378. doi:10.1016/j.cellsig.2007.07.015

Premont, R. T., Inglese, J., & Lefkowitz, R. J. (1995). Protein kinases that phosphorylate activated G protein-coupled receptors. *Faseb j, 9*(2), 175-182. doi:10.1096/fasebj.9.2.7781920

Quoyer, J., Janz, J. M., Luo, J., Ren, Y., Armando, S., Lukashova, V., . . . Bouvier, M. (2013). Pepducin targeting the C-X-C chemokine receptor type 4 acts as a biased agonist favoring activation of the inhibitory G protein. *Proc Natl Acad Sci U S A, 110*(52), E5088-5097. doi:10.1073/pnas.1312515110

Ren, X. D., & Schwartz, M. A. (2000). Determination of GTP loading on Rho. *Methods Enzymol, 325*, 264-272. doi:10.1016/s0076-6879(00)25448-7

Repasky, G. A., Chenette, E. J., & Der, C. J. (2004). Renewing the conspiracy theory debate: does Raf function alone to mediate Ras oncogenesis? *Trends Cell Biol, 14*(11), 639-647. doi:10.1016/j.tcb.2004.09.014

Rhee, S. G., & Bae, Y. S. (1997). Regulation of phosphoinositide-specific phospholipase C isozymes. *J Biol Chem, 272*(24), 15045-15048. doi:10.1074/jbc.272.24.15045

Ridley, A. J. (2001). Rho family proteins: coordinating cell responses. *Trends Cell Biol, 11*(12), 471-477. doi:10.1016/s0962-8924(01)02153-5

Rodbell, M., Birnbaumer, L., Pohl, S. L., & Krans, H. M. (1971). The glucagon-sensitive adenyl cyclase system in plasma membranes of rat liver. V. An obligatory role of guanylnucleotides in glucagon action. *J Biol Chem, 246*(6), 1877-1882.

Rodriguez-Viciana, P., Warne, P. H., Dhand, R., Vanhaesebroeck, B., Gout, I., Fry, M. J., . . . Downward, J. (1994). Phosphatidylinositol-3-OH kinase as a direct target of Ras. *Nature, 370*(6490), 527-532. doi:10.1038/370527a0

Rojas, R. J., Yohe, M. E., Gershburg, S., Kawano, T., Kozasa, T., & Sondek, J. (2007). Galphaq directly activates p63RhoGEF and Trio via a conserved extension of the Dbl homology-associated pleckstrin homology domain. *J Biol Chem, 282*(40), 29201-29210. doi:10.1074/jbc.M703458200

Rondard, P., Iiri, T., Srinivasan, S., Meng, E., Fujita, T., & Bourne, H. R. (2001). Mutant G protein alpha subunit activated by Gbeta gamma: a model for receptor activation? *Proc Natl Acad Sci U S A, 98*(11), 6150-6155. doi:10.1073/pnas.101136198

Rosenbaum, D. M., Rasmussen, S. G., & Kobilka, B. K. (2009). The structure and function of G-protein-coupled receptors. *Nature, 459*(7245), 356-363. doi:10.1038/nature08144

Rovnyak, D., Hoch, J. C., Stern, A. S., & Wagner, G. (2004). Resolution and sensitivity of high field nuclear magnetic resonance spectroscopy. *J Biomol NMR, 30*(1), 1-10. doi:10.1023/b:Jnmr.0000042946.04002.19

Rubio, I. (2005). Use of the Ras binding domain of c-Raf for biochemical and live-cell analysis of Ras activation. *Biochem Soc Trans, 33*(Pt 4), 662-663. doi:10.1042/bst0330662

Salahpour, A., Espinoza, S., Masri, B., Lam, V., Barak, L. S., & Gainetdinov, R. R. (2012). BRET biosensors to study GPCR biology, pharmacology, and signal transduction. *Front Endocrinol (Lausanne), 3*, 105. doi:10.3389/fendo.2012.00105

Samatar, A. A., & Poulikakos, P. I. (2014). Targeting RAS-ERK signalling in cancer: promises and challenges. *Nat Rev Drug Discov, 13*(12), 928-942. doi:10.1038/nrd4281

Santy, L. C., Frank, S. R., Hatfield, J. C., & Casanova, J. E. (1999). Regulation of ARNO nucleotide exchange by a PH domain electrostatic switch. *Curr Biol, 9*(20), 1173-1176. doi:10.1016/s0960-9822(00)80019-6

Schlienger, S., Campbell, S., Pasquin, S., Gaboury, L., & Claing, A. (2016). ADP-ribosylation factor 1 expression regulates epithelial-mesenchymal transition and predicts poor clinical outcome in triple-negative breast cancer. *Oncotarget, 7*(13), 15811-15827. doi:10.18632/oncotarget.7515

Schmidt, A., & Hall, A. (2002). Guanine nucleotide exchange factors for Rho GTPases: turning on the switch. *Genes Dev, 16*(13), 1587-1609. doi:10.1101/gad.1003302

Schrage, R., Schmitz, A. L., Gaffal, E., Annala, S., Kehraus, S., Wenzel, D., . . . Kostenis, E. (2015). The experimental power of FR900359 to study Gq-regulated biological processes. *Nat Commun, 6*, 10156. doi:10.1038/ncomms10156

Seachrist, J. L., Anborgh, P. H., & Ferguson, S. S. (2000). beta 2-adrenergic receptor internalization, endosomal sorting, and plasma membrane recycling are regulated by rab GTPases. *J Biol Chem, 275*(35), 27221-27228. doi:10.1074/jbc.M003657200

Sebolt-Leopold, J. S., Dudley, D. T., Herrera, R., Van Becelaere, K., Wiland, A., Gowan, R. C., . . . Saltiel, A. R. (1999). Blockade of the MAP kinase pathway suppresses growth of colon tumors in vivo. *Nat Med, 5*(7), 810-816. doi:10.1038/10533

Seger, R., & Krebs, E. G. (1995). The MAPK signaling cascade. *Faseb j, 9*(9), 726-735.

Seta, K., Nanamori, M., Modrall, J. G., Neubig, R. R., & Sadoshima, J. (2002). AT1 receptor mutant lacking heterotrimeric G protein coupling activates the Src-Ras-ERK pathway without nuclear translocation of ERKs. *J Biol Chem, 277*(11), 9268-9277. doi:10.1074/jbc.M109221200

Shenoy, S. K., & Lefkowitz, R. J. (2011). beta-Arrestin-mediated receptor trafficking and signal transduction. *Trends Pharmacol Sci, 32*(9), 521-533. doi:10.1016/j.tips.2011.05.002

Shenoy, S. K., McDonald, P. H., Kohout, T. A., & Lefkowitz, R. J. (2001). Regulation of receptor fate by ubiquitination of activated beta 2-adrenergic receptor and beta-arrestin. *Science, 294*(5545), 1307-1313. doi:10.1126/science.1063866

Shih, W., Gallusser, A., & Kirchhausen, T. (1995). A clathrin-binding site in the hinge of the beta 2 chain of mammalian AP-2 complexes. *J Biol Chem, 270*(52), 31083-31090. doi:10.1074/jbc.270.52.31083

Shima, F., Yoshikawa, Y., Ye, M., Araki, M., Matsumoto, S., Liao, J., . . . Kataoka, T. (2013). In silico discovery of small-molecule Ras inhibitors that display antitumor activity by blocking the Ras-effector interaction. *Proc Natl Acad Sci U S A, 110*(20), 8182-8187. doi:10.1073/pnas.1217730110

Simaan, M., Bedard-Goulet, S., Fessart, D., Gratton, J. P., & Laporte, S. A. (2005). Dissociation of beta-arrestin from internalized bradykinin B2 receptor is necessary for receptor recycling and resensitization. *Cell Signal, 17*(9), 1074-1083. doi:10.1016/j.cellsig.2004.12.001

Simon, M. I., Strathmann, M. P., & Gautam, N. (1991). Diversity of G proteins in signal transduction. *Science, 252*(5007), 802-808. doi:10.1126/science.1902986

Snyder, J. T., Worthylake, D. K., Rossman, K. L., Betts, L., Pruitt, W. M., Siderovski, D. P., . . . Sondek, J. (2002). Structural basis for the selective activation of Rho GTPases by Dbl exchange factors. *Nat Struct Biol, 9*(6), 468-475. doi:10.1038/nsb796

Soga, S., Shirai, H., Kobori, M., & Hirayama, N. (2007). Use of amino acid composition to predict ligand-binding sites. *J Chem Inf Model, 47*(2), 400-406. doi:10.1021/ci6002202

Stenmark, H. (2009). Rab GTPases as coordinators of vesicle traffic. *Nat Rev Mol Cell Biol, 10*(8), 513-525. doi:10.1038/nrm2728

Sterne-Marr, R., & Benovic, J. L. (1995). Regulation of G protein-coupled receptors by receptor kinases and arrestins. *Vitam Horm, 51*, 193-234. doi:10.1016/s0083-6729(08)61039-0

Sun, Q., Burke, J. P., Phan, J., Burns, M. C., Olejniczak, E. T., Waterson, A. G., . . . Fesik, S. W. (2012). Discovery of small molecules that bind to K-Ras and inhibit Sos-mediated activation. *Angew Chem Int Ed Engl, 51*(25), 6140-6143. doi:10.1002/anie.201201358

Takai, Y., Sasaki, T., & Matozaki, T. (2001). Small GTP-binding proteins. *Physiol Rev, 81*(1), 153-208. doi:10.1152/physrev.2001.81.1.153

Takatsu, H., Yoshino, K., Toda, K., & Nakayama, K. (2002). GGA proteins associate with Golgi membranes through interaction between their GGAH domains and ADP-ribosylation factors. *Biochem J, 365*(Pt 2), 369-378. doi:10.1042/bj20020428

Thanos, C. D., DeLano, W. L., & Wells, J. A. (2006). Hot-spot mimicry of a cytokine receptor by a small molecule. *Proc Natl Acad Sci U S A, 103*(42), 15422-15427. doi:10.1073/pnas.0607058103

Titushin, M. S., Feng, Y., Lee, J., Vysotski, E. S., & Liu, Z. J. (2011). Protein-protein complexation in bioluminescence. *Protein Cell, 2*(12), 957-972. doi:10.1007/s13238-011-1118-y

Tohgo, A., Choy, E. W., Gesty-Palmer, D., Pierce, K. L., Laporte, S., Oakley, R. H., . . . Luttrell, L. M. (2003). The stability of the G protein-coupled receptor-beta-arrestin interaction determines the mechanism and functional consequence of ERK activation. *J Biol Chem, 278*(8), 6258-6267. doi:10.1074/jbc.M212231200

Trinh, T. B., Upadhyaya, P., Qian, Z., & Pei, D. (2016). Discovery of a Direct Ras Inhibitor by Screening a Combinatorial Library of Cell-Permeable Bicyclic Peptides. *ACS Comb Sci, 18*(1), 75-85. doi:10.1021/acscombsci.5b00164

Urizar, E., Montanelli, L., Loy, T., Bonomi, M., Swillens, S., Gales, C., . . . Costagliola, S. (2005). Glycoprotein hormone receptors: link between receptor homodimerization and negative cooperativity. *Embo j, 24*(11), 1954-1964. doi:10.1038/sj.emboj.7600686

Valencia, A., Chardin, P., Wittinghofer, A., & Sander, C. (1991). The ras protein family: evolutionary tree and role of conserved amino acids. *Biochemistry, 30*(19), 4637-4648. doi:10.1021/bi00233a001

Vetter, I. R., & Wittinghofer, A. (2001). The guanine nucleotide-binding switch in three dimensions. *Science, 294*(5545), 1299-1304. doi:10.1126/science.1062023

Viaud, J., Zeghouf, M., Barelli, H., Zeeh, J. C., Padilla, A., Guibert, B., . . . Chavanieu, A. (2007). Structure-based discovery of an inhibitor of Arf activation by Sec7 domains through targeting of protein-protein complexes. *Proc Natl Acad Sci U S A, 104*(25), 10370-10375. doi:10.1073/pnas.0700773104

Vigil, D., Cherfils, J., Rossman, K. L., & Der, C. J. (2010). Ras superfamily GEFs and GAPs: validated and tractable targets for cancer therapy? *Nat Rev Cancer, 10*(12), 842-857. doi:10.1038/nrc2960

Vikis, H. G., & Guan, K. L. (2004). Glutathione-S-transferase-fusion based assays for studying protein-protein interactions. *Methods Mol Biol, 261*, 175-186. doi:10.1385/1-59259-762-9:175

Vogt, S., Grosse, R., Schultz, G., & Offermanns, S. (2003). Receptor-dependent RhoA activation in G12/G13-deficient cells: genetic evidence for an involvement of Gq/G11. *J Biol Chem, 278*(31), 28743-28749. doi:10.1074/jbc.M304570200

Vojtek, A. B., Hollenberg, S. M., & Cooper, J. A. (1993). Mammalian Ras interacts directly with the serine/threonine kinase Raf. *Cell, 74*(1), 205-214. doi:10.1016/0092-8674(93)90307-c

von Kleist, L., Stahlschmidt, W., Bulut, H., Gromova, K., Puchkov, D., Robertson, M. J., . . . Haucke, V. (2011). Role of the clathrin terminal domain in regulating coated pit dynamics revealed by small molecule inhibition. *Cell, 146*(3), 471-484. doi:10.1016/j.cell.2011.06.025

Wang, Q., Villeneuve, G., & Wang, Z. (2005). Control of epidermal growth factor receptor endocytosis by receptor dimerization, rather than receptor kinase activation. *EMBO Rep, 6*(10), 942-948. doi:10.1038/sj.embor.7400491

Wang, Z., & Moran, M. F. (1996). Requirement for the adapter protein GRB2 in EGF receptor endocytosis. *Science, 272*(5270), 1935-1939. doi:10.1126/science.272.5270.1935

Wei, H., Ahn, S., Barnes, W. G., & Lefkowitz, R. J. (2004). Stable interaction between beta-arrestin 2 and angiotensin type 1A receptor is required for beta-arrestin 2-mediated activation of extracellular signal-regulated kinases 1 and 2. *J Biol Chem, 279*(46), 48255-48261. doi:10.1074/jbc.M406205200

Wei, H., Ahn, S., Shenoy, S. K., Karnik, S. S., Hunyady, L., Luttrell, L. M., & Lefkowitz, R. J. (2003). Independent beta-arrestin 2 and G protein-mediated pathways for angiotensin II activation of extracellular signal-regulated kinases 1 and 2. *Proc Natl Acad Sci U S A, 100*(19), 10782-10787. doi:10.1073/pnas.1834556100

Weis, K. (2003). Regulating access to the genome: nucleocytoplasmic transport throughout the cell cycle. *Cell, 112*(4), 441-451. doi:10.1016/s0092-8674(03)00082-5

Wells, J. A., & McClendon, C. L. (2007). Reaching for high-hanging fruit in drug discovery at protein-protein interfaces. *Nature, 450*(7172), 1001-1009. doi:10.1038/nature06526

Wennerberg, K., Rossman, K. L., & Der, C. J. (2005). The Ras superfamily at a glance. *J Cell Sci, 118*(Pt 5), 843-846. doi:10.1242/jcs.01660

Whyte, D. B., Kirschmeier, P., Hockenberry, T. N., Nunez-Oliva, I., James, L., Catino, J. J., . . . Pai, J. K. (1997). K- and N-Ras are geranylgeranylated in cells treated with farnesyl protein transferase inhibitors. *J Biol Chem, 272*(22), 14459-14464. doi:10.1074/jbc.272.22.14459

Winter, J. J., Anderson, M., Blades, K., Brassington, C., Breeze, A. L., Chresta, C., . . . Wrigley, G. (2015). Small molecule binding sites on the Ras:SOS complex can be exploited for inhibition of Ras activation. *J Med Chem, 58*(5), 2265-2274. doi:10.1021/jm501660t

Wolber, G., & Langer, T. (2005). LigandScout: 3-D pharmacophores derived from protein-bound ligands and their use as virtual screening filters. *J Chem Inf Model, 45*(1), 160-169. doi:10.1021/ci049885e

Yoo, J. H., Shi, D. S., Grossmann, A. H., Sorensen, L. K., Tong, Z., Mleynek, T. M., . . . Li, D. Y. (2016). ARF6 Is an Actionable Node that Orchestrates Oncogenic GNAQ Signaling in Uveal Melanoma. *Cancer Cell, 29*(6), 889-904. doi:10.1016/j.ccell.2016.04.015

Yoshizaki, H., Mochizuki, N., Gotoh, Y., & Matsuda, M. (2007). Akt-PDK1 complex mediates epidermal growth factor-induced membrane protrusion through Ral activation. *Mol Biol Cell, 18*(1), 119-128. doi:10.1091/mbc.e06-05-0467

Zerial, M., & McBride, H. (2001). Rab proteins as membrane organizers. *Nat Rev Mol Cell Biol, 2*(2), 107-117. doi:10.1038/35052055

Zhang, B., Zhang, Y., Wang, Z., & Zheng, Y. (2000). The role of Mg2+ cofactor in the guanine nucleotide exchange and GTP hydrolysis reactions of Rho family GTP-binding proteins. *J Biol Chem, 275*(33), 25299-25307. doi:10.1074/jbc.M001027200

Zhang, Q., Dickson, A., & Doupnik, C. A. (2004). Gbetagamma-activated inwardly rectifying K(+) (GIRK) channel activation kinetics via Galphai and Galphao-coupled receptors are determined by Galpha-specific interdomain interactions that affect GDP release rates. *J Biol Chem, 279*(28), 29787-29796. doi:10.1074/jbc.M403359200

Zheng, H., Loh, H. H., & Law, P. Y. (2010). Agonist-selective signaling of G protein-coupled receptor: mechanisms and implications. *IUBMB Life, 62*(2), 112-119. doi:10.1002/iub.293

Ziarek, J. J., Peterson, F. C., Lytle, B. L., & Volkman, B. F. (2011). Binding site identification and structure determination of protein-ligand complexes by NMR a semiautomated approach. *Methods Enzymol, 493*, 241-275. doi:10.1016/b978-0-12-381274-2.00010-8

Zimmerman, B., Beautrait, A., Aguila, B., Charles, R., Escher, E., Claing, A., . . . Laporte, S. A. (2012). Differential beta-arrestin-dependent conformational signaling and cellular responses revealed by angiotensin analogs. *Sci Signal, 5*(221), ra33. doi:10.1126/scisignal.2002522

Zimmerman, B., Simaan, M., Lee, M. H., Luttrell, L. M., & Laporte, S. A. (2009). c-Src-mediated phosphorylation of AP-2 reveals a general mechanism for receptors internalizing through the clathrin pathway. *Cell Signal, 21*(1), 103-110. doi:10.1016/j.cellsig.2008.09.013

## APPENDIX

Copyright Permissions

ELSEVIER LICENSE
TERMS AND CONDITIONS

Apr 28, 2020

---

This Agreement between Jenna Giubilaro ("You") and Elsevier ("Elsevier") consists of your license details and the terms and conditions provided by Elsevier and Copyright Clearance Center.

| | |
|---|---|
| License Number | 4817990574730 |
| License date | Apr 28, 2020 |
| Licensed Content Publisher | Elsevier |
| Licensed Content Publication | Trends in Pharmacological Sciences |
| Licensed Content Title | G-protein-coupled receptors and signaling networks: emerging paradigms |
| Licensed Content Author | Maria Julia Marinissen,J.Silvio Gutkind |
| Licensed Content Date | Jul 1, 2001 |
| Licensed Content Volume | 22 |
| Licensed Content Issue | 7 |
| Licensed Content Pages | 9 |

| | |
|---|---|
| Start Page | 368 |
| End Page | 376 |
| Type of Use | reuse in a thesis/dissertation |
| Portion | figures/tables/illustrations |
| Number of figures/tables/illustrations | 2 |
| Format | both print and electronic |
| Are you the author of this Elsevier article? | No |
| Will you be translating? | No |
| Title | Characterization of a small molecule inhibitor of small G proteins regulating AT1R trafficking and signaling |
| Institution name | McGill University |
| Expected presentation date | Aug 2020 |
| Portions | Figures 1 and 2 |
| Requestor Location | Jenna Giubilaro<br>5190 Philias-Gagnon<br><br>Montreal, QC H1R3Z6<br>Canada<br><br>Attn: Jenna Giubilaro |

ELSEVIER LICENSE
TERMS AND CONDITIONS

Apr 28, 2020

---

This Agreement between Jenna Giubilaro ("You") and Elsevier ("Elsevier") consists of your license details and the terms and conditions provided by Elsevier and Copyright Clearance Center.

| | |
|---|---|
| License Number | 4817970007742 |
| License date | Apr 28, 2020 |
| Licensed Content Publisher | Elsevier |
| Licensed Content Publication | Trends in Cell Biology |
| Licensed Content Title | GDIs: central regulatory molecules in Rho GTPase activation |
| Licensed Content Author | Céline DerMardirossian,Gary M. Bokoch |
| Licensed Content Date | Jul 1, 2005 |
| Licensed Content Volume | 15 |
| Licensed Content Issue | 7 |
| Licensed Content Pages | 8 |

| | |
|---|---|
| Start Page | 356 |
| End Page | 363 |
| Type of Use | reuse in a thesis/dissertation |
| Portion | figures/tables/illustrations |
| Number of figures/tables/illustrations | 1 |
| Format | both print and electronic |
| Are you the author of this Elsevier article? | No |
| Will you be translating? | No |
| Title | Characterization of a small molecule inhibitor of small G proteins regulating AT1R trafficking and signaling |
| Institution name | McGill University |
| Expected presentation date | Aug 2020 |
| Portions | Figure I in Box 1 |
| Requestor Location | Jenna Giubilaro<br>5190 Philias-Gagnon<br><br>Montreal, QC H1R3Z6<br>Canada<br>Attn: Jenna Giubilaro |

ELSEVIER LICENSE
TERMS AND CONDITIONS

Apr 28, 2020

---

This Agreement between Jenna Giubilaro ("You") and Elsevier ("Elsevier") consists of your license details and the terms and conditions provided by Elsevier and Copyright Clearance Center.

| | |
|---|---|
| License Number | 4817981224264 |
| License date | Apr 28, 2020 |
| Licensed Content Publisher | Elsevier |
| Licensed Content Publication | European Journal of Medicinal Chemistry |
| Licensed Content Title | PI3K/Akt/mTOR and Ras/Raf/MEK/ERK signaling pathways inhibitors as anticancer agents: Structural and pharmacological perspectives |
| Licensed Content Author | Vivek Asati,Debarshi Kar Mahapatra,Sanjay Kumar Bharti |
| Licensed Content Date | Feb 15, 2016 |
| Licensed Content Volume | 109 |
| Licensed Content Issue | n/a |

| | |
|---|---|
| Licensed Content Pages | 28 |
| Start Page | 314 |
| End Page | 341 |
| Type of Use | reuse in a thesis/dissertation |
| Portion | figures/tables/illustrations |
| Number of figures/tables/illustrations | 1 |
| Format | both print and electronic |
| Are you the author of this Elsevier article? | No |
| Will you be translating? | No |
| Title | Characterization of a small molecule inhibitor of small G proteins regulating AT1R trafficking and signaling |
| Institution name | McGill University |
| Expected presentation date | Aug 2020 |
| Portions | Figure 1 |
| Requestor Location | Jenna Giubilaro<br>5190 Philias-Gagnon<br><br>Montreal, QC H1R3Z6<br>Canada<br>Attn: Jenna Giubilaro |

Dear Jenna Giubilaro,

Rockefeller University Press has approved your recent request.

**Request Summary:**
Submit date: 27-Jul-2020
Request ID: 600019836
Publication: The Journal of cell biology
Title: Overexpression of wild-type and mutant ARF1 and ARF6: distinct perturbations of nonoverlapping membrane compartments.
Type of Use: Republish in a thesis/dissertation